INFORMATION TO USERS

This manuscript has been reproduced from the microfilm master. UMI films the text directly from the original or copy submitted. Thus, some thesis and dissertation copies are in typewriter face, while others may be from any type of computer printer.

The quality of this reproduction is dependent upon the quality of the copy submitted. Broken or indistinct print, colored or poor quality illustrations and photographs, print bleedthrough, substandard margins, and improper alignment can adversely affect reproduction.

In the unlikely event that the author did not send UMI a complete manuscript and there are missing pages, these will be noted. Also, if unauthorized copyright material had to be removed, a note will indicate the deletion.

Oversize materials (e.g., maps, drawings, charts) are reproduced by sectioning the original, beginning at the upper left-hand corner and continuing from left to right in equal sections with small overlaps. Each original is also photographed in one exposure and is included in reduced form at the back of the book.

Photographs included in the original manuscript have been reproduced xerographically in this copy. Higher quality 6" x 9" black and white photographic prints are available for any photographs or illustrations appearing in this copy for an additional charge. Contact UMI directly to order.

UMI

A Bell & Howell Information Company
300 North Zeeb Road, Ann Arbor MI 48106-1346 USA
313/761-4700 800/521-0600

UNIVERSITY OF ALBERTA

Molecular Studies of Mammalian Na^+/Nucleoside Cotransporters

by

Meiyi Huang 

A thesis submitted to the Faculty of Graduate Studies and Reseach in partial fulfillment of the requirement for the degree of Master of Science.

DEPARTMENT OF PHYSIOLOGY

Edmonton, Alberta

Spring, 1997

University of Alberta

Library Release Form

Name of Author: Meiyi Huang

Title of Thesis: Molecular Studies of Mammalian Na^+/Nucleoside Cotransporters

Degree: Master of Science

Year this Degree Granted: 1997

Permission is hereby granted to the University of Alberta Library to reproduce single copies of this thesis and to lend or sell such copies for private, scholarly, or scientific research purposes only.

The author reserves all other publication and other rights in association with the copyright in the thesis, and except as hereinbefore provided, neither the thesis nor any substantial portion thereof may be printed or otherwise reproduced in any material form whatever without the author's prior writtern permission.

Meiyi Huang

Meiyi Huang

10929 80ave

Edmonton, Alberta

Canada, T6G, 0P9

Jan. 16, 1997

University of Alberta

Faculty of Graduate Studies and Research

The undersigned certify that they have read, and recommended to the Faculty of Graduate Studies and Research for acceptance, a thesis entitled **Molecular Studies of Mammalian Na^+/Nucleoside Cotransporters** submitted by **Meiyi Huang** in partial fulfillment of the requirements for the degree of **Master of Science.**

J.D. Young (Supervisor)

C. Benishin (Chairperson)

C.I. Cheeseman

W.P. Gati

E. Karpinski

Jan. 16, 1997

Dedicated to the memory of my father, Huang, Zhi,

and to my mother and my family.

ABSTRACT

rCNT1, a pyrimidine-selective, Na^+-dependent nucleoside transporter from rat jejunum/kidney is the first identified mammalian representative of a gene family that also includes the *E. coli* H^+-dependent nucleoside symporter NupC.

ON this study, cDNAs were cloned encoding human CNT1 (hCNT1). A short PCR product homologous to rCNT1 was amplified from a human kidney cDNA library and used to isolate two larger cDNA fragments (Clones A and B) of the same protein. Subsequently, the PCR probe was used to clone the full-length human transporter, which mediated CNT1-type transport activity in *Xenopus* oocytes. Clones A and B encoded 40% of the open reading frame of hCNT1.

Site-directed mutagenesis was used to study the functional role of three conserved amino acid residues from helix 12 of rCNT1. Each mutation individually had little effect on transport activity in oocytes. Double mutants exhibited substantially reduced fluxes, while the triple mutant was devoid of activity. Western analyses confirmed that the mutations altered the intrinsic activity of the transporter.

ACKNOWLEDGEMENT

I wish to extend my sincere gratitude to my supervisor, Dr. J.D.Young, for his guidance and support throughout my project and in writing this thesis. I am grateful to all the other people who have assisted me to complete the project. A special thanks to Mabel Rizel, for giving me the technical assistance in performing the molecular biology studies, and to Sylvia Yao, for her guidance in expression studies. I am most grateful to Dr. C.E. Cass for her support and help and to the members of her Laboratory. I also thank other people who have given me valuable advice. Thank you to Wing Tsang for his help in Dr. Young's Laboratory during the time he was here in Edmonton. Thanks all the people in Dr. Young's Laboratory who have helped me. Thank you also to members of my Thesis Committee for their invaluable contributions to my work.

TABLE OF CONTENTS

CHAPTER			PAGE
1. Introduction			
	1.1	The Functional Classification of Na^+-dependent Nucleoside Transport Processes	5
	1.2	SNST1	7
	1.3	rCNT1	8
		1.3.1 Cloning and Expression of rCNT1	8
		1.3.2 Structure and Evolution of rCNT1	9
		1.3.3 rCNT1 Transmembrane Domains 12 and 13	11
	1.4	rCNT2 (SPNT)	14
	1.5	Bacterial H^+/nucleoside Symporters	15
	1.6	Research Objectives	15
2.	Materials and Methods		26
	2.1	Isolation of cDNAs Encoding Human CNT1 (hCNT1)	27
		2.1.1 PCR Probe	
		2.1.2 Labelling of the PCR Fragment	28
		2.1.3 Library Screening	29
	2.2	Site-directed mutagenesis of Rat CNT1 (rCNT1)	31
		2.2.1 Construction of Mutants	31
		2.2.1.1 First PCR Amplification	33
		2.2.1.2 Purification of First Round PCR Products	34
		2.2.1.3 Second PCR Amplification	34

2.2.1.4 Purification of Second Round PCR Products 35
2.2.1.5 Restriction Endonuclease Digestion 36
2.2.1.6 Ligation 36
2.2.1.7 Calcium Chloride Transformation 37

2.2.2 *In Vitro* Transcription 38

2.2.3 Gel Electrophoresis of RNA 39

2.2.4 Oocyte Preparation 40

2.2.5 Injection of Oocytes 41

2.2.6 Assay of Uridine Transport Activity 42

2.2.7 Statistical Analysis of Transport Data 42

2.2.8 Preparation of Oocyte Plasma Membranes 43

2.2.9 Quantification of Plasma Membrane Protein 43

2.2.10 SDS Polyacrylamide Gel Electrophoresis and Western Blotting 44

3. Results 52

3.1 Isolation of cDNAs Encoding Human CNT1 (hCNT1) 53

3.1.1 Cloning Strategy 53

3.1.2 PCR Probe 55

3.1.3 Library Screening 55

3.2 Site-directed Mutagenesis of Rat CNT1 (rCNT1) 58

3.2.1 Construction of Mutants 59

3.2.1.1 First PCR Amplification 60
3.2.1.2 Second PCR Amplification 60
3.2.1.3 Digestion of PCR Product and rCNT1 cDNA with *BspE*I and *BamH*I 61

3.2.1.4 Subcloning 61
3.2.1.5 Mutant Identification 62
3.2.1.6 Second Mutagenesis 63

3.2.2 *In Vitro* Transcription 63

3.2.3 Uridine Transport Activity of rCNT1 Mutants 64

3.2.4 Western Blotting 66

4. Discussion 110

4.1 Isolation of cDNAs Encoding Human CNT1 (hCNT1) 111

4.1.1 PCR Product 111

4.1.2 Clones A and B 113

4.1.3 hCNT1 115

4.2 Site-directed Mutagenesis Studies of Rat CNT1 (rCNT1) 119

4.2.1 Three Conserved Amino Acid Residues in Transmembrane Domain 12 119

4.2.2 Expression of Recombinant rCNT1 Mutants in the Oocyte Plasma Membrane 121

4.3 Future Directions 123

4.3.1 Human CNT Transporters 123

4.3.2 Mutagenesis Studies 124

5. Reference 130

LIST OF TABLES

TABLE	PAGE
1.1 Na^+-dependent nucleoside transport systems in mammalian cells	18
1.2 Na^+-dependent glucose transporter (SGLT) family	19
3.1 Sequence results of rCNT1 mutagenesis with degenerate primers IP1,IP2	92
3.2 Uridine influx values for wild-type and mutant rCNT1 constructs	93

LIST OF FIGURES

FIGURE		PAGE
1.1	The structure of uridine	20
1.2	Topographical model of rCNT1	21
1.3	Alignment of deduced ECOHU4748, ECOHU4751, NupC and rCNT1 amino acid sequences (location of S459, T466 and P470)	22
1.4	Vertical view of putative α-helix 12 of rCNT1	24
1.5	Vertical view of putative α-helix 13 of rCNT1	25
2.1	Alignment of ECOHU4748, ECOHU4751, NupC and rCNT1 nucleotide sequences (1368-1967 of rCNT1)	46
2.1	Alignment of deduced ECOHU4748, ECOHU4751, NupC and rCNT1 amino acid sequences (location of primers Q1 and Q2)	48
2.3	Mutation of wild-type rCNT1 by sequential PCR	50
3.1	Ethidium bromide-stained agarose gel of the PCR product from a human kidney library	68
3.2	Comparison of the nucleotide sequences of the PCR fragment and correponding region of rCNT1	69
3.3	Comparison of the deduced amino acid sequences of the PCR fragment and corresponding region of rCNT1	70
3.4	Isolation of Clone A	71
3.5	Isolation of Clone B	73
3.6	Nucleotide sequence of the Clone A insert	75
3.7	Comparison of the nucleotide sequences of the Clone A cDNA and the corresponding region of rCNT1	76
3.8	Comparison of the deduced amino acid sequences of the overlapping regions of Clone A and rCNT1	78
3.9	Comparison of the nucleotide sequences of the Clone A between	

primers Q1 and Q2 and the PCR product 79

3.10 Nucleotide sequence of the Clone B insert 80

3.11 Comparison of the overlapping regions of the nucleotide sequences of the Clone B and rCNT1 82

3.12 Comparison of the deduced amino acid sequences of the overlapping regions of Clone B and rCNT1 83

3.13 Comparison of the nucleotide sequences of Clone B between primers Q1 and Q2 and the PCR product 84

3.14 Comparison of the nucleotide sequences of overlapping regions of Clones A and B 85

3.15 Schematic representation of the alignment of Clones A and B and the PCR product 86

3.16 Comparison of the nucleotide sequences of the PCR fragment and the corresponding region of hCNT1 87

3.17 Comparison of the nucleotide sequences of the overlapping region of Clone A and hCNT1 88

3.18 Comparison of the nucleotide sequences of the overlapping region of Clone B and hCNT1 90

3.19 Schematic representation of the alignment between the hCNT1 cDNA, the PCR product and Clones A and B cDNAs 91

3.20 Alignment of relevant regions of the deduced amino acid sequences of ECOHU4748, ECOHU4751, NupC, rCNT1 and hCNT1. 94

3.21 Oligonucleotide sequences of the sense degenerate primer IP1 95

3.22 Agarose gel of the PCR products generated during first PCR amplification 96

3.23 Agarose gel of the PCR product generated during second PCR amplification 97

3.24 Agarose gel of DNA fragments digested with *BspEI* and *BamHI* 98

3.25 Agarose gel of PCR products generated using selected transformant

plasmid DNA as template and two flanking primers, T7 and SP6 99

3.26 The probability of wild-type and different rCNT1 mutants among the transformants 100

3.27 Construction of S459A/P470A and S459A/Y466F/P470A 101

3.28 Agarose gel showing representative PCR products generated from mutant rCNT1 pGEM-3Z DNAs by using the primer T7, the primer IP2 and the corresponding mutant plasmid DNA 102

3.29 Agarose gel of mutant plasmid cDNAs linearized by *Xba*I 103

3.30 Agarose gel of wild-type and mutant rCNT1 RNA transcripts 104

3.31 Uridine transport by wild-type and single mutant rCNT1 constructs 105

3.32 Uridine transport by wild-type, double and triple mutant rCNT1 constructs 107

3.33 Western blots of wild-type and mutant recombinant rCNT1 proteins in enriched plasma membrane fractions prepared from *Xenopus oocytes* 109

4.1 Comparison of the deduced amino acid sequences of hCNT1 and rCNT1 126

4.2 Comparison of the deduced amino acid sequences of hCNT1 and rCNT2 128

ABBREVIATIONS

AIDS	Acquired immunodeficiency syndrome
AZT	3'-azido-3'-deoxythymidine
bp	Nucleotide base pair
BSA	Bovine serum albumin
cDNA	Complementary DNA
cRNA	Complementary RNA
ddC	2',3'-dideoxycytidine
EDTA	Ethylenediaminetetraacetic acid
HEPES	4-(2-hydroxyethyl)-1-piperazineethanesulfonic acid
HPLC	High performance liquid chromatography
LB	Lauria-Bertani medium
kDa	Kilodaltons
K_m	Permeant concentration at half-maximal unidirectional flux
MBM	Modified Barth's medium
NBMPR	Nitrobenzylthioinosine
PCR	Polymerase chain reaction
SDS	Sodium dodecylsulphate
SEM	Standard error of mean
Tris	Tris-(hydroxymethyl)aminomethane
V_{max}	Maximum transport rate

CHAPTER 1

Introduction

1. INTRODUCTION

Nucleosides consist of a pentose sugar (typically ribose or deoxyribose) linked to one of several different purine or pyrimidine nitrogen-containing ring compounds called nucleobases because of their acceptance of protons. For instance, uridine is composed of uracil and ribose (Figure 1.1). Nucleosides have various important biochemical, physiological and pharmacological activities in humans and other mammals. For example, nucleosides serve as the precursors of nucleic acids in some tissues (141) and adenosine functions as a local hormone in regulation of lipolysis, neurotransmitter release, platelet aggregation, coronary vasodilation, and cardiac contractility (5,27,52). Inosine is the physiological energy source for pig erythrocytes (138,139). Some natural nucleosides and synthetic nucleoside analogs are cytotoxic and have been used as chemotherapuetic agents to treat cancer and viral infections such as acquired immunodeficiency syndrome (AIDS)(97). In bacteria such as *E.coli*, nucleotides for DNA and RNA synthesis are supplied by nucleoside salvage as well as by *de novo* synthesis (44,86). Physiological nucleosides and most therapeutic nucleoside analogs are hydrophilic and their permeation across cell membranes requires the presence of nucleoside transporter proteins.

Transporters are a class of integral membrane proteins with multiple transmembrane domains (40,46,105). Functionally, transporters are classified as either equilibrative, where transport of the substrate occurs passively, or concentrative, where transport is coupled to an energy source and is concentrative.

Many concentrative transporters are driven by transmembrane ion gradients. In the situation where the ion and solute move in the same direction, transport is termed symport. Where the ion and solute move in opposite directions, transport is termed antiport. In mammals, the co-transported ion is typically Na^+, while in bacteria it is mostly H^+.

Nucleoside transporter proteins have been studied functionally for many years. Bacteria possess concentrative, H^+/nucleoside symporters. In mammalian cells, both equilibrative nucleoside transporters and concentrative, Na^+/nucleoside symporters are present (21). Equilibrative nucleoside transport processes are widely distributed in mammalian tissues and tumour cells and are typically inhibited by low (nM) concentrations of nitrobenzylthioinosine (NBMPR). These transport processes, designated *es* (equilibrative, sensitive) have a broad substrate selectivity and mediate the transport of physiological nucleosides (purine and pyrimidine ribosides and deoxyribosides) and a variety of nucleoside analogs (16,20,36,86,93,94,97,140). Some mammalian cells express equilibrative nucleoside transport processes that are not inhibited by nM concentrations of NBMPR, and are designated *ei* (equilibrative, insensitive) (6-8,18,19,30,53,55,96). Both the *es* and *ei* processes are inhibited by vasoactive drugs such as dipyridamole and dilazep, although there are species differences (16,20,36,93,94,97,140).

NBMPR has proved to be a powerful tool to identify and purify *es*-type nucleoside transporter proteins (18,19,53,54,57,68,69,129,137). The human erythrocyte transporter is an integral membrane glycoprotein of apparent M_r 55,000

and has been purified to homogeneity by a combination of ion-exchange and immunoaffinity chromatography (54,69). The protein shows some physical and structural similarity to the human GLUT1 glucose transporter (56,128,137,141) but, as described below, belongs to a different gene family. Structurally similar *es*-type nucleoside transporter polypeptides have been identified in other mammalian cells and tissues (1-4,26,47,70,71). The molecular properties of *ei* nucleoside transporters are unknown.

Experiments have been undertaken to clone cDNAs encoding the *es* nucleoside transporter. Several putative *es* cDNA fragments were obtained from a phage expression library prepared from cultured human (BeWo) choriocarcinoma cells by screening with polyclonal antibody against the human erythrocytic *es* transporter (13,20). Antisense transcripts of these cDNAs blocked expression of NBMPR-sensitive uridine transport activity in *Xenopus* oocytes injected with BeWo mRNA (13,20). Very recently, a full-length functional *es* transporter cDNA (hENT1) was isolated from human placental cDNA library by a PCR-based cloning strategy that utilized primers corresponding to the N-terminal amino acid sequence of the purified human erythrocyte *es* transporter (41). The hENT1 cDNA encodes a 456 residue, 11 transmembrane domain protein that is unrelated in amino acid sequence to previously identified transporter families (Table 1.1), including that for GLUT1. Like GLUT1, however, hENT1 possesses a putative large extracellular loop between transmembrane helices 1 and 2, and a large putative intracellular loop between transmembrane helices 6 and 7. hENT1 shows sequence homology to

several proteins of unknown function in yeast, nematodes, plants and mammals (41).

In other studies, a murine cDNA encoding an unrelated putative Golgi membrane-associated nucleoside transporter protein, designated MTP, has been isolated by complementation of the thymidine transport deficiency in *Saccharomyces cerevisiae* (20,48). Human MTP has also been cloned (21).

1.1. THE FUNCTIONAL CLASSIFICATION OF Na^+-DEPENDENT NUCLEOSIDE TRANSPORT PROCESSES

In mammals, Na^+-dependent nucleoside transport processes are present in intestinal (12,116) and renal epithelia (42,73,125), choroid plexus (130,131,132), liver (22), macrophages (98,100) and leukemic cells (10,95), and have been classified functionally into five types (Table 1.1). Each has a different cellular and species distribution (21). Only the N5-type process (also known as *cs*: concentrative, sensitive), which occurs in fresh leukaemia cells from patients, is inhibited by NBMPR (95). The other four processes (systems N1-N4) are not inhibited by NBMPR, but differ from each other in permeant specificity. The N1 system (also known as *cif*: concentrative, insensitive, formycin B) is generally purine-selective (formycin B is regarded as a model permeant), but also transports uridine. The second system, designated N2 or *cit* (concentrative, insensitive, thymidine) is generally pyrimidine-selective (thymidine is regarded as a model permeant), but also transports adenosine. Systems N1 and N2, which represent the two principal Na^+-

dependent nucleoside transporter types in mammalian cells, have been found in tissues and cells of rat, rabbit, murine and bovine origin (21). N3-type nucleoside transporters (also known as *cib*: concentrative, insensitive, broad) have broad selectivity for both purine and pyrimidine nucleosides and have been found to date only in human leukemic cells (9,10), rat jejunum (49,59) and rabbit choroid plexus (130,131,132). A human kidney N2/*cit*-like process that is selective for guanosine in addition to pyrimidine nucleosides and adenosine has been given the designation N4/*cit* (42).

The N1, N2 and N4 systems have a Na^+/nucleoside stoichiometry of 1:1 (22,28,29,42,72,98-100,126). For system N3 of rabbit choroid plexus, however, it has been determined to be 2:1 (130).

Different Na^+-linked nucleoside transport systems have been expressed in *Xenopus* oocytes injected with tissue mRNA. The N1 system has been expressed in oocytes injected with rat jejunal mRNA (49). N2-type activity has been expressed with mRNA from rabbit intestine (49,59). The N3 system has been expressed from rat jejunal mRNA (49) and rabbit choroid plexus mRNA (132). Expression of human kidney N4-type activity has also been reported (43).

Recent studies have isolated cDNAs for several mammalian Na^+-dependent nucleoside transporter proteins. The first to be cloned encodes a putative N3-type transporter protein from rabbit kidney, SNST1, a member of the Na^+/glucose SGLT cotransporter gene family (90). Subsequently, a cDNA encoding an N2-type nucleoside transporter, rCNT1, was isolated from rat jejunum by the laboratory of

my supervisor, Dr. James D. Young (50). rCNT1 is unrelated either to SNST1 (90), hENT1 (41) or MTP (20) and instead belongs to a different gene family that includes the *E. coli* H^+/nucleoside symporter *nupC* (25). After my project was initiated, cDNAs encoding rCNT1-related proteins with N1-type activity were cloned from rat liver and and rat jejunum and have been given the designation rCNT2 (135) or SPNT (23).

1.2 SNST1

Members of the SGLT gene family are Na^+-coupled symporters with a range of different substrate specificities (Table 1.2). The rabbit intestinal SGLT1 Na^+/glucose cotransporter was the first mammalian symporter to be cloned (45). It is a 664-residue protein which is predicted to have 12-14 transmembrane domains. The sequences of SGLT1 from different species are highly conserved (127). SGLT1 homologs from mammalian sources include the low-affinity human renal Na^+/glucose cotransporter SGLT2 (123), the canine renal Na^+/ myo-inositol cotransporter SMIT1 (67) and the putative rabbit renal Na^+/nucleoside cotransporter SNST1 (90). In addition, there are two SGLT homologs from bacteria. These are the *E. coli* Na^+/proline cotransporter PutP (88) and Na^+/pantothenate cotransporter (51). There are also a number of SGLT homologs of undetermined function (101).

The SNST1 cDNA was cloned by screening a rabbit renal cDNA library with a 1.6kb fragment of the rabbit SGLT1 (90). It encodes a protein of 672 amino acid

residues that is 61% identical and 80% similar in amino acid sequence to rabbit SGLT1. Homology between the two proteins is most marked near the N-terminus. The conclusion that SNST1 is a nucleoside transporter protein was based on expression studies in *Xenopus* oocytes that demonstrated low levels of apparent N3-type activity (90). Small SNST1-mediated fluxes of nucleosides have also been observed in *Sf*9 cells (91). The presence of the SNST1 protein in renal epithelia has not been demonstrated and its role in nucleoside physiology is, at present, uncertain.

1.3 rCNT1

1.3.1 Cloning and Expression of rCNT1

The 2.4 kb cDNA encoding rCNT1 was isolated from a size-selected rat jejunum cDNA library by expression selection in *Xenopus* oocytes (50). The cDNA encodes a 648-residue protein with a predicted molecular mass 71,000 (50). rCNT1 was demonstrated to be an N2-type transporter by functional expression of the recombinant protein in oocytes (50) and, subsequently, in transiently transfected COS-1 cells (33).

In oocytes, expressed:basal flux ratios for rCNT1-mediated uridine uptake (10 μM) were > 10^4:1 (50), in marked contrast to the modest 2- to 3-fold flux ratio reported for SNST1 (91). After 30 min, the intracellular content of uridine, which is only slowly metabolized in oocytes (49), reached a concentration 6-fold higher

than that present in the extracellular medium. Transport was saturable (apparent K_m 37 μM), Na^+-dependent and unaffected by NBMPR. Alterations in external pH in the range 5.5 - 8.5 had no effect on transport rate, indicating a lack of H^+-dependence. Pyrimidine nucleosides and adenosine inhibited rCNT1-mediated uridine and thymidine influx, while other purine nucleosides, uracil, UMP, UDP and UTP were without effect, demonstrating that the expressed transport activity was of the N2-type. Expression experiments in COS-1 cells yielded similar results (33).

Northen analysis demonstrated that transcript for rCNT1 was present in rat jejunum and kidney, but absent from heart, brain, spleen, lung, liver, muscle and testis, in accordance with the known distribution of N2-type transport activity in rat tissues (58,72,73,74,116,125,126).

1.3.2. Structure and Evolution of rCNT1

rCNT1 is a polytopic integral membrane protein (50). The N-terminus does not contain a signal sequence, suggesting that it is intracellular. The protein contains three *N*-linked glycosylation sites, four potential protein kinase-dependent phosphorylation sites, and a cluster of four serine residues near the C-terminus. Physiochemical and statistical hydropathy scales (32,118) predict that rCNT1 has between 10 and 14 α-helical transmembrane domains. The topographical model shown in Figure 1.2 has the maximum number of 14 potential transmembrane segments and a (+)-charge difference (extracellular *minus* intracellular) of 21. In this model, one potential *N*-linked glycosylation site is located within transmembrane

segment 13, while the other two are predicted to be intracellular. Four possible *O*-linked glycosylation sites are located in the extracellular loop linking transmembrane domains 13 and 14. All four potential protein kinase C-dependent phosphorylation sites are predicted to be intracellular.

At the time my project was initiated, the only proteins known to be related structurally to rCNT1 were the *E. coli* H^+/nucleoside symporter *nup*C (25) and two other *E. coli* proteins of unknown function, designated ECOHU4748 and ECOHU4751 (101). rCNT1 is 27% identical (58% similar) to *nup*C and 34% identical (63% similar) to the other two proteins. A sequence alignment between the four proteins is shown in Figure 1.3. The 54 amino acid residues that are fully conserved in the four proteins are clustered predominantly in the *C*-terminal half of the rCNT1 sequence and include the motifs "MGV", "NEFVA" and "FANFxSIG". Homology between rCNT1 and its *E. coli* counterparts is particularly noticeable in putative transmembrane domains 12 and 13 and in the loop between them. Other conserved residues also tend to be localized within putative transmembrane domains. rCNT1 is ~ 70 amino acid residues longer than the other proteins and the additional residues are located primarily at the *N*- and *C*-termini. In the alignment shown in Figure 1.3, only 11 of the 14 putative transmembrane domains identified in rCNT1 are shared by *nup*C and ECOHU4748/4751.

Other than the three *E.coli* proteins, rCNT1 showed no detectable homology to known eucaryotic or procaryotic membrane transporter proteins, including members of the transporter families listed in Table 1.1. These families include the

SGLT transporter family, to which SNST1 belongs, and those for hENT1 and MTP. It can be concluded, therefore, that rCNT1 and its *E. coli* homologs constitute a previously unrecognised, new transporter gene family and that rCNT1 is the first mammalian representative of that family to be identified. Subsequent to the cloning of rCNT1, cDNAs encoding a second rat Na^+-dependent nucleoside transporter, this time with N1-type transport activity were isolated from liver (23) and intestine (135) and designated rCNT2 (SPNT). Thus, members of the rCNT1 family are responsible for the two major Na^+-dependent nucleoside transport activites (systems N1 and N2) that have been identified functionally in mammalian cells of rat, rabbit, murine and bovine origin (please see Section 1.1). The rCNT2 (SPNT) transporter and nucleoside transport in bacteria are reviewed further in Sections 1.4 and 1.5, respectively.

1.3.3 rCNT1 Transmembrane Domains 12 and 13

Amino acid residues that are conserved between rCNT1 and its bacterial counterparts are likely to be important for transporter's structure and function and are potential targets for site-directed mutagenesis experiments. The sequence alignment presented in Figure 1.3 shows that transmembrane domains 12 and 13 are particularly well conserved and there is evidence from studies of other transporters and receptors that residues important for substrate and cation binding tends to be localized within membrane-spanning regions (60,82). In the case of *E. coli* lactose

permease for example (82), transport function is not affected by the disruption of most hydrophilic loops. Helices 9 and 10 of this protein (82), and helix 12 of the rat brain GABA transporter have been demonstrated to be critical for transport activity (11). Residues responsible for high-affinity binding of agonists to β-adrenergic receptors are all located within the hydrophobic transmembrane core of the receptor (60).

Transmembrane domains 12 and 13 contain 16 (30%) of the 54 amino acid residues conserved between rCNT1, *nupC* and ECOHU4748/4751 (Figure 1.3). A comparison of the vertical views of these two putative α-helices are shown for rCNT1 in Figures 1.4 and 1.5. In the case of helix 12, it is striking that four of the 8 conserved residues, S459, I463, Y466 and P470, localize to one face of the helix. A similar phenomenon has been found in mammalian sugar transporters and has been used to identify potential pore-forming regions (61).

Two (S459 and Y466) of the four residues are polar and capable of participating in hydrogen bonds. Such residues may potentially be important in substrate binding or, alternatively, bonding to an adjacent helix. A number of studies have demonstrated the importance of serine and tyrosine residues in permeant-transporter and ligand-receptor interactions. S356 and S359 of the rat dopamine transporter (62), for example, have been implicated in transport function. S204 of mammalian α2A-adrenergic receptors (120) and S204, S207, S319 and Y326 of mammalian β-adrenergic receptors (111) are crucial for both agonist binding and receptor activation. Y236 is believed to be involved in substrate binding and

transport by *E. coli* lactose permease (15). When Y143 and Y293 of GLUT4, which are conserved in all mammalian glucose transporters, were substituted, glucose transport activity was reduced and abolished, respectively (119).

The other two conserved residues (I463 and P470) on the same face of rCNT1 helix 12 as S459 and Y466 are nonpolar, and one is a proline residue. Conserved and/or functionally important proline residues have been identified within the transmembrane helices of transporters, channels and receptors (14,109). Most transporter proteins contain membrane-buried proline residues and a number of such residues have been studied by site-directed mutagenesis. For example, mutation of the three proline residues of helix 10 of the human erythrocyte glucose transporter GLUT1 have been shown to abolish 2-deoxy-D-glucose uptake (122). Mutation of P328 in transmembrane domain 4 of the α_1-subunit of rat kidney Na^+/K^+-ATPase influences both cation and ATP binding affinity (117), and P87 in helix 2 of the rat Cx26 voltage-gated gap junction channel has been shown to be critical to the transduction of voltage gating (112). Proline is established as a potent breaker of α-helical structures in soluble proteins (136) and its frequent occurrence in the putative transmembrane helices of integral membrane proteins, particularly transport proteins, presents a structural dilemma. Recent studies suggest that the helical propensity of proline is enhanced greatly in a membrane lipid environment and that relative to alanine, for example, serves to protect transmembrane helical conformations (75). Structurally, the presence of a proline residue in a transmembrane α-helix introduces a bend in the helix longitudinal axis, producing kink angles of between 10° and 40°

(107,108). In addition to having a role in helix stability and packing, it has been found that intrahelical proline residues provide potential binding sites for cations *via* exposure of the backbone carbonyl oxygen atoms of residues *i*-3 and *i*-4 (where *i* is the position of the proline) (109).

1.4 rCNT2 (SPNT)

After I initiated my project, two cDNAs encoding N1-type Na^+-dependent nucleoside transporters were cloned. SPNT from rat liver was cloned by expression selection in *Xenopus* oocytes (23). SPNT is a 659 residue protein that is 64% identical (80% similar) in amino acid sequence to rCNT1. In SPNT, the amino acid residues corresponding to S459, Y466 and P470 of helix 12 in rCNT1 are threonine (replacing serine), tyrosine and proline, respectively. Since threonine and serine are close structural homologs (both are polar with a side-chain hydroxyl group that can form hydrogen bonds), the primary structure of SPNT provides additional evidence of the potential importance of these three residues. Threonine residues have been demonstrated to be involved in substrate and cation binding to procaryotic amino acid transporters (79,115). The other conserved amino acid in this face of helix 12 of rCNT1, I463, is also present in SPNT. Functionally, SPNT was identified as an N1-type transporter by its ability to transport adenosine and by the inhibition of this transport by inosine, guanosine, uridine and formycin B. A cDNA encoding the same transporter protein was subsequently isolated from rat jejunum (135).

1.5 BACTERIAL H^+/NUCLEOSIDE SYMPORTERS

In bacteria, the best characterized nucleoside transporters are in the inner membrane of *E. coli*, where two high-affinity H^+-dependent nucleoside transport processes, designated *nup*G and *nup*C, have been identified (25,63-65,84,86,87,103,104,124). The *nup*G gene maps to 63.4 min on the *E. coli* chromosome and encodes a protein with 418 amino acid residues and a molecular mass of 43,000 (124). *Nup*G has a broad specificity for both purine and pyrimidine nucleosides (86). The *nup*C gene maps to 51.8 min on the *E. coli* chromosome (142) and encodes a 401 amino acid protein, also with molecular mass of 43,000 (25). *Nup*C is structurally related to rCNT1/2 and and to two *E. coli* proteins of undetermined function, ECOHU4748 and ECOHU4751, but not to *nup*G, which has no known homologs either in mammals or bacteria. *Nup*C, like rCNT1, is selective for pyrimidine nucleosides and adenosine. This has been established both by studies of the native protein in bacteria (85,86) and by studies of the recombinant *nupC* expressed in *Xenopus* oocytes (133). Expression experiments in *Xenopus* oocytes have also confirmed the transporter's dependence on protons and not Na^+ (133). Subsequent to the initial molecular cloning of *nup*C from *E. coli*, *nup*C genes have been identified in a range of bacterial species, including *Bacillus subtilis* and *H. influenzae* (17,110).

1.6 RESEARCH OBJECTIVES

When I began my project under Dr.Young's supervision in 1993, rCNT1 from rat jejunum/kidney was the first identified mammalian representative of a gene family that is now known to include the proteins responsible for both the purine-selective N1-type and pyrimidine-selective N2-type Na^+-dependent nucleoside transport processes of mammalian cells. As reviewed in Section 1.1 of this Chapter, system N1 and N2 transport activities had been documented functionally in tissues and cells of rat, rabbit, murine and bovine origin, but not in human cells, which instead featured N3, N4 and N5-type fluxes. Studies of recombinant rCNT1 in *Xenopus* oocytes had established that it transported the antiviral pyrimidine nucleosides AZT and ddC, in addition to physiological pyrimidine nucleosides (and adenosine). Therefore, it was hypothesized that the human homolog of rCNT1, if such an entity existed, might potentially be involved in the intestinal absorption and renal handling of drugs used to treat AIDS.

The first research objective of my project was to attempt to isolate cDNAs encoding human CNT1 (hCNT1). Results of these investigations have been published (102, in press).

In 1994, the genomic nucleotide and deduced amino acid sequence of *E. coli* NupC was published. As reviewed in Sections 1.3.2, 1.3.3 and 1.5 of this Chapter, NupC is a structural and functional homolog of rCNT1. Sequence alignments between rCNT1, NupC and two other related *E. coli* proteins of unknown function established that one face of helix 12 was highly conserved, leading to the hypothesis that amino acid residues on this face of helix 12 might be important for transport activity.

The second research objective of my project was to use site-directed mutagenesis to study the functional role of three of these conserved rCNT1 amino acid residues, S459, Y466 and P470.

Table 1.1 Na^+-dependent nucleoside transport systems in mammalian cells

---

N1 (*cif*) - Purine selective (also uridine)

N2 (*cit*) - Pyrimidine selective (also adenosine)

N3 (*cib*) - Broad specificity (purine and pyrimidine nucleosides)

N4 (*cit*) - Pyrimidine selective (also adenosine and guanosine)

N5 (*cs*) - NBMPR - sensitive (permeant selectivity not determined)

Table 1.2 Sodium-dependent glucose transporter (SGLT) family

SGLT1	: High-affinity mammalian Na^+-dependent glucose transporter
SGLT2	: Low-affinity mammalian Na^+-dependent glucose transporter
SNST1	: Putative rabbit renal Na^+-dependent nucleoside transporter
SMIT1	: Dog renal Na^+-dependent myoinositol transporter
PutP	: *E. coli* Na^+-dependent proline transporter
PanF	: *E. coli* Na^+-dependent pantothenate transporter

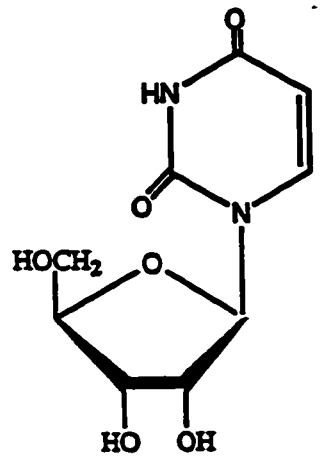

Uridine
(Urd)

Figure 1.1 The structure of uridine.

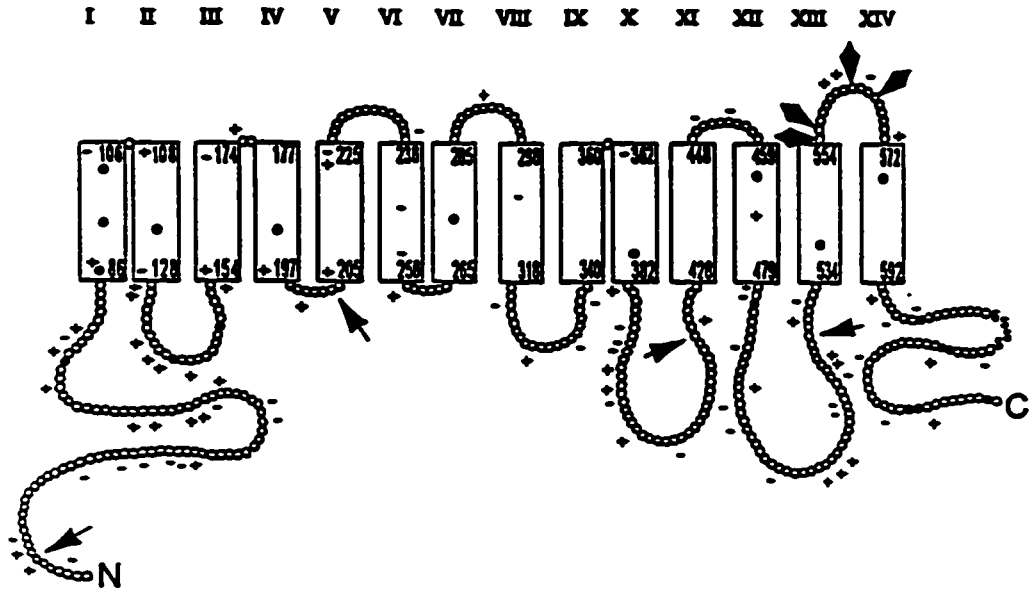

Figure 1.2 Topographical model of rCNT1 (50). Putative transmembrane domains are numbered and shown as rectangles. The acidic, basic and Cys residues are marked by (-), (+) and (●), respectively. Four potential *O*-linked glycosylation sites are located in the extracellular loop between the helices 13 and 14 (♦). Potential PKC-dependent phosphorylation sites are indicated by (↑).

Figure 1.3 Alignment of deduced ECOHU4748, ECOHU4751, NupC and rCNT1 amino acid sequences by using the GCG program PILEUP. Fully conserved residues are indicated by asterisks. Presumed transmembrane helices of rCNT1 are underlined. S459, Y466 and P470 are marked with an arrow.

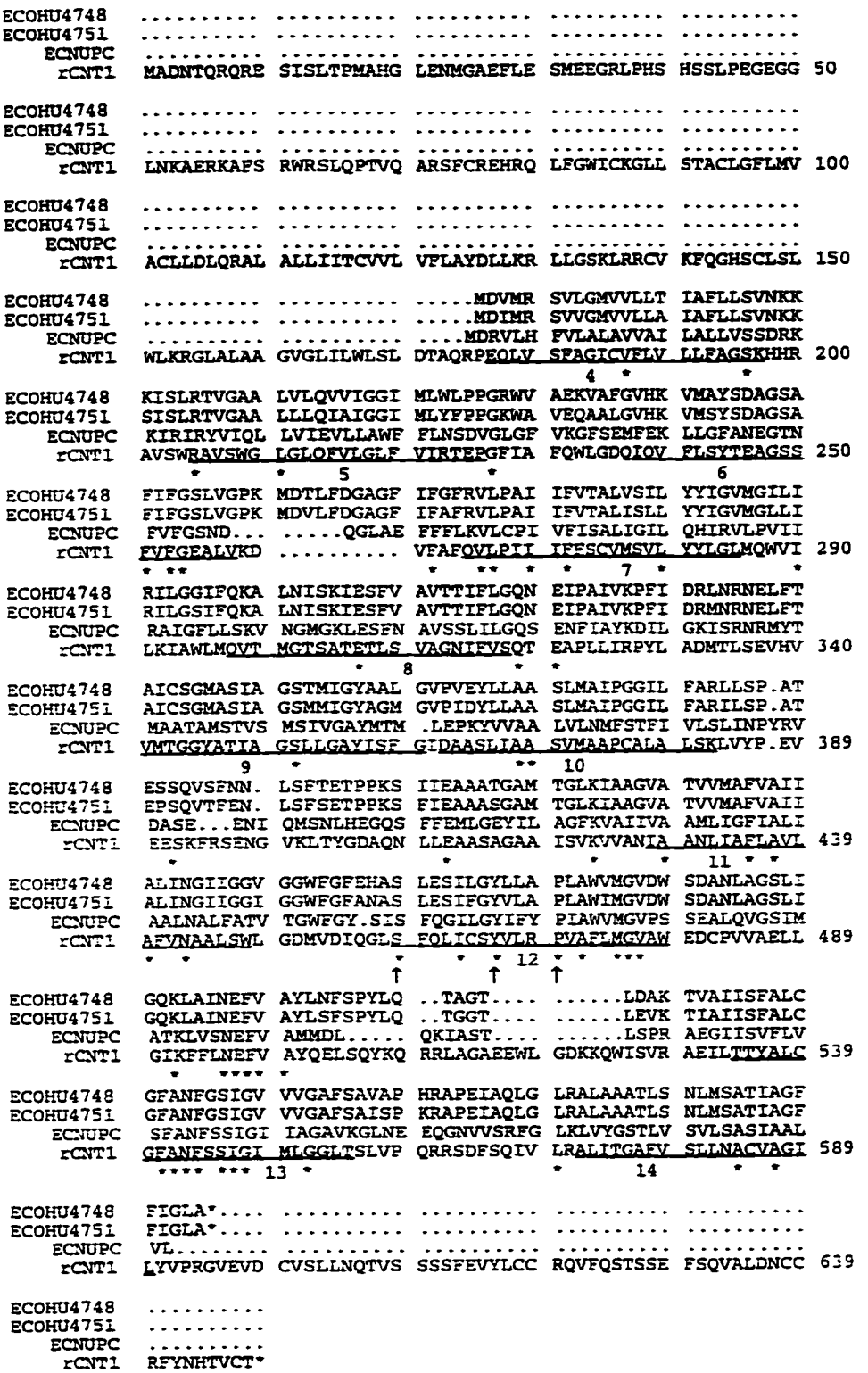

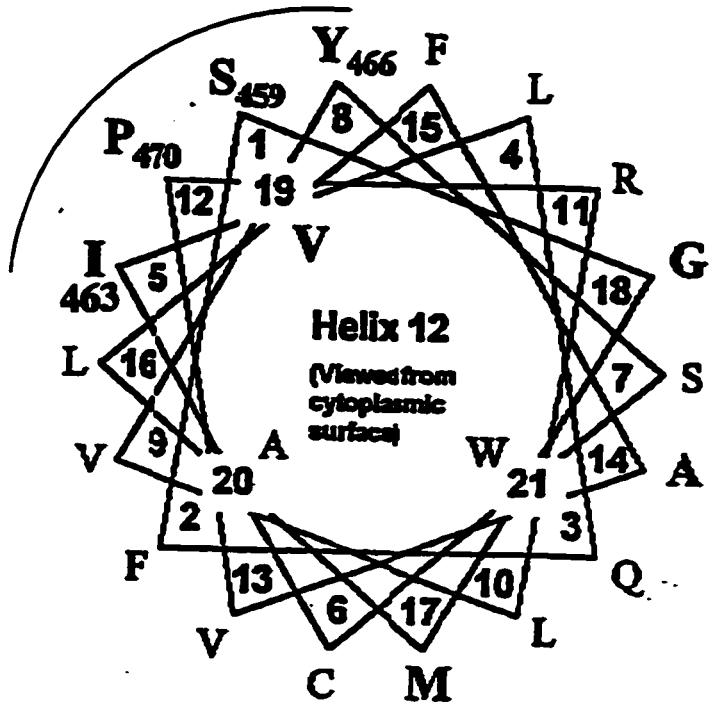

SFQLICSYVLRPVAFLMGVAW
459 479

Figure 1.4 Vertical view of putative α-helix 12 of rCNT1. Conserved residues are in bold.

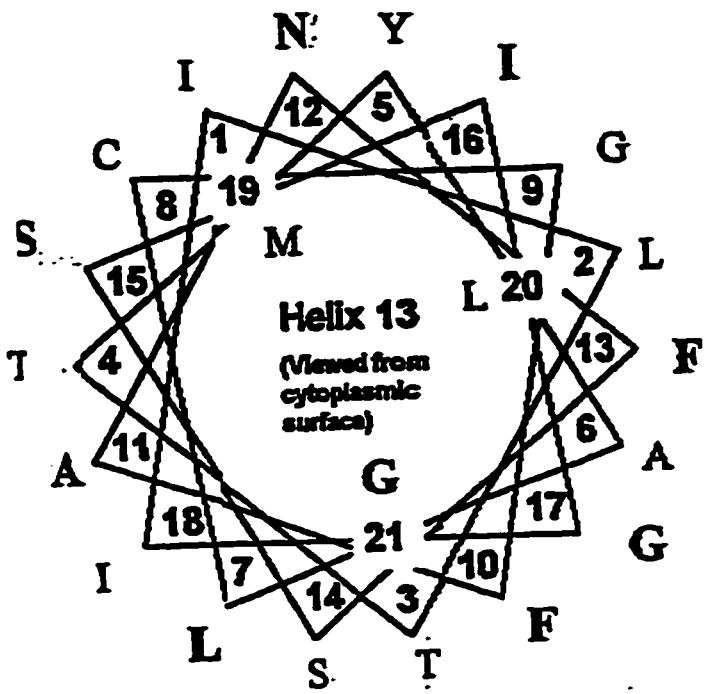

ILTTYALCGFANFSSIGIMLG

531 552

Figure 1.5 Vertical view of putative α-helix 13 of rCNT1. Conserved residues are in bold.

CHAPTER 2

Materials and Methods

2. MATERIALS AND METHODS

Molecular biology procedures described in this thesis were performed by protocols described in Molecular cloning - A laboratory manual (106).

2.1 ISOLATION OF cDNAS ENCODING HUMAN CNT1 (hCNT1)

2.1.1 PCR Probe

PCR amplification of hCNT1 partial cDNA was performed on plasmid DNA from a Clontech 5'-Stretch pYEUra3 human kidney cDNA library using primers (Q1,Q2) complementary to two conserved 3'-coding regions of rCNT1 cDNA (Figures 2.1 and 2.2). The PCR mixture (100 μl), covered with mineral oil to prevent evaporation, contained 10mM Tris(Tris-(hydroxymethyl)aminomethane)-acetate (pH 8.4 at 20°C), 50mM KCl, 1.5mM $MgCl_2$, 0.1 mg/ml gelatin, 200 μM each or dATP, dCTP, dGTP and dTTP, 5ng template DNA, 2.5 units Taq DNA polymerase and 50 pmol of each primer. Q1 and Q2 were synthesized by the DNA Sequencing Laboratory, Department of Biochemistry, University of Alberta, and corresponded to rCNT1 cDNA nucleotide positions 1565-1588 (sense, 5'-CTGTGGCCTTCTTGATGGGTGTGG -3') and nucleotide positions 1777-1801 (antisense, 5' - CCCGATGGAGCTGAAGTTGGCAAA -3'), respectively.

Amplification (30 cycles) was at 94°C for 1 min (denaturation), 50°C for 1.5 min (primer annealing) and 72°C for 1.5 min (primer extension) using a Robocycler™ 40 Temperature Cycler (Stratagene). After PCR, the reaction mixture

was combined with 0.1 volumes of DNA gel loading buffer (20% (w/v) Ficoll 400, 0.1M disodium EDTA (Ethylenediaminetetraacetic Acid) (pH 8.0), 1% (w/v) sodium dodecyl sulphate (SDS), 0.25% (w/v) Bromophenol Blue), applied to a 1.5% (w/v) agarose gel (1.5% (w/v) agarose, 0.5 μg/ml ethidium bromide, 2 mM disodium EDTA and 40 mM Tris-acetate, pH 8.5) and run in Tris-acetate-EDTA (TAE) buffer (2 mM disodium EDTA, 40 mM Tris-acetate, pH 8.5) at 5-10 V/cm until the tracking dye from the loading buffer had migrated to a distance judged sufficient for the analysis and isolation of the PCR DNA fragment (~2 cm). A 312 nm UV light box (Fisher Science) and a Polaroid camera were used to view and photograph the PCR product, which was excised from the gel and extracted into sterile water using the Geneclean II method as described in the kit's protocol for the recovery of DNA (Bio 101 Inc.).

Sequencing of the PCR-generated DNA in both directions was performed by *Taq DyeDeoxy* terminator cycle sequencing using an automated Model 373A Sequencer (Applied Biosystem, Inc.) located in the Department of Biochemistry, University of Alberta. Sequence analysis and alignments were undertaken using the program BESTFIT from the Sequence Analysis Software (GCG) package (Genetics Computer Group Inc.).

2.1.2 Labelling of the PCR Fragment

The PCR fragment was radiolabelled with ^{32}P by the random priming method ($[^{\gamma}]$QuickPrime Kit, Pharmacia Biotech.) and separated from unincorporated

nucleotides by chromatography through a Sephadex G-50 (fine) column prepared in a 1 ml syringe plugged with a glass filter. The labelled probe was eluted from the column with TE buffer (10 mM Tris-HCl, 1 mM disodium EDTA, pH 8.0) and the incorporated radioactivity quantified by liquid scintillation counting (LS 6000IC, Beckman Canada Inc.).

2.1.3 Library Screening

The Clontech 5'-Stretch pYEUra3 human kidney cDNA library, containing ~ $1.1x10^6$ independent clones in the *E.coli* strain XL1-blue, was screened by hybridization using the ^{32}P PCR probe prepared as described in Sections 2.1.1 and 2.1.2. Bacteria were plated out onto 150 mm LB/ampicillin plates (Luria-Bertani Medium containing 10 g tryptone, 5 g yeast extract, 5 g NaCl, 15 g agar and 100 μg/ml ampicillin per litre, pH 7.0) at a density of $2x10^4$ cells per plate. The plates, containing a total number of ~ $6x10^5$ colonies, were incubated overnight at 37°C. Filters wetted by placing on an LB plate were then laid onto each plate for 1 min. The orientation of the filters was marked, and the filters were carefully lifted from the plates. Filters with the bacteria side up were soaked in denaturing solution (1.5 M NaCl, 0.5 M NaOH) for 7 min, then in neutralizing solution (0.5 M Tris-HCl (pH 7.5), 1.5 M NaCl) for 3 min, and finally in fresh neutralizing solution for a further 3 min before being air dried and fixed by UV crosslinking (UV Crosslinker, Amersham Life Science).

Fixed filters were prehybridized for 1h at 42°C in a buffer solution containing

50% (w/v) formamide, 0.75M NaCl, 75mM sodium citrate (pH 7.0), 0.2% (w/v) bovine serum albumin, 0.2% (w/v) Ficoll, 0.2% (w/v) polyvinylpyrrolidone, 0.5% (w/v) SDS and 50 ug/ml denatured herring sperm DNA. The filters were then hybridized overnight at the same temperature and in the same buffer supplemented 10% (w/v) dextran sulfate and $1x10^6$ cpm/ml of the PCR probe.

After hybridization, filters were washed twice in the wash solution containing 15 mM NaCl, 1.5 mM sodium citrate and 0.1% (w/v) SDS for 10-30 min at room temperature and twice in the same wash solution at 65°C to remove non-specific binding. Then, the blots were autoradiographed by exposure to X-AR film (Kodak) in X-ray cassettes with intensifying screens and autoradiographed. Positive colonies were plated out at low concentration and subjected to secondary and tertiary rounds of screening until single positive clones had been isolated.

The insert sizes of positive clones were determined by diagnostic PCR and by direct sizing of crude, phenol-extracted plasmid DNA run on an agarose gel. When PCR was employed, a portion of bacteria from a positive colony were picked and suspended in TE buffer (pH 8.0). Amplification was accomplished using flanking primers on the pYEUra3 vector: URA 3 (5'-GCTAAGATCTAAACTCACAAATTAGAGC-3') and Gal 10 (5'-GCTACYGCAGTTCACACACTGTGGTAG-3'). The procedure for PCR was the same as that described in Section 2.1.1. To make crude plasmid DNA, cloned bacteria were picked after amplification on a plate and were suspended in water (20μl) and extracted with phenol (20μl) at 20°C. The PCR mixtures or plasmid DNA

preparations were run on a 1% (w/v) agarose gel, and their sizes compared with linear or supercoil marker (Gibco/BRL), respectively.

Selected individual colonies were streaked onto 150mm LB plates and incubated at 37°C overnight. Cells were harvested by centrifugation at 1500*g* for 7 min at 4°C. Plasmid DNA from the pellets was isolated and purified using the Qiagen Mini-Script method (QIAGEN Inc.). The resulting plasmid DNA was suspended in sterile water and its concentration estimated using a Sequoia/Turner Model 450 fluorimeter (excitation at 525nm, emission at 600nm).

Cloned pYEUra3 cDNAs and restriction endonuclease fragments subcloned into the pBluescript II KS+/- vector were sequenced bidirectionally by *Taq DyeDeoxy* terminator cycle sequencing (Section 2.1.1) using a combination of vector (T_7 and T_3) and internal primers. Procedures for restriction enzyme digestion and subcloning are detailed in Sections 2.2.3, 2.2.4 and 2.2.5. Sequence analysis and alignments were performed using the GCG BESTFIT program.

2.2 SITE-DIRECTED MUTAGENESIS OF RAT CNT1 (rCNT1)

2.2.1 Construction of Mutants

Mutations were introducted into transmembrane domain 12 of rCNT1 by sequential PCR as outlined in Figure 2.3. During the first PCR amplification, two separate reactions were performed, each containing one flanking primer and one inside primer. The flanking primers (FP1,FP2) corresponded to internal regions of

the rCNT1 coding sequence on either side of the sites to be mutated and enclosed two unique rCNT1 restriction sites (*BspEI*, *BamHI*) for insertion of the final mutated PCR cassette into the wild-type rCNT1 cDNA. The inside primers (IP1,IP2) contained the mutation(s) to be introduced into the rCNT1 sequence. PCR products from the first PCR amplification were used as templates for a second PCR reaction employing only the two flanking primers (FP1,FP2). The final PCR product was subjected to restriction enzyme digestion, ligated into the corresponding restriction sites of rCNT1.

The three amino acid residues in wild-type rCNT1 identified in Chapter 1, Sections 1.3.3 and 1.6 (S459, Y466, P470) were mutated to alanine, phenylalanine and alanine, respectively, using mixed, degenerate IP1 and IP2 oligonucleotide primers designed to generate seven different combinations of the three residue mutations (*ie* three single, three double and one triplet substitution). As described in Chapter 3, Section 3.2.1.5, this strategy resulted in isolation of all of the mutant combinations, with the exception of S459A/P470A and the rare triplet substitution S459A/Y466F/P470A. These were obtained by a separate series of sequential PCR reactions using P470A and Y466F/P470A rCNT1 constructs as templates and new nondegenerate inside primers, IP3 and IP4, to introduce the S459A substitution.

To minimise the possible introduction of PCR sequence errors, the flanking primers FP1 and FP2 were selected to be as close as possible to the site(s) of mutation. The nucleotide sequences of cassette regions of each of the rCNT1 constructs described in this thesis was confirmed by *Taq DyeDeoxy* terminator DNA

sequencing (Chapter 2, Section 2.1.1).

2.2.1.1 First PCR Amplification

PCR amplification of wild-type or P470A and Y466F/P470A rCNT1 mutant plasmids DNAs (in the vector pGEM-3Z) (Promega) was performed using one inside primer and one flanking primer. Each PCR reaction (100 μl) contained 10 mM Tris-HCl (pH 8.4 at 20°C), 1.5 mM $MgCl_2$, 50 mM KCl, 100 μg/ml gelatin, 50 pmol of each primer, 200 μM 4dNTP, 10 ng template DNA and 2.5 units *Taq* polymerase in a 0.5 ml tube covered with mineral oil. Primers were synthesized by the DNA sequencing Laboratory, Department of Biochemistry, University of Alberta.

The two flanking primers (FP1, FP2) corresponded to rCNT1 nucleotide positions 1304-1323 (sense, 5'-AGCTGGTCTACCCAGAGGTG-3') and nucleotide positions 1941-1960 (antisense, 5'-ACACGCAGTCCACCTCGACC-3'), respectively. The two degenerate inside primers (IP1,IP2) corresponded to rCNT1 nucleotide positions 1531-1570 (sense, 5'-(A/**G**)(G/**C**)CTTCCAGCTCATCTGCTCCT(A/**T**)CGTCCTGCGG(C/**G**)CTGTGG-3') and 1526-1564 (antisense, 5'-(G/**C**)CCGCAGGACG(T/**A**)AGGAGCAGATGAGCTGGAAG(C/**G**)(T/**C**)GAGTC-3'), respectively (mutated nucleotides in **bold** letters). The two other inside primers (IP3,IP4), designed without mixed nucleotides to introduce only the S459A mutation, corresponded to rCNT1 nucleotide positions 1521-1544 (sense, 5'-CCAGGGACTC**GC**CTTCCAGCTCAT-3') and 1519-1542 (antisense, 5'-

GAGCTGGAAGGCGAGTCCCTGGAT-3'), respectively (mutated nucleotides in **bold** letters).

The primers used in each reaction comprised one flanking primer and one inside primer of the opposite cDNA strand, two reactions being performed with each template. Amplification (25 cycles) was at 94°C for 1 min, 53°C for 1.5 min and 72°C for 1.5 min.

2.2.1.2 Purification of First Round PCR Products

First round PCR reaction mixtures were loaded on a 0.7% (w/v) agarose gel containing 0.5 μg/ml of ethidium bromide and 0.7% agarose in TAE buffer and run in TAE buffer at 5-10V/cm. The separated PCR products were excised from the gel and extracted into sterile water using the Geneclean II method (Chapter 2, Section 2.1.1).

2.2.1.3 Second PCR Amplification

Each PCR reaction (100 μl) contained 10 mM Tris-HCl (pH 8.4 at 20°C), 1.5 mM $MgCl_2$, 50 mM KCl, 100 μg/ml gelatin, 50 pmol of each primer, 200 μM 4dNTP, 10 ng template DNA and 2.5 units *Taq* polymerase in 0.5 ml tubes covered with mineral oil. The primers used were FP1 and FP2, and the template DNA for each reaction comprised an equal mixture of the two PCR products derived from each of original template cDNAs used in the first round PCR amplification. Amplification (25 cycles) was at 94°C for 1 min, 58°C for 1.5 min and 72°C for 1.5

min.

2.2.1.4 Purification of Second Round PCR Products

The sizes of second round PCR products were verified by agarose gel electrophoresis (Chapter 2, Section 2.1.1), after which the PCR mixtures were subjected to DNA extraction with phenol:chloroform. Phenol (Gibco/BRL) was first equilibrated to pH 8.0 by mixing with an equal volume of 0.5 M Tris-HCl (pH 8.0). The Tris/phenol mixture was stirred well, separated at room temperature and the upper aqueous phase discarded. This process was repeated until the pH of the phenol had reached 8.0 when tested with pH paper. Equal volumes of this buffered phenol and PCR reacion mixture were vortexed together, then centrifuged at 10,000*g* until the organic and aqueous phases had separated. The upper, aqueous phase was transferred to a fresh polypropylene tube. An equal volume of buffer-saturated phenol mixed with chloroform and isoamyl alcohol at a ratio of 25:24:1 (v/v/v) was added to the aqueous phase and the above steps were repeated. The DNA was extracted for a third time with an equal volume of chloroform/isoamyl alcohol alone at a ratio of 24:1 (v/v). Finally, the DNA was precipitated by addition of 0.1 volumes of 3M sodium acetate (pH 5.2) and 2 volumes of cold ethanol (-20°C). The contents were mixed and kept at -20°C for several hours, after which the DNA was recovered by centrifugation at 12,000g for 30 min at 4°C. The pellet was washed with 1 ml of 70% (v/v) ethanol, recovered by centrifugation and dried in either air or by use of a Savant (SVC 200) SpeedVac (Savant Instrument, Inc.). The purified

DNA was dissolved in water at a concentration of 0.5 μg/μl for restriction enzyme digestion.

2.2.1.5 Restriction Endonuclease Digestion

cDNA products from the second PCR amplification were digested (at the flanking sites) with the restriction enzymes *Bsp*EI and *Bam*HI for subcloning into wild-type rCNT1 in the vector pGEM-3Z, which was cut with the same enzymes. Incubations were performed at 37°C for 6h in reaction mixtures containing 0.1 volumes of React Buffer (buffer III, New England Biolabs), 10 units of each restriction enzyme and 2 μg of cDNA, after which the digestion products were run on 1% (v/v) normal agarose or low-melting-point agarose gels (Gibco/BRL) in TAE buffer containing ethidium bromide (0.5 μg/ml). For normal agarose gels, cDNA fragments of the correct size were excised under UV light and subjected to Geneclean II purification for later ligation (Chapter 2, Section 2.2.1.6). In the case of low-melting-point agarose gels, gel slices were used directly for ligation.

2.2.1.6 Ligation

Ligation reactions between PCR amplification products and rCNT1 plasmid cDNA contained 100 ng digested plasmid, 50 ng PCR cDNA, 0.2 volumes of 5X concentrated ligase buffer (Gibco/BRL), 1 μl of T4 DNA ligase (Gibco/BRL) and sterile water in a total volume of 10μl. Incubations were for 24 h at 15°C. Low-melting-point agarose gel slices were heated to 70°C for 10 min, then cooled to 37°C

before addition to reaction mixtures.

2.2.1.7 Calcium Chloride Transformation

XL1-Blue *E. coli* were streaked on a 150 mm LB plate and incubated overnight at 37°C. A well-isolated colony from the plate was inoculated into 500 ml LB medium in a sterile 2-liter flask and incubated at 37°C with shaking to an OD_{600} of 0.3-0.6. The culture was aliquoted into 50 ml prechilled, sterile polypropylene tubes and left on ice for 10 min, after which the cells were centrifuged for 7 min at 1600g and 4°C. Each pellet was resuspended in 10 ml of ice-cold $CaCl_2$ solution (100 mM $CaCl_2$, 70 mM $MgCl_2$ and 40 mM sodium acetate, pH 5.5), collected by centrifugation at 1100g for 5 min at 4°C, then resuspended in a further 10 ml ice-cold $CaCl_2$ solution and kept on ice for 30 min. The last step was repeated, except that cells were resuspended in 2 ml $CaCl_2$ solution containing 15% (v/v) glycerol. The cells were dispensed (0.5-1 ml) into sterile polypropylene tubes, prechilled in dry ice and frozen at -70°C.

Competent cells (200 μl), prepared as described above, were thawed and transformed by addition of 5 μl of ligation mixture (Chapter 2, Section 2.2.1.6). The suspensions were mixed by swirling gently, placed on ice for 10 min, heated to 42°C for 2 min, then returned to ice for 2 min before addition of 1 ml LB medium. The mixture was placed on a Gyrotory shaker (Model G2, New Brunswick Scientific) for 1 h at 37°C, then plated on 150 mm LB plates containing ampicillin (100 μg/ml) and incubated overnight at 37°C. The sizes of plasmid inserts of randomly selected

transformant colonies were checked by diagnostic PCR (Chapter 2, Section 2.1.3) using the pGEM-3Z flanking primers T7 (5'-TAATACGACTCACTATAG-3') and SP6 (5'-ATTTAGGTGACACTATAG-3') and by running crude plasmid DNA preparations on an agarose gel (Chapter 2, Section 2.1.3). Clones of the same size as wild-type prCNT1 were selected for plasmid preparation (Chapter 2, Section 2.1.3) and DNA sequencing (Chapter 2, Section 2.1.1). Plasmid cDNA inserts with the correct mutations were transcribed into RNA for expression in *Xenopus* oocytes (Chapter 2, Section 2.2.2).

2.2.2 *In Vitro* Transcription

Native and mutant rCNT1 cDNAs were transcribed *in vitro* with T7 RNA polymerase in the presence of the ^{m7}GpppG cap using the MEGAscript (Ambion) transcription system.

To ensure synthesis of run-off transcripts of defined length, cDNAs in the vector pGEM-3Z with T7 (5'), SP6(3') orientation were first digested with the restriction enzyme *Xba*I, resulting in cleavage of plasmids at the 3'-ends of cDNA inserts distal to the T7 promoter. After digestion, the DNA templates were purified by phenol/chloroform extraction and ethanol precipitation (Chapter 2, Sections 2.2.1.4) and dissolved in water.

Each 20 μl of transcription reaction contained 2 μl 10x transcription buffer (Ambion), 2 μl each of ATP, CTP and UTP (75 mM), 0.5 μl GTP (75 mM), 3 μl

^{m7}GpppG (40 mM), 2 μl bacteriophage T7 polymerase containing placental ribonuclease inhibitor (Ambion) and 1 μg linearised plasmid cDNA in RNase-free water. The contents were mixed gently and incubated at 37°C for 6 h. After the reaction, 1 μl RNase-free DNase I (2 U/μl, Ambion) was added, and the incubation continued at 37°C for a further 15 min to remove the template DNA.

The RNA transcript was recovered by adding 30 μl RNase-free water and 25 μl lithium chloride precipitation solution (7.5 M lithium chloride, 50 mM disodium EDTA). After mixing thoroughly, the contents were chilled to -20°C for 30 min. Then the RNA was collected by centrifugation at 12,000*g* for 20 min. The supernatant solution was carefully removed and the pellet resuspended in 200 μl RNase-free water. The RNA was subjected to phenol/chloroform/isoamyl alcohol (25:24:1, v/v/v) extraction and ethanol precipitation as described in Section 2.2.2 of this Chapter for DNA extraction and precipitation. The RNA pellet was then resuspended in RNase-free water, quantified using a Sequoia/Turner Model 450 fluorimeter, and diluted to a concentration of 1 μg/μl. Approximately 0.5 μg of each of the RNA transcripts were run on an agarose gel to check for integrity and size (Chapter 2, Section 2.2.3). The remainder of each preparation was stored in aliquots (10 μl) at -70°C.

2.2.3 Gel Electrophoresis of RNA

To confirm the quality of the RNA that was produced, RNA transcripts

obtained by *in vitro* transcription of rCNT1 cDNAs (Section 2.2.7) were run on a 1% (w/v) agarose-formaldehyde gel (1% (w/v) agarose in MOPS (3-[N-morpholino]propanesulfonic acid) electrophoresis buffer (20 mM MOPS, 5 mM sodium acetate, 1 mM EDTA, pH 7.0) and 2.2 M formaldehyde). RNA samples were mixed with 5 volumes of RNA loading buffer (20 mM MOPS, 2.2 M formaldehyde, 50% (v/v) formamide, 7% (v/v) glycerol and 0.5% (w/v) bromophenol blue diluted to 1.5 ml in RNAase-free water). One microliter of 1 mg/ml ethidium bromide was added to the sample mixtures, which were then incubated for 10 min at 65 °C. Electrophoresis was performed in MOPS electrophoresis buffer at 5 V/cm, after which the gel was viewed and photographed as described for DNA gels (Chapter 2, Section 2.1.3). The size of the RNA was judged by comparison with RNA molecular weight standards (Novagen) run on the same gel.

2.2.4 Oocyte Preparation

Mature oocyte-positive female *Xenopus laevis* (Nasco) were anesthetised by ice immersion and sacrificed by a standard pithing procedure. Ovarian lobes were removed, opened and washed into modified Barth's medium (MBM: 88 mM NaCl, 1 mM KCl, 0.33 mM $Ca(NO_3)_2$, 0.41 mM $CaCl_2$, 0.82 mM $MgSO_4$, 2.4 mM $NaHCO_3$, 2.5 mM Na-pyruvate, 0.1 mg/ml penicillin, 0.1 mg/ml gentamicin, 10 mM HEPES, pH 7.5). Small clumps of ovarian tissue were dissected and incubated

in 2 mg/ml collagenase (Type 1, 326 U/mg, Worthington Biochemical Corporation) in MBM for 2 h at room temperature on a Gyrotory Shaker (Model G2, New Brunswick Scientific) to separate oocytes from connective tissue. Individual oocytes were washed five times in MBM containing 0.1% (w/v) bovine serum albumin, five times in MBM alone, sorted, and allowed to recover overnight in MBM before incubation in hypertonic phosphate buffer (100 mM K_2HPO_4, pH 6.5, 0.1% (w/v) bovine serum albumin) for 1h at room temperature to remove remaining follicular layers. Mature healthy stage VI oocytes were again washed into MBM, sorted, and maintained at 18°C for 24h in MBM before injection either with RNA transcript dissolved in RNAase-free water or with water alone.

2.2.5 Injection of Oocytes

Defolliculated oocytes were immobilised in rows along the edges of Petri dishes and injected either with 10 nl of RNA transcript (1 μg/μl) or water using microcapillary tips (diameter 10-20 μm) attached to a pneumatic microinjector (Inject + Matic System, Singer Instrument Co. Ltd.). Tips were prepared from microcapillary tubes using an Inject + Matic puller (Singer Instrument Co. Ltd.). Injected oocytes were maintained for 3 days in MBM at 18°C, with a daily change of medium, and then either assayed for uridine transport activity or processed for preparation of oocyte plasma membranes.

2.2.6 Assay of Uridine Transport Activity

After 3 days in MBM at 18°C, which previous work has shown to maximize rCNT1 expression (133), injected oocytes were assayed for uridine transport activity using a conventional radioisotope flux technique (50). The initial rate of uridine influx (10 μM, 20°C) was traced with [5, 6-^{3}H]uridine (5 μCi/ml)(Moravek Biochemicals) that was repurified by high performance liquid chromatography (HPLC) and provided by Dr. Carol E. Cass (Departments of Oncology and Biochemistry, University of Alberta). As an additional precaution against ^3H_2O contamination of the [^{3}H]uridine, aliquots of HPLC-repurified [^{3}H]uridine were lyophilized immediately before use (Savant (SVC 200) SpeedVac, Savant Instrument,Inc.). Incubations were performed on groups of 10-12 oocytes for 1 min (transport is linear during this uptake interval) in transport buffer (0.2 ml) containing 100 mM NaCl, 2 mM KCl, 1 mM $CaCl_2$, 1 mM $MgCl_2$ and 10 mM HEPES, pH 7.5 (50). At the end of the flux incubation, the extracellular label was removed by six rapid ice-cold washes in Na^+-free transport buffer (100 mM NaCl replaced by 100 mM choline chloride), discarding the supernatant between washes. All washes were completed within 1 min. Individual oocytes were dissolved in 5% (w/v) SDS for 2 h and assayed for intracellular ^{3}H by liquid scintillation counting (LS 6000 IC, Beckman Canada Inc.).

2.2.7 Statistical Analysis of Transport Data

Results of the flux studies are presented as means ± the standard error of the mean (SEM) of 4 experiments, each comprising typically 10-12 oocytes. The significance of differences was tested using Student's *t*-test.

2.2.8 Preparation of Oocyte Plasma Membranes

The procedure that was used has been described previously (113). Three days postinjection, groups of 30 oocytes were placed in petri dishes on ice with 1 ml of ice-cold homogenization buffer (83 mM NaCl, 1 mM $MgCl_2$, 10 mM HEPES-NaOH, pH 7.9) containing the protease inhibitors phenylmethanesulphonyl fluoride (0.5 mM), pepstatin A (5 μl/ml) and leupeptin (5 μl/ml). The oocytes were disrupted using a watchmaker's forceps. The resulting oocyte ghosts were stirred on ice for 10 min, after which the homogenate was centrifuged at 1000*g* for 10 min at 4°C. The supernatant containing the plasma membrane fraction was centrifuged again at 10,000*g* for 20 min at 4°C. The resulting plasma membrane pellet was resuspended in homogenization buffer containing protease inhibitors and stored at -70°C.

2.2.9 Quantification of Plasma Membrane Protein

Protein quantification of oocyte plasma membrane protein (31) was performed by the bicinchoninic acid (BCA) assay (Pierce Chemical Co.). The protein concentrations of unknown samples, diluted to 50 μl with water, were determined

from a standard curve constructed with bovine serum albumin (BSA) and water was used as a blank. Working reagent was freshly prepared by mixing 50 parts Reagent A with 1 part Reagent B. One milliliter of the working reagent was added to each sample in duplicate. Mixtures were incubated at 60°C for 30 min, then cooled to room temperature. Absorbance was measured at 562 nm (Ultrospec, LKB Biochrom Ltd.).

2.2.10 SDS Polyacrylamide Gel Electrophoresis and Western Blotting

Oocyte plasma membrane samples, adjusted to a protein concentration of 0.5 μg/μl, were mixed with gel sample buffer (2% (w/v) SDS, 10% (w/v) glycerol, 5% (v/v) β-mercaptoethanol, 0.005% (w/v) bromophenol blue, 40 mM Tris-HCl pH 6.8 at 20°C). Proteins (10 μg) were fractionated on preformed 8 x 7 x 0.075 cm 12% SDS polyacrylamide gels (BioRad) using the Mini-PROTEAN II cell (BioRad) electrophoresis system. Prestained molecular weight markers (Sigma) were run in a lane adjacent to the samples. After electrophoresis at 200 V for 1 h, separated proteins were immobilized onto polyvinylidene difluoride (PVDF) membranes (Amersham Life Science) by electrotransfer (100 V) for 1 h with the Mini Trans-Blot cell (BioRad) in transfer buffer containing 192 mM glycine, 20% (v/v) methanol and 25 mM Tris-HCl, pH 8.3 at 20°C. Membrane blots were immunoprobed by the following method. Blots were first washed with TBS (20 mM Tris-HCl, 500 mM NaCl, pH 7.5 at 20°C) for 5 min. Non-specific binding sites on

the membrane were blocked for 2 h with TTBS (TBS with 0.2% (v/v) Tween-20) containing 5% (w/v) dried milk powder, then washed twice for 15 min with the same solution. rCNT1-immunoreactivity was detected by incubation for 16 h with a rabbit affinity-purified polyclonal antipeptide antibody at concentration of 1 μg/ml in TTBS containing 1% milk powder. The antibody was directed against amino acid residues 505-524 of rCNT1 and was a gift from Dr. Steve A. Baldwin, Department of Biochemistry, University of Leeds. The membranes were washed three times for 15 min each in TTBS and then incubated for 1 h with horseradish peroxidase (HRP)-conjugated anti-rabbit secondary antibody (Amersham Life Science) diluted 1:5000 in the same solution as used for the primary antibody. After washing as described above, blots were detected by an enhanced chemiluminesence (ECL) method (Amersham Life Science) and exposed to Hyperfilm-ECL (Amersham Life Science). All procedures were performed at room temperature.

Figure 2.1 Alignment of ECOHU4748, ECOHU4751, NupC and rCNT1 nucleotide sequences between bases 1368 and 1967 by using the GCG program PILEUP. The locations of primers Q1 and Q2 are arrowed. Fully conserved nucleotides are indicated by asterisks.


1401 1450
ECOHU4748 AACACCGCCA AAAAGCATTA TTGAAGCCGC TGCGACAGGG GCAATGACCG
ECOHU4751 AACGCCGCCA AAAAGCTTTA TCGAAGCGGC GGCGAGCGGT GCGATGACCG
ECNUPC GCACGAAGGT CAGAGCTTCT TCGAAATGCT GGGTGAATAC ATTCTGGCAG
rCNT1 TGGAGACGCT CAGAACCTCT TGGAAGCAGC CAGTGCTGGG GCTGCCATCT 1417
1451 1500
ECOHU4748 GGCTGAAAAT CGCCGCAGGT GTGGCAACAG TGGTGATGGC ATTTGTTGCA
ECOHU4751 GGCTAAAAAT CGCCGCTGGT GTGGCGACGG TGGTAATGGC GTTTGTCGCA
ECNUPC GTTTCAAAGT TGCCATTATC GTTGCCGCGA TGCTGATTGG CTTTATCGCC
rCNT1 CAGTGAAGGT CGTTGCCAAC ATTGCTGCCA ATCTGATTGC CTTCCTGGCT
1501 1550
ECOHU4748 ATAATTGCGT TGATTAACGG TATTATCGGC GGCGTTGGTG GCTGGTTTGG
ECOHU4751 ATTATTGCGC TGATCAACGG CATTATCGGC GGAATTGGCG GCTGGTTTGG
ECNUPC CTGATCGCCG CGCTGAACGC ACTGTTTGCC ACCGTTACTG GCTGGTTTGG
rCNT1 GTACTAGCCT TCGTCAATGC TGCCCTCTCC TGGCTAGGGG ACATGGTGGA
1551 1600
ECOHU4748 TTTTGAACAT GCCTCGCTGG AGTCCATTTT AGGTTACCTG CTGGCTCCAC
ECOHU4751 TTTCGCCAAT GCCTCTCTGG AAAGTATTTT TGGCTATGTG CTGGCACCGC
ECNUPC CT...ACAGC ATCTCCTTCC AGGGCATCCT GGGCTACATC TTCTATCCGA
rCNT1 CATCCAGGGA CTCAGCTTCC AGCTCATCTG CTCCTACGTC CTGCGGCCTG
1601 1650
ECOHU4748 TGGCGTGGGT GATGGGTGTG GACTGGAGTG ATGCGAATCT TGCCGGGAGT
ECOHU4751 TGGCGTGGAT CATGGGTGTG GACTGGAGTG ATGCCAATCT TGCGGGTAGC
ECNUPC TTGCATGGGT GATGGGTGTT CCTTCCAGTG AAGCACTGCA AGTGGGCAGT
rCNT1 TGGCCTTCTT GATGGGTGTG GCCTGGGAGG ACTGTCCGGT AGTGGCTGAG
1651 1700
ECOHU4748 TTGATTGGAC AGAAACTGGC AATAAATGAA TTTGTCGCTT ATCTCAATTT
ECOHU4751 CTGATTGGGC AGAAACTGGC GATTAACGAA TTCGTCGCTT ACCTGAGTTT
ECNUPC ATCATGGCGA CCAAACTGGT TTCCAACGAG TTCGTTGCGA TGATGGA..T
rCNT1 TTGCTGGGCA TCAAGTTCTT TCTGAATGAG TTTGTGGCCT ATCAAGAGCT
1701 1750
ECOHU4748 CTCACCCTAT CTGCAA..AC GGCTGGCA.. ....
ECOHU4751 CTCCCCATAC CTGCAA..AC GGGCGGCA.. ....
ECNUPC CTGCAGAAAA TTGCTTCCAC G......... ....
rCNT1 TTCCCAGTAC AAGCAACGAC GCCTGGCAGG GGCTGAGGAG TGGCTTGGTG
1751 1800
ECOHU4748 ....CTCTCGAT GCTAAAACTG TGGCGATTAT TTCCTTCGCG
ECOHU4751 ....CGCTGGAA GTGAAAACCA TTGCGATTAT CTCCTTTGCG
ECNUPC ....CTCTCT CCGCGTGCTG AAGGCATCAT CTCTGTGTTC
rCNT1 ACAAGAAACA GTGGATCTCT GTCAGAGCAG AAATCCTGAC TACATACGCC
1801 1850
ECOHU4748 TTGTGCGGTT TCGCTAACTT TGGTTCTATC GGGGTGGTGG TGGGGGCGTT
ECOHU4751 CTTTGTGGTT TTGCTAACTT TGGTTCTATC GGTGTTGTCG TTGGCGCATT
ECNUPC CTGGTTTCCT TCGCTAACTT CTCTTCAATC GGGATTATCG CAGGTGCAGT
rCNT1 CTCTGTGGAT TTGCCAACTT CAGCTCCATC GGCATCATGT TGGGAGGCCT
1851 1900
ECOHU4748 TTCTGCGGTT GCGCCACACC GTGCGCCGGA AATCGCCCAG CTTGGTTTAC
ECOHU4751 TTCGGCTATT TCGCCAAAAC GCGCGCCGGA AATCGCCCAG CTTGGTTTAC
ECNUPC TAAAGGCCTG AATGAAGAGC AAGGTAACGT GGTTTCTCGC TTCGGTCTGA
rCNT1 GACCTCCCTA GTCCCCCAGC GGAGGAGCGA CTTCTCCCAG ATTGTACTCC
1901 1950
ECOHU4748 GGGCGCTGGC GGCGGCGACG CTTTCCAACT TGATGAGTGC GACCATTGCC
ECOHU4751 GGGCGCTGGC AGCAGCAACG CTTTCCAACC TGATGAGTGC GACTATTGCC
ECNUPC AGCTGGTTTA CGGCTCTACC CTGGTGAGTG TGCTGTCTGC GTCAATCGCA
rCNT1 GGGCACTGAT CACAGGGGCT TTCGTGTCCC TGCTAAACGC CTGTGTGGCA
1951 2000
ECOHU4748 GGGTTCTTTA TTGGTTTAGC TTGA...... ....
ECOHU4751 GGGTTCTTTA TTGGTCTGGC GTAA...... ....
ECNUPC GCACTGGTGC TGTAAGACCA TACATAAAAA AGCCGGGGAT AATTCCCATA
rCNT1 GGGATCCTCT ATGTACCCAG GGGGGTCGAG GTGGACTGCG TGTCCCTTCT 1967

Figure 2.2 Alignment of deduced ECOHU4748, ECOHU4751, NupC and rCNT1 amino acid sequences by using the GCG program PILEUP. The locations of primers Q1 and Q2 are indicated by arrows and fully conserved amino acid residues are indicated by asterisks. Presumed transmembrane helices of rCNT1 are underlined.

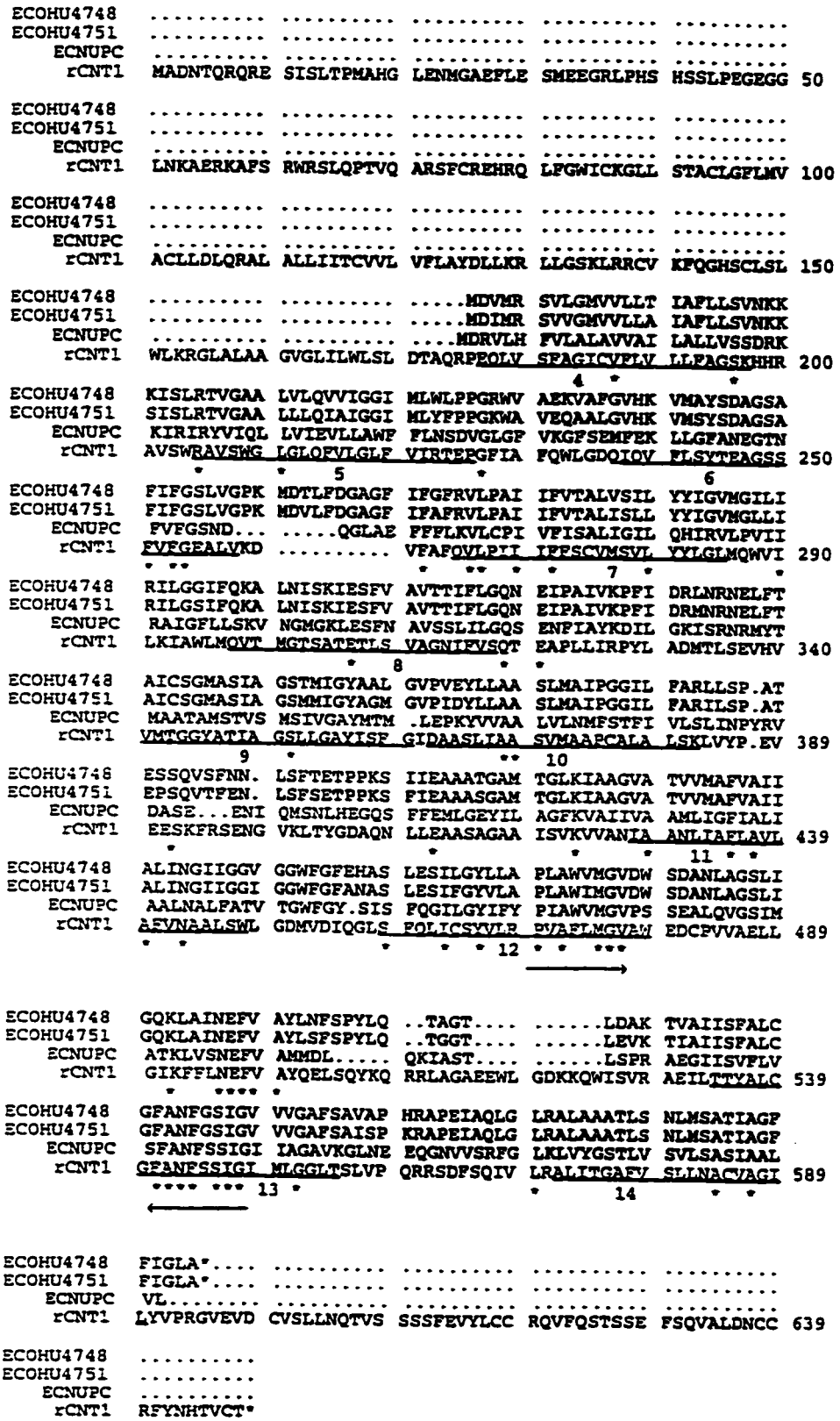

Figure 2.3. Mutation of wild-type rCNT1 by sequential PCR. FP are two primers flanking the region of the rCNT1 insert to be mutated. IP are two inside primers containing the mutation to be introduced. In the first PCR amplification, two separate reactions were performed with the two pairs of flanking and inside primers. In the second PCR amplification, the amplified fragments from the first PCR were mixed and amplified using flanking primers only. The final products were digested and subcloned into the corresponding restriction sites of the rCNT1 plasmid. ^: mutation. ↓: restriction site.

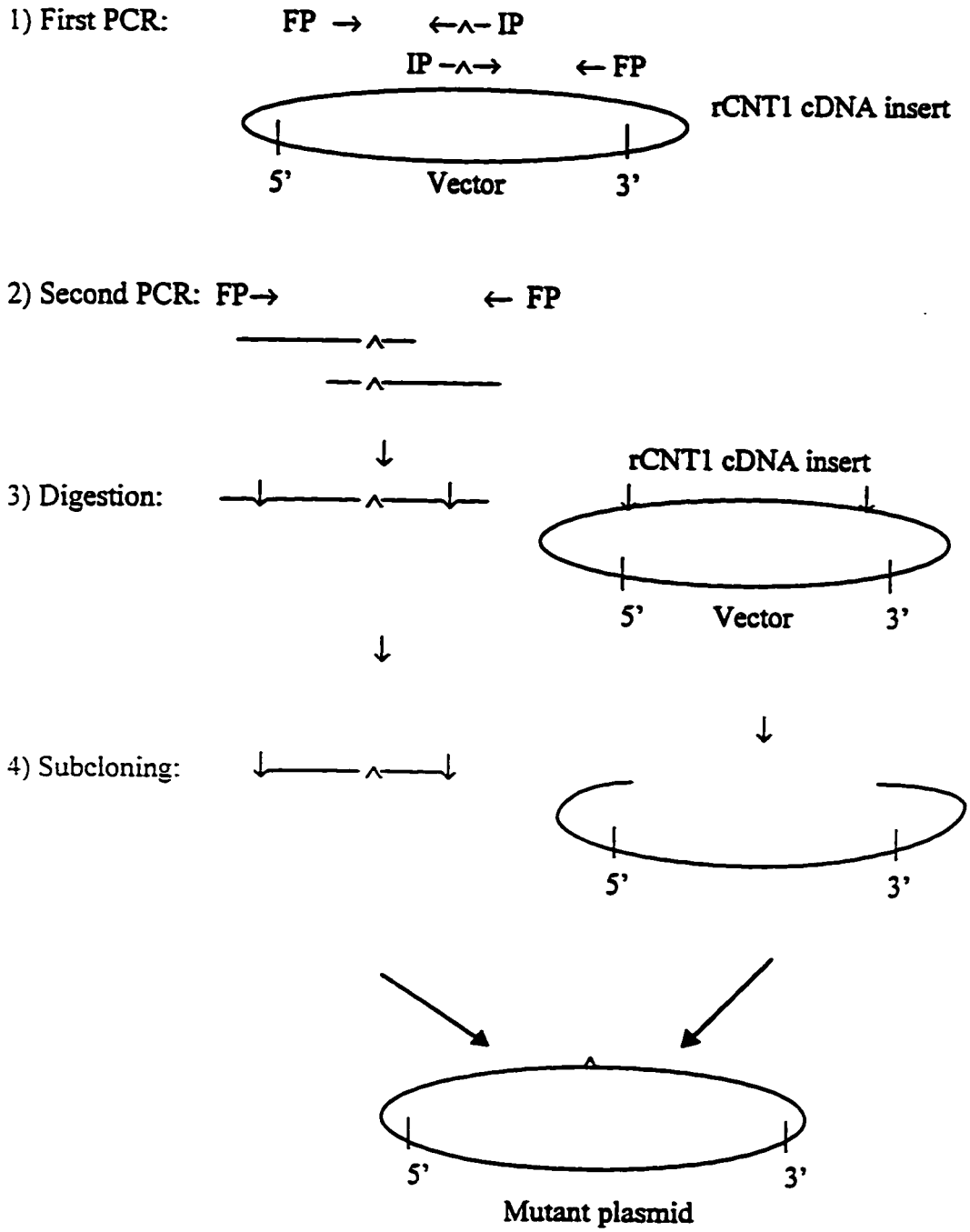
1) First PCR:
FP →
←^– IP
IP –^→
← FP
rCNT1 cDNA insert
5'
Vector
3'
2) Second PCR: FP→
← FP
3) Digestion:
rCNT1 cDNA insert
5'
Vector
3'
4) Subcloning:
5'
3'
5'
3'
Mutant plasmid

CHAPTER 3

Results

3. RESULTS

3.1 ISOLATION OF cDNAS ENCODING HUMAN CNT1 (hCNT1)

As described in the Introduction to this thesis (Chapter 1, Section 1.3), rCNT1 (50) and rCNT2 (23,135), which are expressed in jejunum/kidney and jejunum/liver, respectively, are the first recognised mammalian representatives of a new transporter gene family that also includes *E. coli* and other bacterial *nupC* proton/nucleoside symporters (23,25). rCNT1 and rCNT2 are selective for pyrimidine and purine nucleosides, respectively, and correspond functionally to the two major Na^+-dependent nucleoside transport processes that have been observed in mammalian cells of rodent, rabbit and bovine origin (21). In addition to transporting physiological pyrimidine nucleosides, recombinant rCNT1 has also been shown to transport the pyrimidine nucleoside analogs AZT and ddC, two important antiviral drugs used in the treatment of AIDS (50,134). The research described in Sections 3.1.1 and 3.1.2 below had the objective of isolating cDNA(s) encoding the human homolog of rCNT1.

3.1.1 Cloning strategy

Hybridization of rat jejunal mRNA at high stringency with a radiolabelled probe of rCNT1 corresponding to amino acid residues 75-213 has been shown to

identify a single transcript at 3.4 kb (50). When a rat multiple tissue Northern blot[1] (heart, brain, spleen, lung, liver, muscle (skeletal), kidney, testis) was screened with the same probe under identical conditions, only kidney gave a positive hybridization signal (50). I selected kidney in preference to intestine as a potential tissue source of hCNT1 cDNAs because of the ready availability of commercial human kidney cDNA libraries. The human kidney Clontech 5'-Stretch pYEUra3 cDNA library that was used in my experiments contained $1.1x10^6$ primary recombinants, with an average insert size of 1.6 kb (range 0.5 to 3.5 kb).

Two strategies to isolate hCNT1 cDNAs from this library were attempted. The first was low stringency screening using an rCNT1 hybridization probe corresponding to a C-terminal domain between amino acid residues 385 and 588 that is conserved between rCNT1 and its *E.coli* homologs (Figure 2.2). The second approach involved initial PCR amplification of pYEUra3 library plasmid cDNA using C-terminal primers corresponding to localised regions of high homology within transmembrane domains 12 and 13 (amino acid residues 470 to 477 and 541 to 548, respectively: Figure 2.2) to generate a partial hCNT1 cDNA, followed by high stringency screening of the library with this hCNT1-specific PCR probe. The first strategy, although more direct, was unsuccessful: cross-species hybridization with the non-identical probe under low stringency conditions produced high background

[1] Part of this Chapter is in press. Rizel, M.W.L., Yao, S.Y.M., Huang, M.Y., Elliott, J.F., Cass, C.E. and Young, J.D. (1996). Molecular cloning, functional expression and chromosomal localization of cDNAs encoding a human Na^+/nucleoside cotransporter (hCNT1). Am. J. Physiol,

autoradiograms and a high incidence of false positive clones. The second approach overcame these limitations by generating a hybridization probe with a high degree of identity to the targeted sequence. Subsequent screening of the library under hybridization conditions of high stringency gave low background autoradiograms with few false positive clones. This greatly facilitated the identification hCNT1-positive clones, which were present in the library in relatively low abundance.

3.1.2 PCR probe

Amplification of hCNT1 partial cDNA from the Clontech 5'-Stretch pYEUra3 human kidney cDNA library, performed as described in Chapter 2, Section 2.1.1, generated a single PCR product that was separated by agarose gel electrophoresis as shown in Figure 3.1. The PCR cDNA was extracted from the gel and sequenced. The 235 bp fragment, which was of the predicted size, was 86% identical in nucleotide sequence to the corresponding region of rCNT1 cDNA (Figure 3.2). The corresponding predicted amino acid sequences were 89% identitical and 98% similar (Figure 3.3).

The high homology between the two sequences suggested that the PCR reaction had successfully amplified a cDNA fragment of a human rCNT1 homolog. The specificity of the PCR reaction was confirmed in control experiments in which the PCR reaction was repeated either in the absence of one of the two primers or in the absence of pYEUra3 template. No PCR products were obtained under these conditions (data not shown).

3.1.3 Library Screening

The above PCR cDNA product was labeled with ^{32}P, and used as a hybridization probe to screen the Clontech 5'-Stretch YEUra3 human kidney cDNA library as described in Chapter 2, Sections 2.1.2 and 2.1.3. Two positive clones were identified (Figures 3.4 and 3.5). One, Clone A, had an 857 bp insert (Figure 3.6). Sequence comparison showed that 557 bp (183 amino acid residues) at the 3' end of the insert were homologous to rCNT1. This region of the insert begins 350 bp upstream of the sense primer for the PCR probe (Q1) and ends 45 bp upstream of the antisense primer sequence (Q2). Most of the homologous region is therefore upstream of the PCR product and corresponds to rCNT1 nucleotide and amino acid positions 1216-1732 (87% identical) and 342-525 (91% identical, 96% similar), respectively (Figure 3.7 and 3.8). The region of Clone A between primers Q1 and Q2 was identical in nucleotide sequence (except for one position) to the PCR product (Figure 3.9). The remaining 292 bp of insert in Clone A was unrelated either to rCNT1 or to other known sequences in the databases and most probably represents an artifact of library construction (please see Chapter 4, Section 4.1.2).

The other positive clone, Clone B, contained 1066 bp of insert and exhibited the nucleotide sequence shown in Figure 3.10. Again, only part of the sequence (450 bp, 150 amino acids) at the 3' end was homologous to rCNT1. The homologous region extended beyond both ends of the PCR fragment, beginning 66 bp upstream of the sense primer (Q1) and 172 bp downstream of the antisense primer (Q2), and corresponded to rCNT1 nucleotide and amino acid positions 1499-1949 (86%

identical) and 450-597 (88% identical, 97% similar), respectively (Figures 3.11 and 3.12). The nucleotide sequence of Clone B between Q1 and Q2 was identical (except for one position) to that of the PCR product (Figure 3.13). As was the case for Clone A, the remaining 615 bp of insert sequence was unrelated either to rCNT1 or to other published sequences and may be an artifact of library construction.

The nucleotide sequences of shared regions of Clone A and Clone B are compared in Figure 3.14. The nucleotide sequences common to the two cDNAs were identical except for two positions. The relatioship between Clone A, Clone B and the PCR product is shown schematically in Figure 3.15.

In summary, Clones A and B both contain sequence 99% identical to the PCR probe. They are therefore authentic positive cDNAs. Both are highly homologous to rCNT1 and their overlap regions of sequence were essentially identical. Therefore, it can be concluded that they encode portions of the same human kidney rCNT1 homolog.

A full length version of hCNT1 cDNA was subsequently isolated from a second human kidney cDNA library (Clontech 5'-Stretch Plus pCDNAI human kidney cDNA library) by Ms. Mabel W.L. Rizel in Dr. Young's laboratory (102). The nucleotide sequence of the full length hCNT1 cDNA, which was obtained by hybridization screening using the PCR probe generated in this study, is compared with those of the PCR product and Clones A and B in Figures (3.16, 3.17 and 3.18). The nucleotide and deduced amino acid sequences of the PCR product and Clones A and B corresponded to hCNT1 nucleotide positions at 1620-1807, 1207-1763 and

1530-1980, respectively and amino acid positions 484-545, 344-527 and 454-603, respectively. The nucleotide sequences of the PCR fragment and Clone A are 100% identical to the corresponding region of full length hCNT1 (Figures 3.16 and 3.17), while that of Clone B is identical to that of hCNT1 except in three positions (Figure 3.18). The relationship between the PCR product, Clone A, Clone B and the full length rCNT1 product are shown schematically in Figure 3.19.

3.2 SITE-DIRECTED MUTAGENESIS OF RAT CNT1 (rCNT1)

Recombinant jejunal/kidney CNT1 transports physiological pyrimidine nucleosides and adenosine, and also accepts as permeants the antiviral pyrimidine nucleoside analogs AZT and ddC (50,102,134). The experiments described in the first part of this Chapter (Section 3.1) led to the discovery and isolation of cDNAs encoding a protein (hCNT1) from human kidney homologous to rCNT1. hCNT1 may play a role in the intestinal absorption and renal handling of drugs used to treat HIV infection in patients suffering from AIDS (Chapter 4, Section 4.1.3). The remainder of the present Chapter describes experiments that investigated the functional roles of three evolutionarily conserved amino acid residues that are common to both rCNT1 and hCNT1.

Structurally, rCNT1 is a membrane protein of 648 amino acid residues which are predicted to form 14 potential transmembrane domains. At the time I commenced my project, four CNT1 family members were known: rCNT1, NupC, ECOH4748

and ECOH4751 (Chapter1, Section 1.3.2). Their deduced amino acid sequences are aligned and correlated with the predicted secondary structure of rCNT1 in Figure 1.3. Approximately one-third of the fully conserved amino acid residues are localized in predicted transmembrane helices 12 and 13. Analysis of vertical views of these two transmembrane segments revealed that helix 12 has a striking conserved face composed of S459, I463, Y466 and P470 (Figures 1.4 and 1.5). All four of these residues are also present in hCNT1 (Figures 3.20), suggesting that this face of helix 12 is important for the transport function of proteins belonging the CNT gene family.

To test this hypothesis, three of these conserved residues (S459 and Y466, which are conventional α-amino acids with polar side chains that can participate in hydrogen bonds, and the nonpolar imino acid P470, which may have a role in helix stability and packing and, possibly, cation binding), were mutated in rCNT1 into corresponding non-hydrogen-bonding α-amino acids of similar size. Therefore, S459, Y466 and P470 were mutated into Ala, Phe and Ala, respectively.

The effects of these mutations, both singly and in combination, on the function of the recombinant rCNT1 transporter expressed in *Xenopus* oocytes were investigated. The remainder of the present Chapter describes the construction and expression of the following rCNT1 mutants: S459A, Y466F, P470A, S459A/Y466F, S459A/P470A, Y466F/P470A and S459A/Y466F/P470A.

3.2.1 Construction of Mutants

The codons of the wild-type targeted residues of rCNT1 were changed into the least altered codons corresponding to amino acid residues to be substituted. Therefore, the codons AGC(Ser), TAC(Tyr) and CCT(Pro) were changed into GCC(Alanine), TTC(Phenylalanine) and GCT(Alanine), respectively. The mutations were introduced by a sequential PCR methodology (Chapter 2, Section 2.2.1).

3.2.1.1 First PCR Amplification

During the first PCR amplification, two separate reactions were performed. Each reaction contained one flanking primer (FP) and one inside primer (IP). The inside primers contained the mutations to be introduced and were designed to be degenerate in order to generate simultaneously the seven different mutants to be studied (Chapter 2, Section 2.2.1) (Figure 3.21). Wild-type rCNT1 cDNA was used as template. After amplification, the PCR products were run on an agarose gel. The reactions with the primers FP1/IP1 and FP2/IP2 (Chapter 2, Section 2.2.1.1) generated products (~ 260 bp and ~ 430 bp, respectively) of the expected size (Figure 3.22). These products were extracted from the gel, mixed, and subjected to a second PCR amplification.

3.2.1.2 Second PCR Amplification

The second PCR amplification, performed with the two flanking primers FP1 and FP2 and the mixed first-round PCR products as template, produced, as expected, a ~ 656 bp fragment (Figure 3.23), which was extracted from the gel for restriction

enzyme digestion and subsequent insertion into rCNT1 plasmid DNA.

3.2.1.3 Digestion of PCR product and rCNT1 cDNA with BspEI and BamHI

The second-round PCR product was ligated into wild-type rCNT1 cDNA in the plasmid expression vector pGEM-3Z using the two unique restricion sites (*BspEI* and *BamHI*) closest to the segment of rCNT1 to be mutated. The strategy of subcloning the shortest possible PCR fragment into the rCNT1 plasmid was designed to (i) reduce, as far as possible, the introducion of PCR-induced mutations and (ii) minimise the amount of DNA sequencing required to select mutant clones and verify their structures.

Digestion of each end of the ~ 656 bp second-round PCR cDNA with *BspEI* and *BamHI* produced a prominant fragment of ~ 580bp (Figure 3.24). Digestion of the 5144bp rCNT1 pGEM-3Z DNA with the same two restriction enzymes also produced a fragment of ~ 580bp and a strong top band of ~ 4564bp(Figure 3.24). The latter was used in the subsequent subcloning of the restriction enzyme-digested PCR product.

3.2.1.4 Subcloning

The digested PCR product and rCNT1 pGEM-3Z DNA, ligated together to reform plasmids of ~ 5144bp, were transformed into *E. coli*. The sizes of constructs were confirmed by subjecting plasmid DNA to agarose gel electrophoresis and by PCR with T7 and SP6 vector primers. Representative PCR results for a

number of randomly selected transformants are shown in Figure 3.25.

3.2.1.5 Mutant Identification

After subcloning, isolated transformants were randomly selected and sequenced. Because the degenerate inside primers were designed to include four nucleotide substitutions (Section 3.2.1, this Chapter and Chapter 2, Section 2.2.1.1), 16 different kinds of transformants should have been produced, including the original wild-type sequence (Figure 3.26). Therefore, the theoretical frequency of each of the transformants shown in Figure 3.26 is 1/16. We would expect, however, an over-representation of the wild-type transformant because its degenerate inside primer would to anneal more easily to the template cDNA during PCR.

Thirty eight transformants (Table 3.1) were randomly selected, grown and sequenced using T7 and SP6 primers. Of these, 9 had nucleotide sequences corresponding to wild-type rCNT1 and 21 had unusable single nucleotide base changes in the S459 codon, resulting in conversion of AGC(Ser) to either ACC(Thr) or GGC(Gly). There was one each of mutants S459A, Y466F and Y466f/P470A, and two of P470A. One corresponded to mutant S459A/P470A, but contained a spurious additional PCR-induced mutation (frame shift: 1544delA, ATC→TC) and two of the clones were S459A/Y466F, one having an additional PCR mutation (S496: AGT→AGC) that did not change the encoded amino acid sequence.

Thus, the 38 clones yielded five out of the seven expected mutants. These five mutants included each of the three anticipated single mutants (S459A,

Y466F,P470A) and two of the expected double mutants (S459A/Y466F and Y466F/P470A, but not S459A/P470A). No clone corresponding to the triple mutant (S459A/Y466F/P470A) was found. To avoid sequencing a large number of additional clones, it was decided to obtain the missing two constructs (S459A/P470A and S459A/Y466F/P470) directly by means of a second round of mutagenesis experiments.

3.2.1.6 Second Mutagenesis

In the second round of mutagenesis experiments, the first PCR amplification was performed using two new nondegenerate inside primers (IP3, IP4) designed to introduce the S459A substitution (Chapter 2, Section 2.2.1.1). The flanking primers were the same as used previously. The template used to make the S459A/P470A mutant was P470A rCNT1 cDNA (Section 3.2.1.5), while that used to make the triple mutant (S459A/Y466F/P470) was Y466F/P470A rCNT1 cDNA (Section 3.2.1.5, this Chapter and Chapter 2, Section 2.2.1) (Figure 3.28).

PCR amplifications with the two sets of primers (FP1/IP3 and FP2/IP4) generated fragments of the expected sizes (~ 260bp and ~ 430 bp, respectively). These PCR products were used in a second PCR amplification with FP1 and FP2 primers and ligated into wild-type rCNT1 pGEM-3Z as described previously in Sections 3.2.1.2, 3.2.1.3 and 3.2.1.4 of this Chapter. The resulting transformants were sequenced until clones corresponding to the correct mutants (without PCR-induced errors) were obtained.

3.2.2 *In Vitro* Transcription

Plasmid DNA of the seven different mutants and wild-type rCNT1 were subjected to *in vitro* transcription to make sense RNA for expression in *Xenopus* oocytes.

Correct orientation of each insert with respect to the vector T7 RNA polymerase site was first confirmed by PCR with T7 primer and the inside primer, IP2 (Chapter 2, Section 2.2.1.1). A clear band of the expected size (~ 1.5 kb) was obtained for all of the constructs (Figure 3.28). Therefore, T7 RNA polymerase was used in the transcription reaction. Before transcription, plasmid DNA was linearized with *Xba*I, which cleaved the vector DNA at a unique site distal to the 3'-ends of the inserted cDNAs. Digestion was confirmed by running the linearized DNA on an agarose gel against both linear and supercoil DNA markers (Figure 3.29). Gel electrophoresis was used to verify the sizes (~ 2.4 kb) and integrity of each of the RNA transcripts (Figure 3.30).

3.2.3 Uridine Transport Activity of rCNT1 Mutants

Uridine influx was assayed three days after injection of *Xenopus* oocytes with 10nl of water or 10nl of water containing 10ng of wild-type or mutant rCNT1 transcript. A conventional radioisotope flux technique was used (50), in which the initial rate of [^{3}H]uridine influx (10μM, 20°C, 1min flux) was measured in transport buffer containing 100mM NaCl. The transport activities of the mutants, wild-type rCNT1 and control water-injected oocytes were compared in the same flux experiment in oocytes from the same frog under identical expermental conditions.

Four independent flux experiments were performed for each mutant. Each experiment utilized oocytes from a different frog and different preparations of DNA and RNA. In one series of 4 experiments, each of the 3 single mutations were compared with wild-type rCNT1. In a second series of 4 experiments, the 3 double mutants and the triple mutant were compared with wild-type rCNT1. Figures 3.31 and 3.32 show the mean fluxes (± SE) obtained in each of the two sets of experiments. Uridine uptake by water-injected oocytes was < 0.03 pmol/oocyte.min^{-1} in both series of experiments, and is not subtracted from the flux values given below and summarised in Table 3.2.

Influx values for S459A, Y466F and P470A were 3.45 ± 1.16, 4.49 ± 0.34 and 3.64 ± 1.11 pmol/oocyte.min^{-1}, respectively, compared with 4.35 ± 1.03 pmol/oocyte.min^{-1} for wild-type rCNT1 (Figure 3.31, Table 3.2). Expressed as a percentage of the wild-type flux, the mutant activities were 79%, 103% and 84%, respectively. Analysis of the data by Student's *t*-test determined that the decrease for S459A, but not that for P470A, was statistically significant ($P<0.05$).

Influx values for the double mutants were in the order Y466F/P470A > S459A/Y466F > S459A/P470A (Figure 3.32, Table 3.2). Expressed as a percentage of the wild-type flux (3.62 ± 0.98 pmol/oocyte.min^{-1}), the mutant activities were 49% (Y466F/P470A: 1.79 ± 0.74 pmol/oocyte.min^{-1}), 20% (S459A/Y466F: 0.73 ± 0.28 pmol/oocyte.min^{-1}) and 8% (S459A/P470A: 0.29 ± 0.13 pmol/oocyte.min^{-1}). In each case, the decrease in activity was statistically significant ($P<0.05$) relative to the wild-type flux. The fluxes for the three combination mutants were

smaller in magnitude than that observed in Figure 3.31 (Table 3.2) for the single mutant S459A (79% of control). The triple mutant S459A/Y466F/P470A had no detectable transport activity. A comparison between the double mutant S459A/Y466F and the triple mutant S459A/Y466F/P470A established that their uridine transport activities were significantly different ($P<0.05$).

3.2.4 Western Blotting

Loss of transport activity, such as that described above in Section 3.2.3 of this Chapter for rCNT1 mutants, may be secondary to decreased expression of the recombinant proteins in the plasma membrane. To test for this possibility, plasma membranes were prepared from oocytes expressing each of the different recombinant rCNT1 constructs, using experimental conditions for oocyte preparation, injection and incubation that were identical to those used in the transport studies described in the previous Section. These enriched plasma membrane fractions were then separated by SDS-polyacrylamide gel electrophoresis and subjected to Western analysis. Immunostaining was performed with a rabbit polyclonal antipeptide antibody raised against amino acid residues 505-524 of wild-type rCNT1. As shown in the representative blots presented in Figures 3.33, the antibody recognised a protein (58-84 kDA) of the predicted size in plasma membranes prepared from oocytes injected with wild-type rCNT1 RNA transcript. Immunoreactive protein migrating either as a singlet or doublet was also observed for each of the mutant samples, including that for the functionally-inactive triplet mutant S459A/Y466F/P470A. In contrast, no

immunostaining was observed in membranes prepared from control oocytes injected with water. The intensities of staining suggest that wild-type and mutant rCNT1 transporters were expressed in the oocyte plasma membrane in comparable amounts.

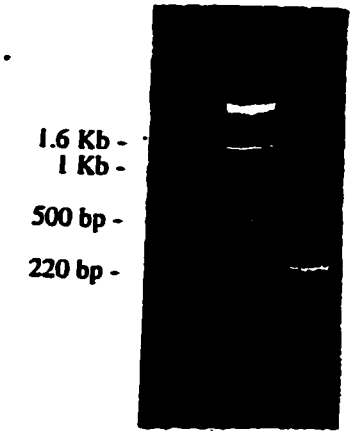

Figure 3.1. Ethidium bromide-stained 1.5% agarose gel of the PCR product generated from a human kidney cDNA library with two primers (Q1, Q2) corresponding to conserved regions of rCNT1. This PCR fragment corresponds to rCNT1 amino acid residues 469-548. The migration of the fragment (235 bp) is compared with linear DNA markers (Gibco BRL, left hand lane).

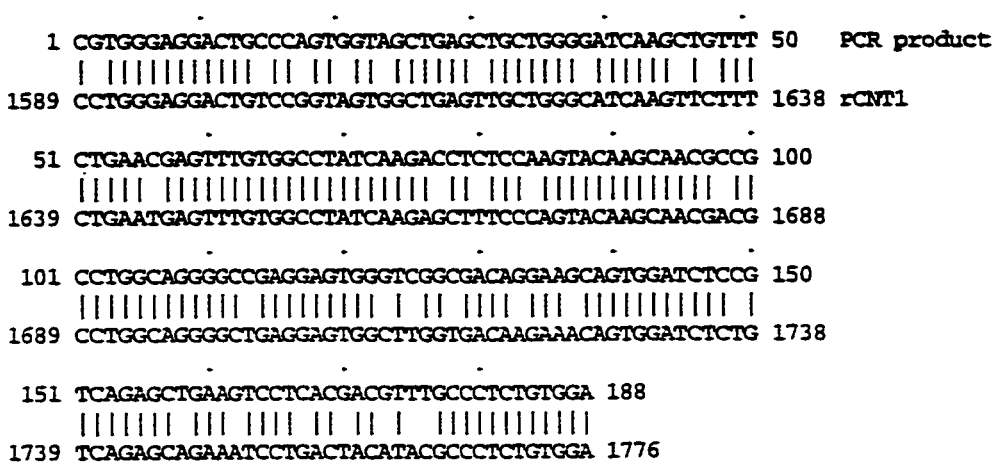

Figure 3.2. Comparison of the nucleotide sequences of the PCR fragment (top) and the corresponding region of rCNT1 (bottom). The alignment was performed using the GCG BESTFIT program. Identical nucleotides are indicated by vertical lines. The two sequences are 86% identical.

```
  1 WEDCPVVAELLGIKLFLNEFVAYQDLSKYKQRRLAGAEEWVGDRKQWISV 50  PCR product
    ||||||||||||||:|||||||||:||-|||||||||||||:||:||||||
479 WEDCPVVAELLGIKFFLNEFVAYQELSQYKQRRLAGAEEWLGDKKQWISV 528 rCNT1

 51 RAEVLTTFALCG 62
    |||:|||:||||
529 RAEILTTYALCG 540
```

Figure 3.3. Comparison of the deduced amino acid sequences of the PCR product and the corresponding region of rCNT1. The alignment was performed using the GCG BESTFIT program. Lines denote identical residues. Two dots represent highly conserved residues and a single dot shows weakly conserved residues. The two sequences are 89% identical and 98% similar.

Figure 3.4. Isolation of Clone A from a pYEUra3 human kidney cDNA library by hybridization screening with the PCR probe: (a) Clone A was identified by first round of screening; (b) the positive colony was picked, plated and rescreened: ↑, example of positive signal; ■, marker for orientation.


a)
b)

Figure 3.5. Isolation of Clone B from a pYEUra3 human kidney cDNA library by hybridization screening with the PCR probe: (a) Clone B was identified by first round of screening; (b) the positive colony was picked, plated and rescreened: ↑, example of positive signal; ■, marker for orientation.

a)

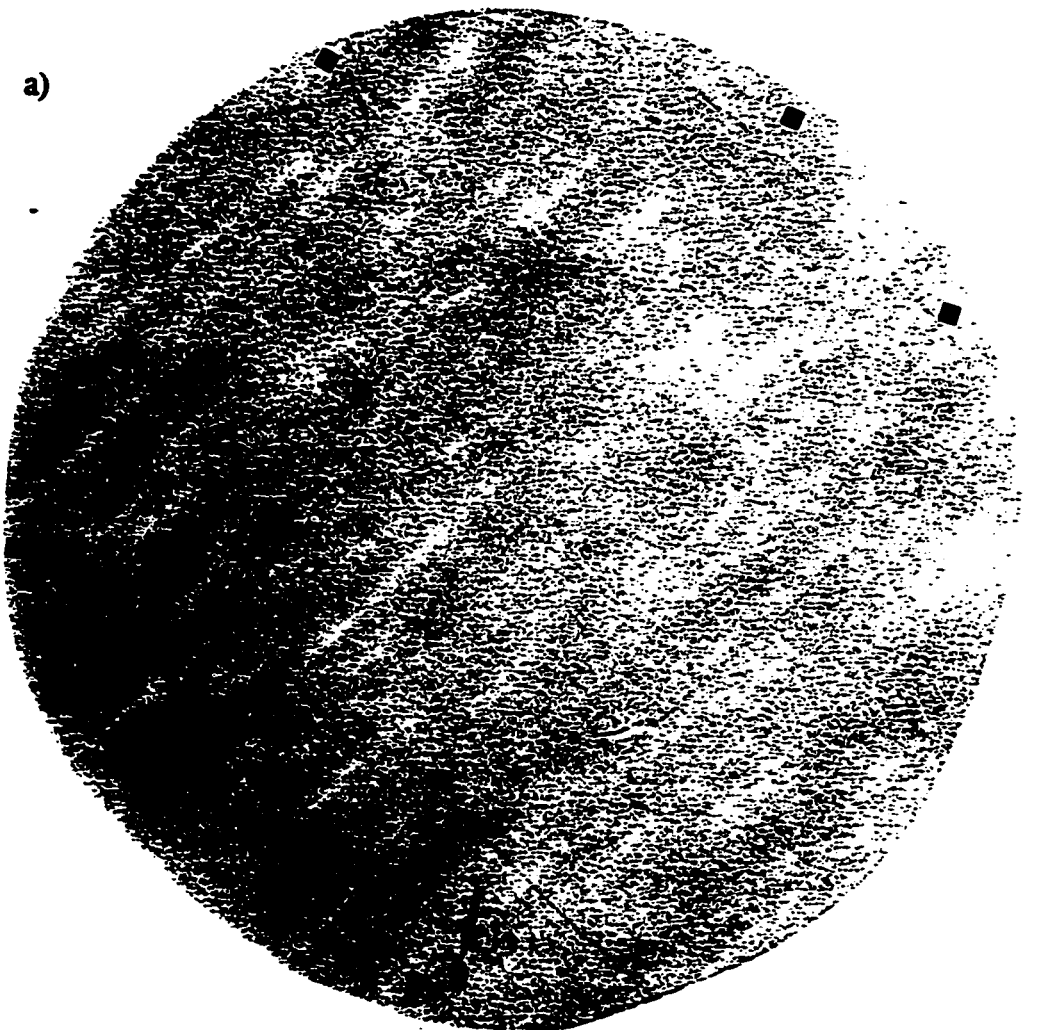

b)

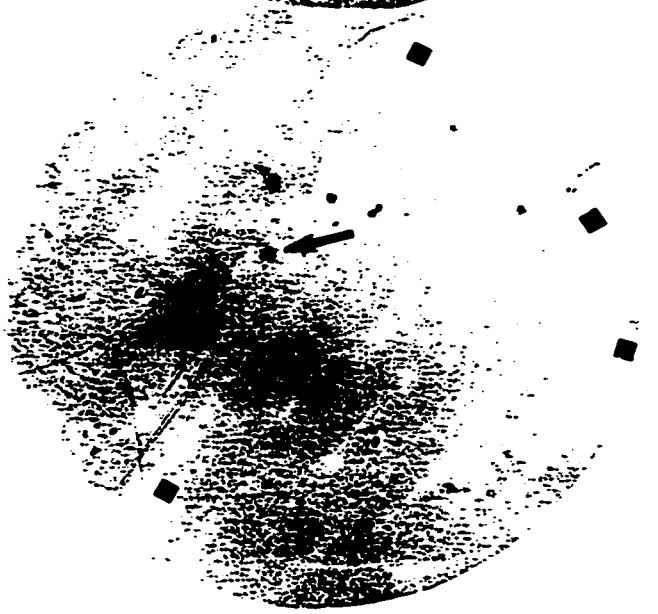

```
  1  AATTCCGGTT TTTTTTTTG GA*TGGACAA TAAGCTTTTA TTGCATTGAA
 51  AGGTCATTGC AGTGAAAGGT TGGGGATTGC TTGCTGCTAC AGCTGAATGG
101  ATTCTATTCT GAACACACAG AAAGAGATCA CAGACTCCCT ACCCTAAGAA
151  GAAGGGAGGT GGTAGATGAA ATGGACTTGA TTGAAGAGAC TAGCCTGGCC
201  CACACACAGA AGGAGGACTG GCCCTCTTCT TGGAGCCCAT GCTCTGGTAG
251  AGGGCCATAA CAAGAGAGCT GGATGGTGCC GGTGTCCAGG ATAACTTCAC
301  tgtcatgacc ggaggttacg ccaccattgc tggcagcctg ctgggtgcct
351  acatctcctt tgggatcgat gccacctcgt tgattgcagc ctctgtgatg
401  gctgcccctt gtgccttggc cctctccaaa ctggtctacc cggaggtgga
451  ggagtccaag tttaggaggg aggaaggagt gaaactgacc tatggagatg
501  ctcagaacct catagaagca gccagcactg gggccgccat ctccgtgaag
551  gtggtcgcca acatcgctgc caacctgatt gcgttcctgg ctgtgctgga
601  ctttatcaat gctgccctct cctggctggg agaaatggtg gacatccagg
651  ggctcagctt ccagctcatc tgctcctaca tcctgcggcc tgtagccttc
701  ttgatgggtg tggcgtggga ggactgccca gtggtagctg agctgctggg
751  gatcaagctg tttctgaacg agtttgtggc ctatcaagac ctctccaagt
801  acaagcaacc ccgcctggca ggggccgagg agtgggtcgg cgacaggaag
851  cagtgga
```

Figure 3.6. Nucleotide sequence of the Clone A insert. It is a 857 bp fragment, of which 557 bp (183 amino acid residues) are homologous to rCNT1 cDNA. The homologous region is indicated by lower case letters.

Figure 3.7. Comparison of the nucleotide sequences of the Clone A cDNA (top) and the corresponding region of rCNT1 (bottom). The alignment was performed using the GCG BESTFIT program. Identical nucleotides are indicated by vertical lines. The two sequences are 87% identical.

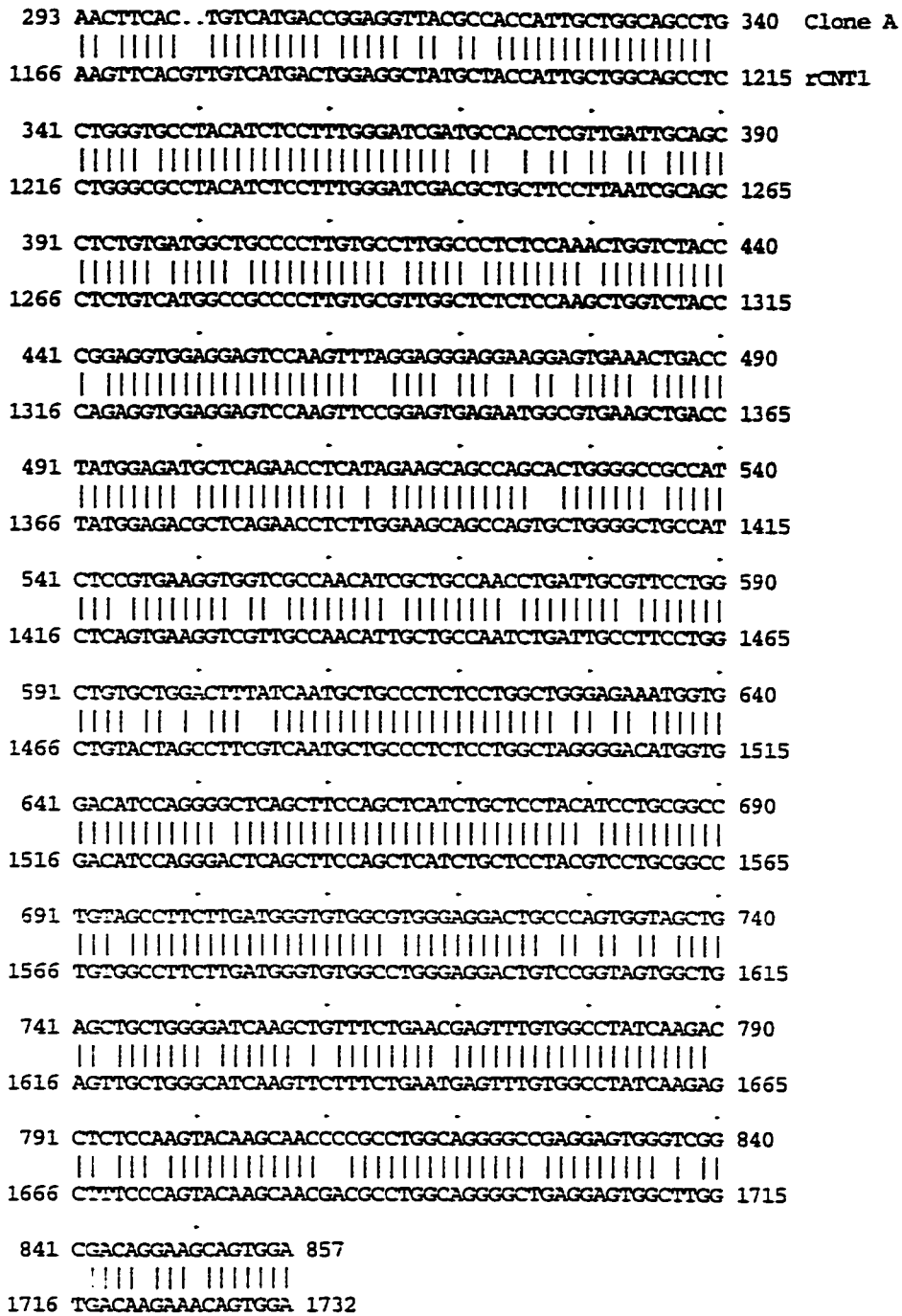
293 AACTTCAC..TGTCATGACCGGAGGTTACGCCACCATTGCTGGCAGCCTG 340 Clone A
1166 AAGTTCACGTTGTCATGACTGGAGGCTATGCTACCATTGCTGGCAGCCTC 1215 rCNT1
341 CTGGGTGCCTACATCTCCTTTGGGATCGATGCCACCTCGTTGATTGCAGC 390
1216 CTGGGCGCCTACATCTCCTTTGGGATCGACGCTGCTTCCTTAATCGCAGC 1265
391 CTCTGTGATGGCTGCCCCTTGTGCCTTGGCCCTCTCCAAACTGGTCTACC 440
1266 CTCTGTCATGGCCGCCCCTTGTGCGTTGGCTCTCTCCAAGCTGGTCTACC 1315
441 CGGAGGTGGAGGAGTCCAAGTTTAGGAGGGAGGAAGGAGTGAAACTGACC 490
1316 CAGAGGTGGAGGAGTCCAAGTTCCGGAGTGAGAATGGCGTGAAGCTGACC 1365
491 TATGGAGATGCTCAGAACCTCATAGAAGCAGCCAGCACTGGGGCCGCCAT 540
1366 TATGGAGACGCTCAGAACCTCTTGGAAGCAGCCAGTGCTGGGGCTGCCAT 1415
541 CTCCGTGAAGGTGGTCGCCAACATCGCTGCCAACCTGATTGCGTTCCTGG 590
1416 CTCAGTGAAGGTCGTTGCCAACATTGCTGCCAATCTGATTGCCTTCCTGG 1465
591 CTGTGCTGGACTTTATCAATGCTGCCCTCTCCTGGCTGGGAGAAATGGTG 640
1466 CTGTACTAGCCTTCGTCAATGCTGCCCTCTCCTGGCTAGGGGACATGGTG 1515
641 GACATCCAGGGGCTCAGCTTCCAGCTCATCTGCTCCTACATCCTGCGGCC 690
1516 GACATCCAGGGACTCAGCTTCCAGCTCATCTGCTCCTACGTCCTGCGGCC 1565
691 TGTAGCCTTCTTGATGGGTGTGGCGTGGGAGGACTGCCCAGTGGTAGCTG 740
1566 TGTGGCCTTCTTGATGGGTGTGGCCTGGGAGGACTGTCCGGTAGTGGCTG 1615
741 AGCTGCTGGGGATCAAGCTGTTTCTGAACGAGTTTGTGGCCTATCAAGAC 790
1616 AGTTGCTGGGCATCAAGTTCTTTCTGAATGAGTTTGTGGCCTATCAAGAG 1665
791 CTCTCCAAGTACAAGCAACCCCGCCTGGCAGGGGCCGAGGAGTGGGTCGG 840
1666 CTTTCCCAGTACAAGCAACGACGCCTGGCAGGGGCTGAGGAGTGGCTTGG 1715
841 CGACAGGAAGCAGTGGA 857
1716 TGACAAGAAACAGTGGA 1732

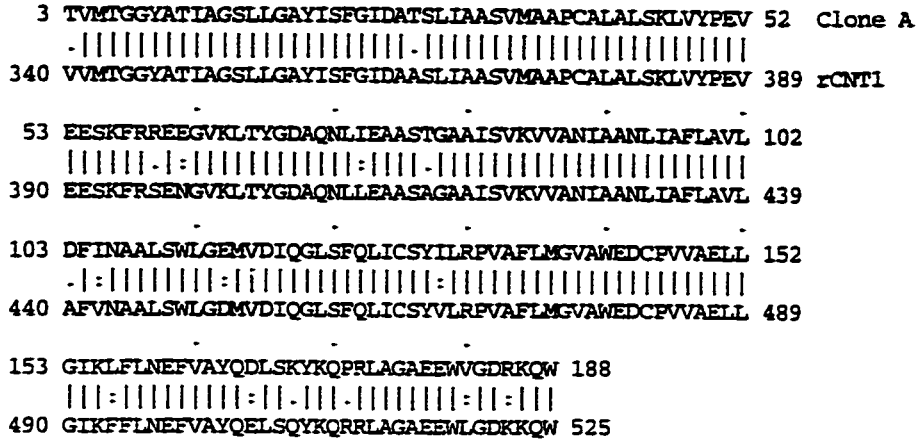

Figure 3.8. Comparison of the deduced amino acid sequences of the overlapping regions of Clone A and rCNT1. The alignment was performed using the GCG BESTFIT program. Lines denote identical residues. Two dots represent highly conserved residues and a single dot shows weakly conserved residues. The two sequences are 91% identical and 96% similar.

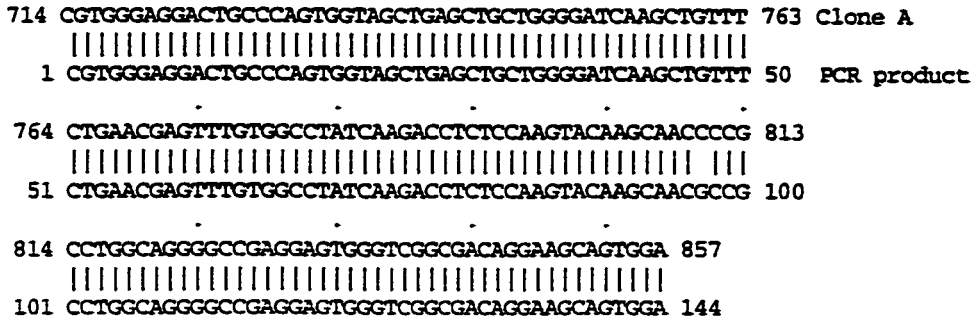

Figure 3.9. Comparison of the nucleotide sequences of Clone A between primers Q1 and Q2 (top) and the PCR product (bottom). The alignment was performed using the GCG BESTFIT program. Identical nucleotides are indicated by vertical lines. The two sequences are identical, except for one position.

Figure 3.10. Nucleotide sequence of the Clone B insert. It is a 1066 bp fragment, of which 450 bp (150 amino acid residues) are homologous to rCNT1 cDNA. The homologous region is indicated by lower case letters.

```
   1  ATTCCGGCAG ACAAAAAAGA ACCATTCCTG AGAGCATCTG GAATTAAATG
  51  AATAGCTATG GTGAAGTCTG GCTGCTGGTA CTGCGCTTTT TTTTAAACTT
 101  GCTGATTTGT GGTGCCATGA AAAATCAGCA TCATCACAAC CAGATTCAAA
 151  AAGGTATTGT TTCTATTCAT CATTGTACTG GAAAAGAAGT AGAAAATAAA
 201  AAAGGTATCG ACACCCGAAA GCAGTGTATT CTACAATTAA GTATTCTACG
 251  TAAAGTAAAA GTTCTGCACC TTTACTTATA AGGCATTAGA ATCAAGGAAA
 301  GCAAAATGTT ATCTAAAAGA AGTTGAAAGA ACACCTAACT CTATTTGATT
 351  ATTTGCTAAA TAACATTTCT TTTCCCTTAA AAAGGAATGT TAGTGAATGT
 401  ATTTCTTATT CCTCATACCT TGATAGGAAA TAAAATGTTT GAATTTTTAA
 451  AAAGTTATCA CCTGTGACCA AAACTTATTT TTTAATAAAG ATTAGAAACA
 501  AGTCGGCTTT GAGGTATTTT ATTGATTTAA AGGGAAAGCT ACAATTGCAG
 551  GCTAAACAGA AAATGAAAGC AGATACTTTA ACTGAACACC ACTCAAGATA
 601  ATATGATATA TGATGGGctg ggcgacatgg tggacatcca ggggctcagc
 651  ttccagctca tctgctccta catcctgcgg cctgtagcct tcttgatggg
 701  tgtggcgtgg gaggactgcc cagtggtagc tgagctgctg gggatcaagc
 751  tgtttctgaa cgagtttgtg gcctatcaag acctctccaa gtacaagcaa
 801  ccccgcctgg caggggccga ggagtgggtc ggcgacagga agcagtggat
 851  ctccgtcaga gctgaagtcc tcacgacgtt tgccctctgt ggatttgcca
 901  atttcagctc cattgggatc atgctgggag gcgtgacctc catggtcccc
 951  caacggaaga gcgacttctc ccagatagtg ctccgggcgc tcttcacggg
1001  agcctgtgtg tccctggtga acgcctgtat ggcagggatc ctctacatgc
1051  ccaggggggc tgaagt
```

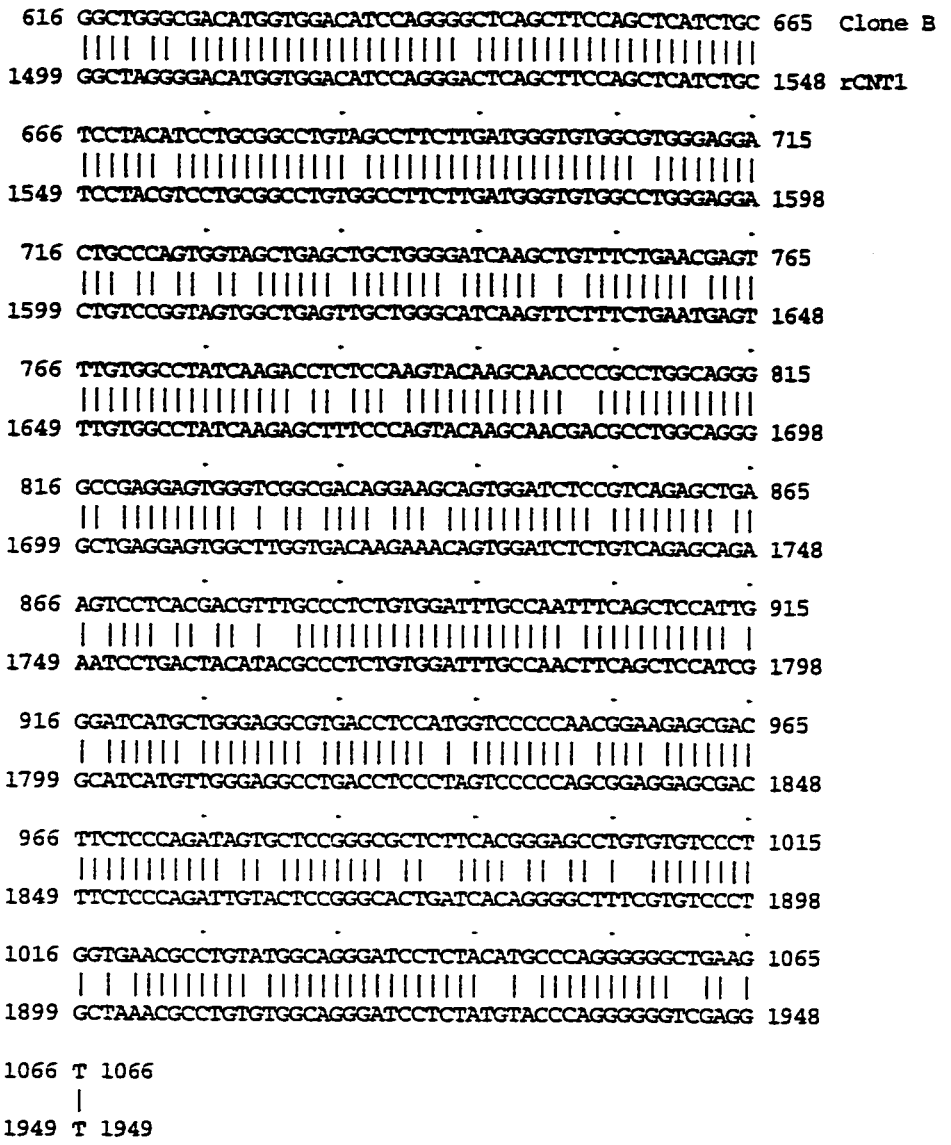

Figure 3.11. Comparison of the overlapping regions of the nucleotide sequences of the Clone B (top) and rCNT1 (bottom). The alignment was performed using the GCG BESTFIT program. Identical nucleotides are indicated by vertical lines. The two sequences are 86% identical.

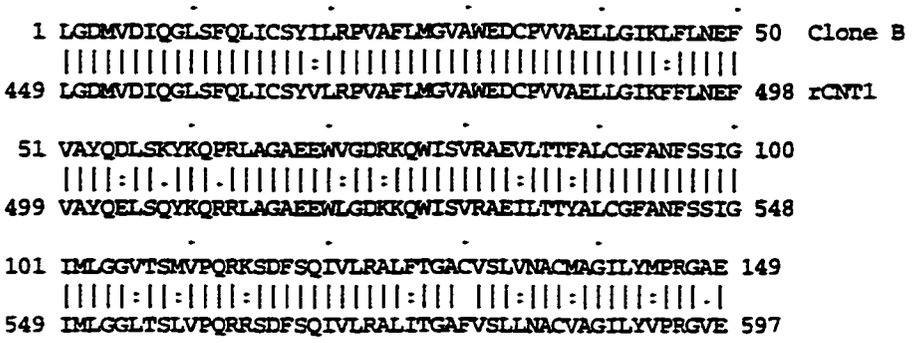

Figure 3.12. Comparison of the deduced amino acid sequences of the overlapping regions of Clone B and rCNT1. The alignment was performed using the GCG BESTFIT program. Lines denote identical residues. Two dots represent highly conserved residues and a single dot shows weakly conserved residues. The two sequences are 88% identical and 97% similarity.

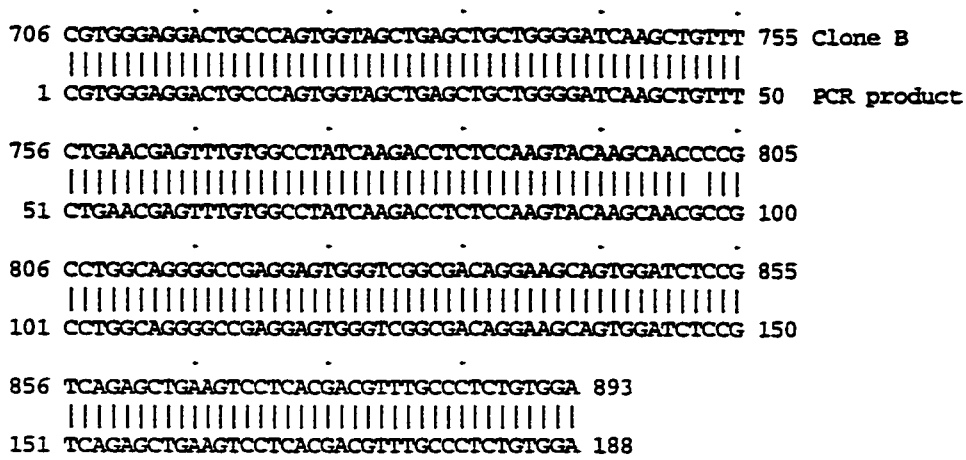

Figure 3.13. Comparison of the nucleotide sequences of Clone B between primers Q1 and Q2 (top) and the PCR product (bottom). The alignment was performed using the GCG BESTFIT program. Identical nucleotides are indicated by vertical lines. The two sequences are identical. except for one position.

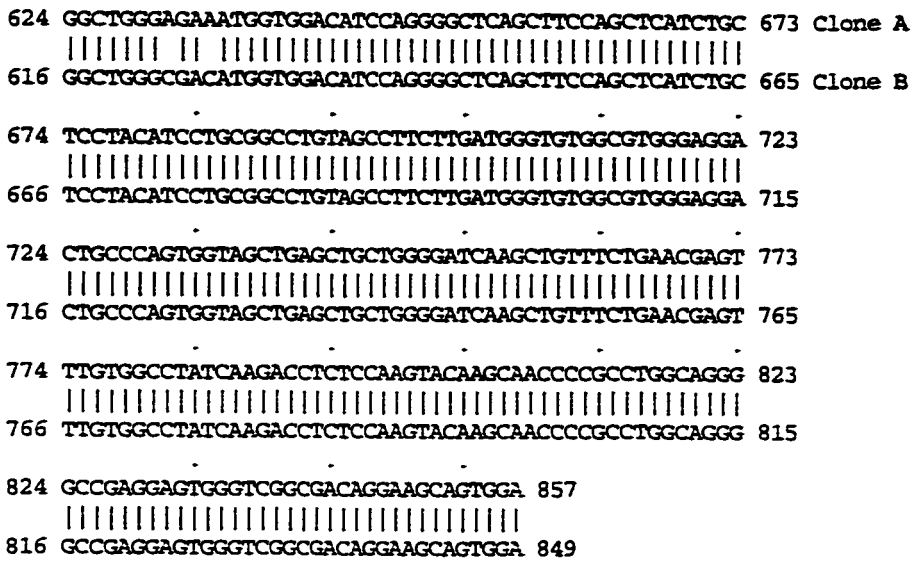

Figure 3.14. Comparison of the nucleotide sequences of overlapping regions of Clone A (top) and Clone B (bottom). The alignment was performed using the GCG BESTFIT program. Identical nucleotides are indicated by vertical lines. The two sequences are identical. except for two positions.

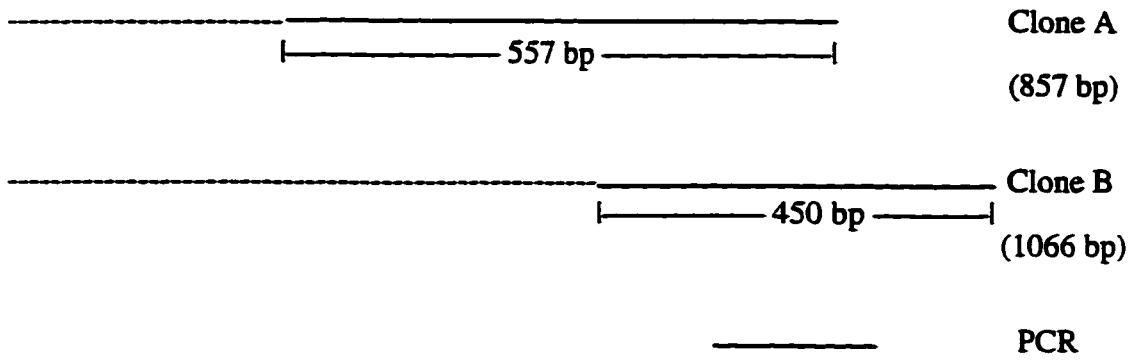

Figure 3.15. Schematic representation of the alignment of Clones A and B and the PCR product. Solid lines indicate homologous region. Broken lines indicate regions of sequence unrelated to rCNT1.

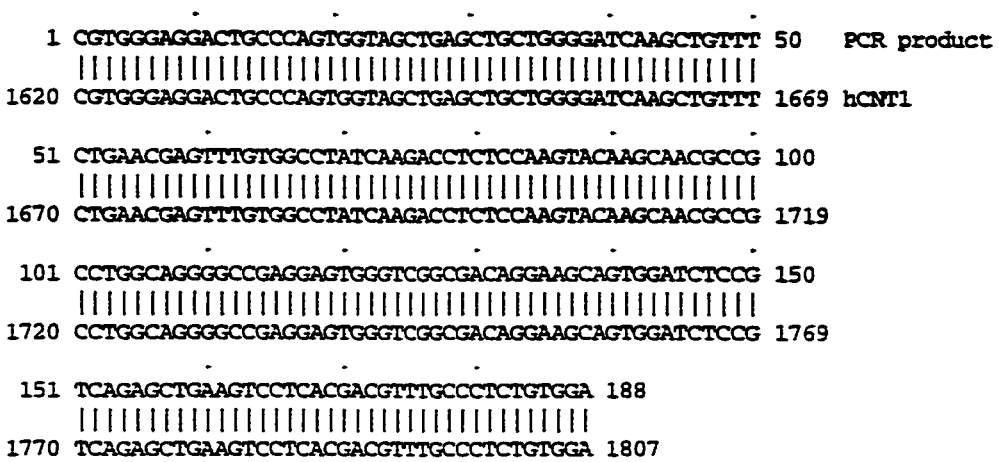

Figure 3.16. Comparison of the nucleotide sequences of the PCR fragment (top) and the corresponding region of hCNT1 (bottom). The alignment was performed using the GCG BESTFIT program. Identical nucleotides are indicated by vertical lines. The two sequences are identical.

Figure 3.17. Comparison of the nucleotide sequences of the overlap region of Clone A (top) and hCNT1 (bottom). The alignment was performed using the GCG BESTFIT program. Identical nucleotides are indicated by vertical lines. The two sequences are identical.

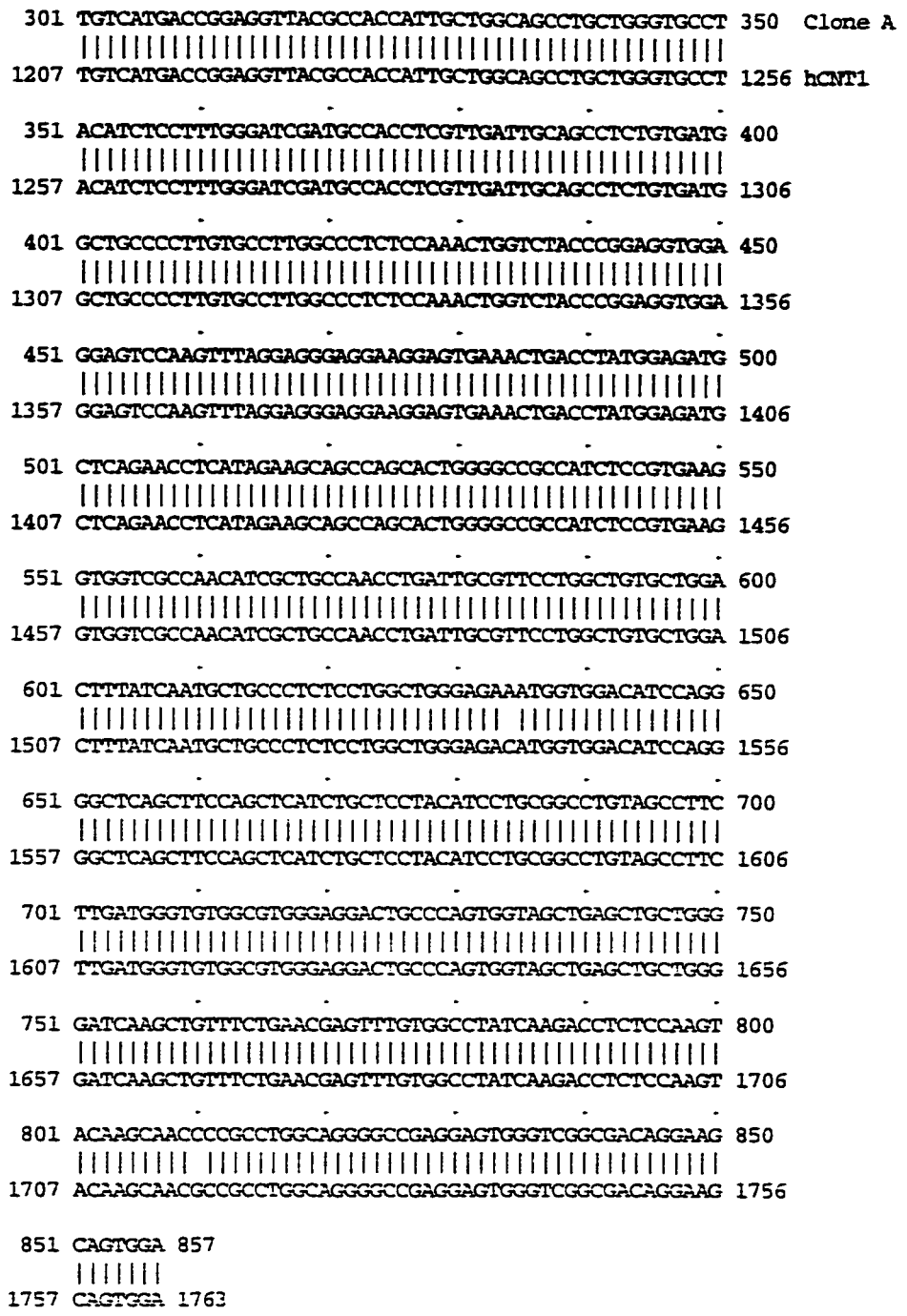
301 TGTCATGACCGGAGGTTACGCCACCATTGCTGGCAGCCTGCTGGGTGCCT 350 Clone A
1207 TGTCATGACCGGAGGTTACGCCACCATTGCTGGCAGCCTGCTGGGTGCCT 1256 hCNT1
351 ACATCTCCTTTGGGATCGATGCCACCTCGTTGATTGCAGCCTCTGTGATG 400
1257 ACATCTCCTTTGGGATCGATGCCACCTCGTTGATTGCAGCCTCTGTGATG 1306
401 GCTGCCCCTTGTGCCTTGGCCCTCTCCAAACTGGTCTACCCGGAGGTGGA 450
1307 GCTGCCCCTTGTGCCTTGGCCCTCTCCAAACTGGTCTACCCGGAGGTGGA 1356
451 GGAGTCCAAGTTTAGGAGGGAGGAAGGAGTGAAACTGACCTATGGAGATG 500
1357 GGAGTCCAAGTTTAGGAGGGAGGAAGGAGTGAAACTGACCTATGGAGATG 1406
501 CTCAGAACCTCATAGAAGCAGCCAGCACTGGGGCCGCCATCTCCGTGAAG 550
1407 CTCAGAACCTCATAGAAGCAGCCAGCACTGGGGCCGCCATCTCCGTGAAG 1456
551 GTGGTCGCCAACATCGCTGCCAACCTGATTGCGTTCCTGGCTGTGCTGGA 600
1457 GTGGTCGCCAACATCGCTGCCAACCTGATTGCGTTCCTGGCTGTGCTGGA 1506
601 CTTTATCAATGCTGCCCTCTCCTGGCTGGGAGAAATGGTGGACATCCAGG 650
1507 CTTTATCAATGCTGCCCTCTCCTGGCTGGGAGACATGGTGGACATCCAGG 1556
651 GGCTCAGCTTCCAGCTCATCTGCTCCTACATCCTGCGGCCTGTAGCCTTC 700
1557 GGCTCAGCTTCCAGCTCATCTGCTCCTACATCCTGCGGCCTGTAGCCTTC 1606
701 TTGATGGGTGTGGCGTGGGAGGACTGCCCAGTGGTAGCTGAGCTGCTGGG 750
1607 TTGATGGGTGTGGCGTGGGAGGACTGCCCAGTGGTAGCTGAGCTGCTGGG 1656
751 GATCAAGCTGTTTCTGAACGAGTTTGTGGCCTATCAAGACCTCTCCAAGT 800
1657 GATCAAGCTGTTTCTGAACGAGTTTGTGGCCTATCAAGACCTCTCCAAGT 1706
801 ACAAGCAACCCCGCCTGGCAGGGGCCGAGGAGTGGGTCGGCGACAGGAAG 850
1707 ACAAGCAACGCCGCCTGGCAGGGGCCGAGGAGTGGGTCGGCGACAGGAAG 1756
851 CAGTGGA 857
1757 CAGTGGA 1763

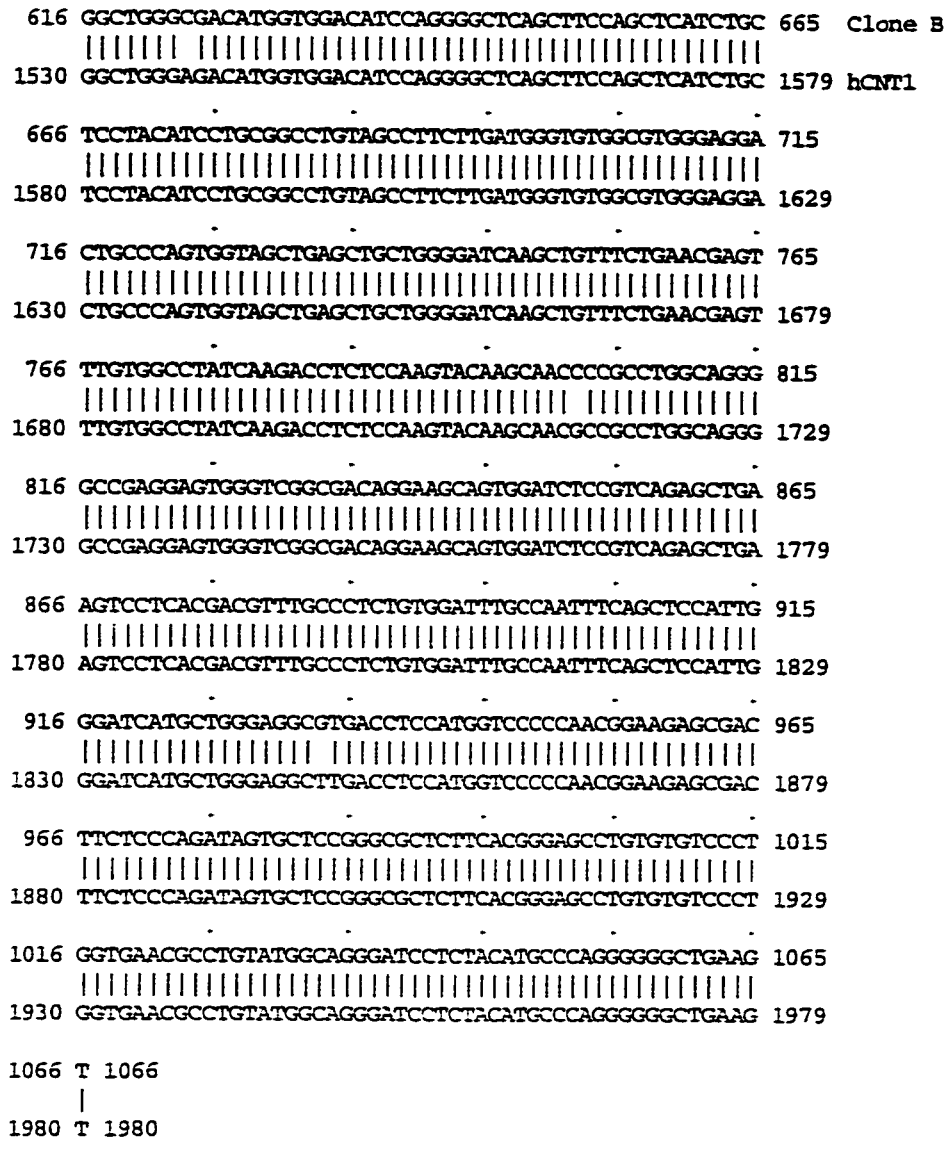

Figure 3.18. Comparison of the nucleotide sequences of the overlap region of Clone B (top) and hCNT1 (bottom). The alignment was performed using the GCG BESTFIT program. Identical nucleotides are indicated by vertical lines. The two sequences are identical, except for three positions.

Figure 3.19. Schematic representation of the alignment between the hCNT1 cDNA. the PCR product and homologous regions of Clones A and B.

Table 3.1 Sequence results of rCNT1 mutagenesis with degenerate primers IP1, IP2

Wild-type	9
S459A	1
Y466F	1
P470A	2
S459A/Y466F	2 (1 with a PCR mutation)
Y466F/P470A	1
S459A/P470A	1 (with a PCR mutation)
S459A (single base mutation)	21
Total	38

Table 3.2 Uridine influx values for wild-type and mutant rCNT1 constructs

Experimental Group	Constructs	Influx Values (pmol/oocyte.min^{-1})
Series 1	Wild-type rCNT1	4.35 ± 1.03
	S459A	3.45 ± 1.16
	Y466F	4.49 ± 0.34
	P470A	3.64 ± 1.11
	Water control	0.024 ± 0.02
Series 2	Wild-type	3.62 ± 0.98
	S459A/Y466F	0.73 ± 0.28
	S459A/P470A	0.29 ± 0.13
	Y466F/P470A	1.79 ± 0.74
	S459A/Y466F/P470A	0.02 ± 0.01
	Water control	0.02 ±0.02

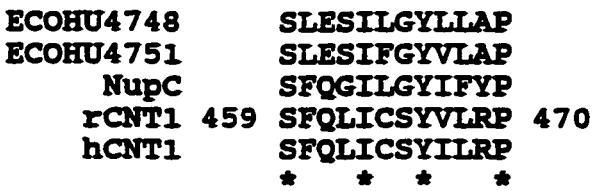

Figure 3.20. Alignment of relevant regions of the deduced amino acid sequences of ECOHU4748, ECOHU4751, NupC, rCNT1 and hCNT1. S459, I463, Y466 and P470 that form a conserved face in helix 12 are indicated by asterisks.

```
------AGC TAC  CCT-----> Wildtype
------GGC TAC  CCT----->
------ACC TAC  CCT----->
------AGC TTC  CCT-----> Y466F
------AGC TAC  GCT-----> P470A
------GCC TAC  CCT-----> S459A
------GGC TTC  CCT----->
------GGC TAC  GCT----->
------GCC TTC  CCT-----> S459A/Y466F
------GCC TAC  GCT-----> S459A/P470A
------GGC TTC  GCT----->
------GCC TTC  GCT-----> Triple mutant
------ACC TTC  CCT----->
------ACC TAC  GCT----->
------ACC TTC  GCT----->
------AGC TTC  GCT-----> Y466F/P470A
```

Figure 3.21. Oligonucleotide sequences of the sense degenerate primer IP1. Targeted nucleotides are shown in **bold and underlined**. Substitute nucleotides are shown in *italics*.

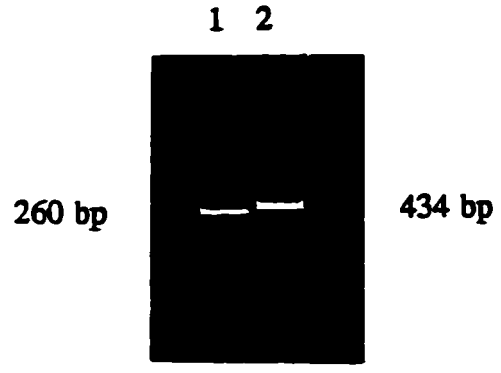

Figure 3.22. Ethidium bromide-stained 1% agarose gel of the PCR products generated from rCNT1 plasmid DNA during first PCR amplification. Lane 1: 260 bp fragment from the reaction using the flanking primer FP1 and the degenerate inside primer IP2; Lane 2: 434 bp fragment from the reaction using the flanking primer FP2 and the degenerate inside primer IP1.

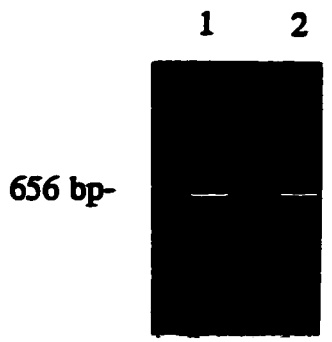

Figure 3.23 Ethidium bromide-stained 1% agarose gel of the PCR product (565 bp) generated from rCNT1 plasmid DNA during second PCR amplification with the two flanking primers FP1 and FP2. Lane 1: control reaction using the wildtype cDNA as template; Lane 2: aliquots of the reaction using the first PCR products as templates.

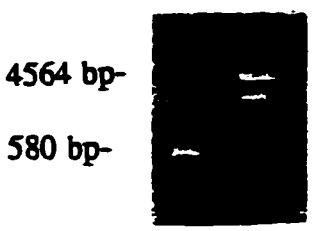

Figure 3.24. Ethidium bromide-stained 1% agarose gel of DNA fragments digested with *BspEI* and *BamHI*. Left hand lane: digestion of second PCR product; Right hand lane: digestion of rCNT1 plasmid DNA. A band at 580 bp in the right hand lane was visible on the original gel, but is only faintly visible here.

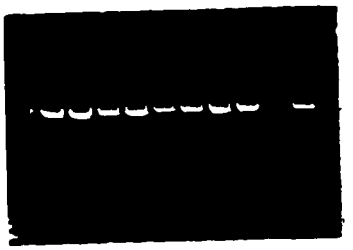

Figure 3.25. Ethidium bromide-stained 1% agarose gel of PCR products (~ 2.4 kb) generated using randomly selected transformant plasmid DNA as template and two flanking primers for the pGEM-3Z vector, T7 and SP6. Left hand lanes: selected transformants. Right hand lane: control rCNT1 plasmid DNA.

			W	1	Wild-type
		W			
			G	2	P470A
	W				
			W	3	Y466F
		T			
			G	4	Y466F/P470A
W					
			W	5	
		W			
			G	6	
	C				
			W	7	
		T			
			G	8	
			W	9	
		W			
			G	10	
	W				
			W	11	
		T			
			G	12	
G					
			W	13	S459A
		W			
			G	14	S459A/P470A
	C				
			W	15	S459A/Y466F
		T			
			G	16	Triple mutant

A(G)	G(C)	A(T)	C(G)
1532	1533	1553	1564

Figure 3.26. The probability of wild-type and different rCNT1 mutants among the transformants produced by mutagenesis of wild-type rCNT1 using the degenerate inside primers IP1 and IP2. W: original nucleotides.

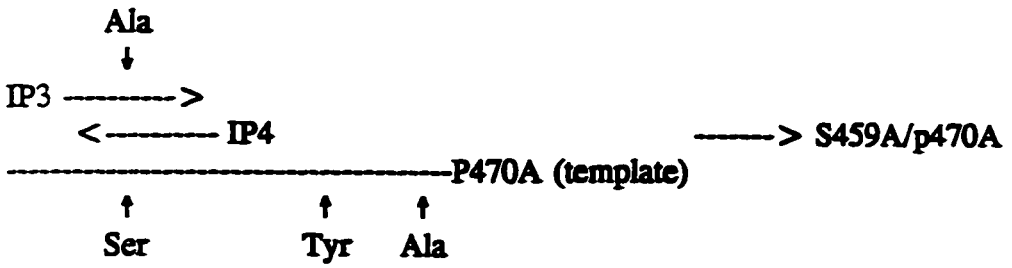

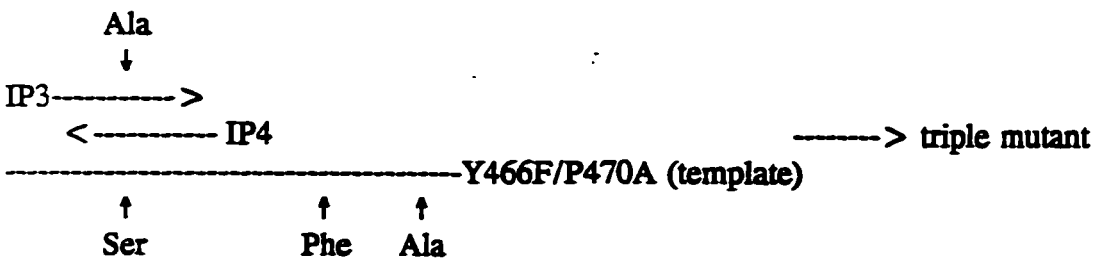

Figure 3.27. **Construction of S459A/P470A and S459A/Y466F/P470A using non-degenerate primers IP3 and IP4 and mutant templates P470A and Y466F/P470A,** respectively.

Figure 3.28. Ethidium bromide-stained 1% agarose gel showing representative PCR products generated from mutant rCNT1 pGEM-3Z DNAs by using the flanking primer T7, the internal primer IP2 and the corresponding mutant plasmid DNA as template.

Figure 3.29. Ethidium bromide-stained 1% agarose gel of mutant plasmid cDNAs linearized by *Xba*I. Left to right: S459A, Y466F, P470A, S459A/Y466F, S459A/P470A, Y466F/P470A, S459A/Y466F/P470A and control, wild-type rCNT1.

Figure 3.30. A 1% agarose gel of wild-type and mutant rCNT1 RNA transcripts. Left to right: S459A, Y466F, P470A, S459A/Y466F, S459A/P470A, Y466F/P470A, S459A/Y466F/P470A and wild-type control rCNT1.

Figure 3.31. Uridine transport by wild-type and single mutant rCNT1 constructs. *Xenopus* oocytes were injected with water alone or with water containing wild-type or mutant rCNT1 RNA transcripts (10ng). After 3 days, influx of [^{3}H]uridine (10μM, 20°C, 1min) was determined in transport buffer containing 100mM NaCl. Each value is the mean$\pm$SEM of four experiments. S, mutant S459A; Y, mutant Y466F; P, mutant P470A. * denotes values that are statistically different ($P < 0.05$) from control.

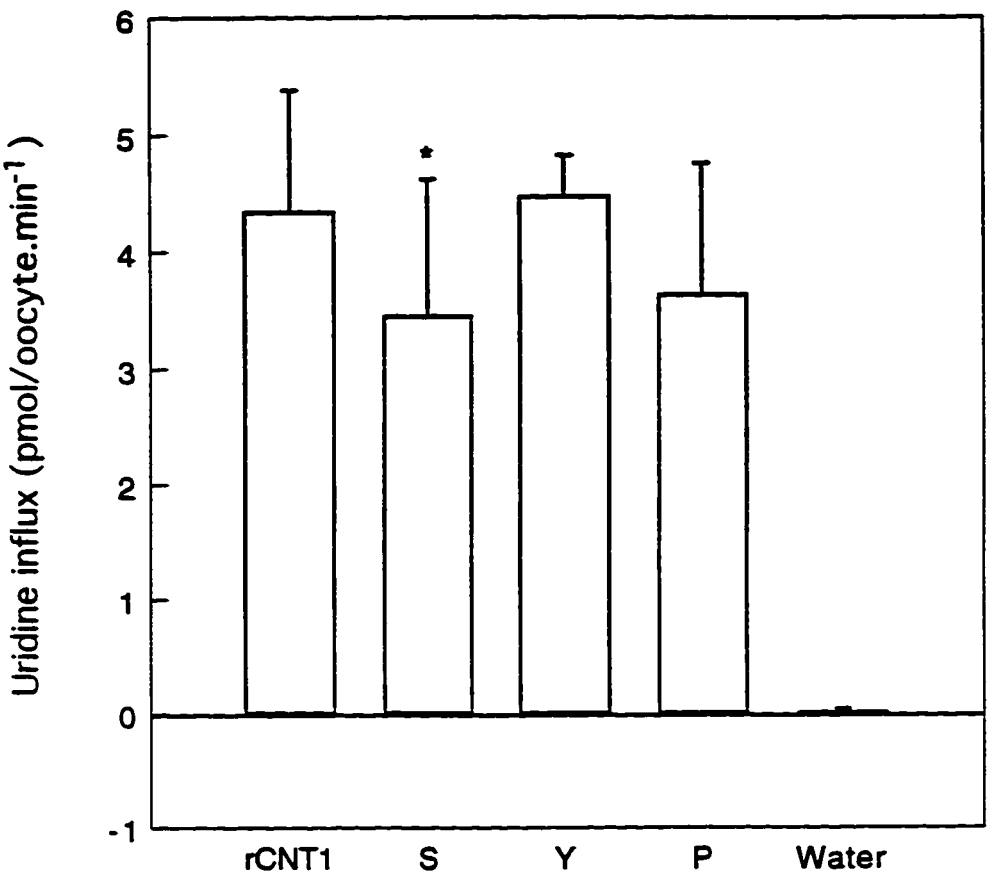
Uridine influx (pmol/oocyte.min-1)
6
5
4
3
2
1
0
-1
*
rCNT1
S
Y
P
Water

Figure 3.32. Uridine transport by wild-type, double and triple mutant rCNT1 constructs. *Xenopus* oocytes were injected with water alone or with water containing wildtype or mutant rCNT1 RNA transcripts. After 3 days, influx of [^{3}H]uridine (10μM, 20°C, 1min) was determined in transport buffer containing 100mM NaCl. Each value is the mean$\pm$SEM of four experiments. SY, mutant S459A/Y466F; SP, mutant S459A/P470A; YP, mutant Y466F/P470A; SYP, mutant S459A/Y466F/P470A. * denotes values that are statistically different ($P < 0.05$) from control.

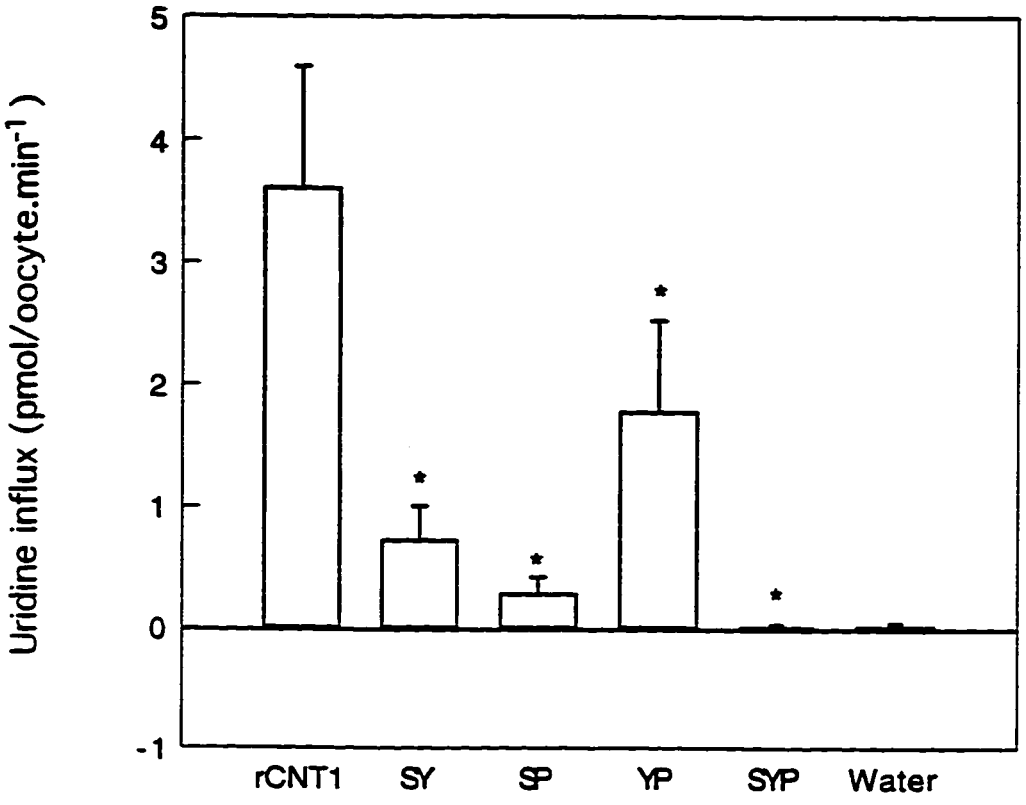
Uridine influx (pmol/oocyte.min-1)
5
4
3
2
1
0
-1
rCNT1
SY
SP
YP
SYP
Water

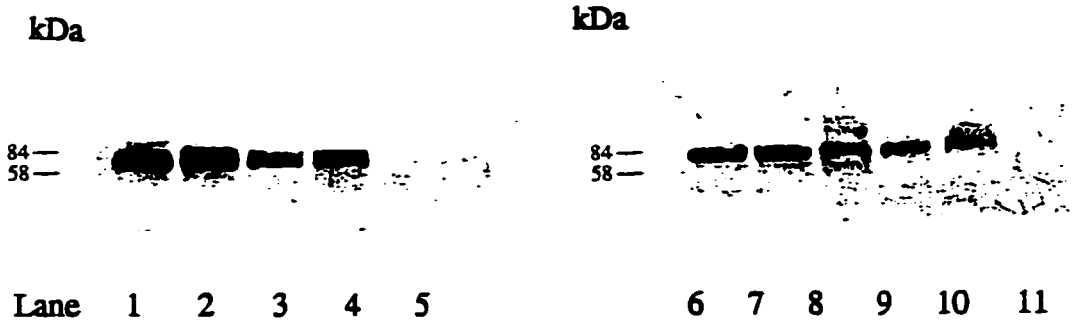

Lane 1: S459A

2: Y466F

3: P470A

Lane 6: S459A/Y466F

7: S459A/P470A

8: Y466F/P470A

9: S459A/Y466F/P470A

Lanes 4 and 10: wild-type controls

5 and 11: water control

11: water controls.

CHAPTER 4

Discussion

4. DISCUSSION

Expression selection in *Xenopus* oocytes has been used to isolate a cDNA from rat jejunal epithelium encoding a Na^+-dependent nucleoside transporter protein named rCNT1 (50). rCNT1, which is also present in kidney and corresponds functionally to one of the two major concentrative nucleoside transporter subtypes found in mammalian cells (system N2/*cit*), was the first identified mammalian representative of a new gene family of transporters that includes the *E. coli* H^+/nucleoside symporter *nup*C (25,50). In addition to transporting physiological pyrimidine nucleosides (and adenosine), recombinant rCNT1 expressed in *Xenopus* oocytes has been shown to accept the antiviral pyrimidine nucleoside analogs AZT and ddC as permeants, suggesting a potential role for the human homolog of this transporter in the intestinal absorption and renal handling of these drugs (50,134). The first part of my thesis describes the isolation of cDNAs encoding the human homolog of this protein, hCNT1. The second part of this thesis describes the construction and functional expression of a series of rCNT1 mutants involving amino acid substitutions in a putative transmembrane domain (helix 12) that is highly conserved between human and rat CNT1 and their bacterial counterpart.

4.1 ISOLATION OF cDNAS ENCODING HUMAN CNT1 (hCNT1)

4.1.1 PCR Product

A PCR product was amplified from a human kidney pYEUra3 cDNA library that proved to belong to a human rCNT1 homolog (Chapter 3, Section 3.1.2). The nucleotide sequence of the 235 bp PCR fragment was 86% identical to the corresponding region of rCNT1 cDNA. When the deduced amino acid sequence of the human PCR product was compared with that encoded by the same region of rCNT1, they were 98% similar and 89% identical. There were sufficient sequence differences between the human kidney PCR product and rCNT1 to exclude the possibility that the former was a PCR artifact derived from contaminating rCNT1 template present in the human kidney cDNA amplification reaction.

Subsequent to the cloning of rCNT1 and the isolation of my human kidney PCR fragment, cDNAs encoding a second rat nucleoside transporter protein, rCNT2, with N1/*cif* transport activity were isolated from rat liver (23) and rat jejunum (135). The nucleotide and deduced amino acid sequences of the human kidney PCR product were less similar to the corresponding region of rCNT2 (70% and 63% identity, respectively) than they were to rCNT1 (86% and 89% identity, respectively), suggesting that I had isolated a cDNA belonging to a hCNT1-type nucleoside transporter.

This cDNA, labelled with ^{32}P, was used subsequently as a hybridization probe to isolate two further hCNT cDNA fragments (clones A and B) from the same pYEUra3 human kidney cDNA library (Chapter 3, Section 3.1 and this Chapter, Section 4.1.2 below). In later studies, the same probe, generated by PCR amplification using Clone B as template, played an important role in experiments

which ultimately led to the successful isolation of a full-length hCNT cDNA (102). As discussed in Section 4.1.3 below, functional expression of the full-length cDNA in *Xenopus* oocytes confirmed that the PCR product (and clones A and B) encoded a CNT1-type transporter (designated hCNT1).

4.1.2 Clones A and B

Hybridization cloning of Clones A and B from the same human kidney pYEUra3 cDNA library that yielded the PCR fragment provided strong supporting evidence for the presence of an rCNT1 homolog in human kidney. As described in Chapter 3, Section 3.1.3, sequence alignments established that the two partial-length cDNAs (i) encoded overlapping regions of the same rCNT-related protein and (ii) contained nucleotide sequence identical to the PCR probe. As was the case for the PCR product, the nucleotide and deduced amino acid sequences of Clones A and B more closely resembled rCNT1 (87% and 91% identity, respectively, for Clone A and 86% and 88%, identity, respectively, for Clone B) than rCNT2 (73% and 72% identity, respectively, for Clone A and 75% and 70%, identity, respectively, for Clone B) suggesting that the cDNAs belong to a hCNT1-type transporter.

In addition to rCNT1/2-related sequence, the cDNA inserts of Clones A and B also contained regions of sequence unrelated to either rCNT1 or rCNT2, which were different in the two clones (Chapter 3, Section 3.1.3). Neither matched known sequences in the databases. Their open reading frames were not continuous with the adjacent regions of rCNT1/2-related sequence and it is likely that the inserts of both

clones were produced by artifactual ligation of two different cDNAs into the same plasmid during assembly of the library. It is also possible that the clones were produced by recombination events in *E. coli*. The probability of this occuring, however, is small because the *E. coli* strain used to make the library and in my experiments (XL1-Blue) is a *recA*$^-$ host, where homologous recombination does not occur. A final possibility is that the mRNA used to make the library was contaminated with genomic DNA, in which case the non-homologous regions of sequence might be introns in the hCNT1 gene.

The Clone B insert included both primer regions of the PCR product (Figure 3.16). This cDNA was used subsequently as template to provide an additional PCR probe to screen a different pCDNA1 human kidney cDNA library (Section 4.1.3 below). The choice of using Clone B as template to make the PCR probe, rather than using the PCR product itself, was to lessen the chance amplifying PCR-induced mutations. These experiments, which were performed in a study separate from this thesis by Mrs. Mabel W.L. Ritzel and Dr. Sylvia Y.M. Yao, resulted in the eventual isolation and functional expression of cDNAs encoding full-length hCNT1 (102). Together, Clones A and B encoded 40% of the full open reading frame of hCNT1 (Figure 3.19).

Finally, my experiments suggest that Clone A may contain a novel endonucleoase, *Acc*I, restriction site. During subcloning and sequencing of the clone, I discovered that the *Acc*I restriction enzyme, under experimental conditions recommended by the supplier, unexpectedly cleaved this cDNA at a site ~170 bp

from the 5'-end (results not shown). Analysis of the original insert and the digested fragments established that *Acc*I cleaved the cDNA at a site with the sequence CTAT↓TCAT. The normal *Acc*I restriction site has the sequence GT↓(A/C)(T/G)AC.

4.1.3 hCNT1

rCNT1 and rCNT2 are pyrimidine- and purine-selective, respectively, and correspond functionally to the two major Na^+-dependent nucleoside transporter processes that have been observed in cells of rodent, rabbit and bovine origin (21). As outlined in Section 4.1.2 above, the conclusion that my human kidney PCR product and Clones A and B encoded fragments of a human homolog of rCNT1 was verified in subsequent experiments by the isolation and expression of cDNAs encoding the full-length transporter in *Xenopus* oocytes (102). In fact, a series of cDNAs encoding two human homologs (hCNT1a and hCNT1b) of rCNT1 were obtained.

hCNT1a was a composite full-length cDNA assembled from two incomplete, overlapping cDNAs cloned from a pCDNA1 human kidney cDNA library by hybridization screening with the PCR probe described in this thesis (102). The open reading frame encoded a 650 amino acid residue protein (compared with 648 for rCNT1) that was 83% identical in sequence to rCNT1 (Figure 4.1). The sequence identity between hCNT1a and rat liver rCNT2 (also known as SPNT)(23) was 64% (Figure 4.2). Northern blot analysis of human kidney mRNA identified a single

transcript at 3.4 kb (118). The rat kidney rCNT1 transcript was of similar size (50). hCNT1b was isolated by reverse transcriptase (RT)-PCR amplification of human kidney RNA using primers flanking the hCNT1a open reading frame (102). The predicted amino acid sequence was similar (> 99% correspondence), but not identical, to hCNT1a.

Compared with hCNT1a, hCNT1b contained four amino acid substitutions (G34E, V109I, N410S, D522N) and deletion of V141. These differences, which may reflect hCNT1 genetic polymorphism (the cDNAs for hCNT1a and hCNT1b were obtained from different donors) and/or PCR-induced changes, were found to have no detectable effect on hCNT1 function (102). hCNT1-mediated uridine flux was rapid, Na^+-dependent and saturable, giving kinetic constants (apparent K_m ~ 40 μM, V_{max} ~ 25 pmol/oocyte.min^{-1}) similar to those reported previously for rCNT1 (50). Na^+-independent uridine influx by hCNT1 exhibited a linear concentration-dependence (up to 1 mM) that was also similar in magnitude to that found previously for rCNT1 (50) and suggests ordered binding of Na^+ and nucleoside to the transporter, with the cation binding first, thereby increasing the protein's affinity for nucleosides.

Classification of rCNT1 as a pyrimidine-selective (N2/*cit*-type) nucleoside transporter was based upon selective inhibition of uridine and thymidine fluxes by pyrimidine nucleosides and adenosine (adenosine, thymidine, cytidine, uridine > > guanosine, inosine)(50). Uridine fluxes in oocytes expressing recombinant hCNT1 were inhibited by adenosine, thymidine, cytidine and uridine, but not by guanosine

and inosine, suggesting close functional homology of the human nucleoside transporter with rCNT1 (102).

With respect to transport of adenosine, both hCNT1 and rCNT1 treated this physiologically important purine nucleoside as a high-affinity but low capacity permeant (102, 135). In human, mouse and rat kidney, adenosine undergoes net renal reabsorption by a high-affinity, low-capacity process (66,114). For example, adenosine is reabsorbed at plasma concentrations $< 50\ \mu M$, but is secreted at higher concentrations in isolated perfused rat kidneys (114). Unlike adenosine, deoxyadenosine undergoes net renal secretion in humans and mice (66). Other sugar-modified adenosine analogs (tubercidin compounds) are also secreted (89). In experiments with oocytes expressing recombinant hCNT1, deoxyadenosine inhibited transport activity with an apparent K_i value (46 μM) similar to that determined for adenosine, demonstrating high-affinity binding of deoxyadenosine to the transporter (102). Consistent with the kidney's ability to differentiate its handling of adenosine (reabsorption) and deoxyadenosine (secretion), however, transport of deoxyadenosine by hCNT1 (and rCNT1) was much slower than for adenosine (102). These findings establish that the ribose moiety of adenosine is important for transport by hCNT1 and rCNT1 and are compatible with CNT1 participation in renal adenosine reabsorption. The relative contribution of hCNT1 to that process, assuming that the transporter is located in the brush border membrane, will depend on the extent to which human kidney expresses other Na^+-linked nucleoside transporters.

Unlike adenosine and deoxyadenosine, hCNT1 transport of uridine was not

inhibited by guanosine, a presumed N4/*cit* permeant (102)(please also see Chapter 1, Section 1.1). Direct measurements of [^{3}H]guanosine fluxes by oocytes expressing hCNT1 and rCNT1 confirmed that guanosine was a poor CNT1 permeant (50,102). Human kidney brush border membrane vesicles (42) and oocytes injected with human kidney mRNA (43) have previously been shown to exhibit a nucleoside transport activity that accepts pyrimidine nucleosides, adenosine and guanosine as permeants. The role of hCNT1 in these processes remains to be determined. The conclusion that guanosine is a permeant of the human kidney pyrimidine-selective nucleoside transporter was based upon results from indirect inhibition and *trans*-acceleration assays (42,43), and not, as described here, from direct measurements of guanosine fluxes.

In a final series of functional studies (102), it was established that hCNT1, like rCNT1, also transports AZT, a pyrimidine nucleoside analog widely used in the treatment of AIDS (24). This drug is administered orally, is absorbed efficiently by the gastrointestinal systems of both rats and humans (24,83,92), and is secreted in the urine either unchanged or as the glucuronide conjugate (38,39). Therefore, although AZT undergoes net renal secretion (39), the results with recombinant hCNT1 demonstrate the existence in human kidney of an active transport system that may contribute to AZT reabsorption.

It can be concluded, therefore, that hCNT1 is both a structural and functional homolog of rCNT1. The isolation of cDNAs encoding hCNT1 represented the first molecular cloning of a human nucleoside transporter and the first demonstration that

members of the CNT family of NT proteins and their associated transport activities exist in human cells. hCNT1 represents a potential mechanism for renal reabsorption of physiological nucleosides and synthetic nucleoside drugs.

4.2 SITE-DIRECTED MUTAGENESIS STUDIES OF RAT CNT1 (rCNT1)

4.2.1 Three Conserved Amino Acid Residues in Transmembrane Domain 12

My experiments tested the hypothesis that three amino acid residues common to rCNT1 and its *E. coli* homologs may play an important role in the structure/function of the transporter. These rCNT1 residues, S459, Y466 and P470, are spatially arranged on the same face of presumed helix 12 of the protein and are also conserved in hCNT1. My studies mutated each of these residues singly and in combination to investigate the effect(s) of their substitution on the transport activity of recombinant rCNT1 expressed in *Xenopus* oocytes. S459 and P470 were mutated to alanine residues, and Y466 was mutated to phenylalanine.

My experiments provided an unexpected observation. In the situation where each residue was mutated in isolation, only S459A showed a significant decrease in transport activity (10 μM uridine influx), and even here the decrease in transport activity was small (79% of wild-type). The double mutants, in contrast, exhibited intermediate uridine fluxes (8-49% of wild-type), while the triple mutant was totally devoid of transport activity. Thus, while the mutagenesis experiments verified the original hypothesis (that the three residues were important for transport activity), my

results demonstrated that none of the amino acids, in isolation, were essential for transport activity. Instead, their mutation had a cumulative effect on the function of the protein. My studies provided evidence that none of the mutations (either singly or in combination) adversely affected trafficking of the recombinant proteins to the oocyte plasma membrane (Section 4.2.2, below). Therefore, it can be concluded that the observed changes in transport activity reflect alterations in the intrinsic transport activity of the protein.

Two of the amino acid residues under investigation (S459 and Y466) are polar and capable of forming hydrogen bonds either with the permeant or with other structural elements of the transporter protein itself (*eg* helix-helix interactions). Whichever possibility is correct, neither residue on its own or in combination with the other is essential for activity (the double mutant showed an 80% decrease in uridine influx relative to the wild-type protein). A potential analogy for this situation is provided by X-ray crystallographic data for the lactose binding site of human S-lac lectin (76,77). The resolved crystal structure of this sugar-binding protein demonstrated that there are nine specific interactions, mostly hydrogen bonds, between the lactose substrate and the side chains of specific amino acid residues in the protein. In such a circumstance, it might be anticipated that loss of one or perhaps two of these interactions might reduce the affinity of the protein for its substrate, but that partial binding (and transport) might still occur. The transport assay used in my experiments employed a sub-K_m uridine concentration (10 μM) to maximise the chance of observing changes in either K_m or V_{max}. My data provide

no information on which kinetic parameter(s) were altered in the different mutants and would not have detected situations in which both K_m and V_{max} changed in parallel to maintain the wild-type V_{max}:K_m ratio.

The third amino acid residue under investigation was P470. This nonpolar amino acid residue is particularly interesting because of its postulated location within the middle of helix 12 (Figure 1.3). The role of proline residues in transmembrane α-helices and their potential involvement in cation binding is reviewed in Chapter 1, Section 1.3.3).

4.2.2 Expression of Recombinant rCNT1 Mutants in the Oocyte Plasma Membrane

Xenopus oocytes can translate foreign eukaryotic mRNA efficiently into protein and process and target the resultant heterologous proteins to the appropriate cellular compartment. This expression system in combination with site-directed mutagenesis is a popular and useful methodology to study structure-function relationships of cloned membrane transporter proteins (*eg* 31,35,78,80).

Changes in fuctional activity associated with amino acid substitutions are most usually interpreted in terms of alterations in intrinsic activity. They can, however, result from altered trafficking of the protein to the plasma membrane. Recent studies of two human genetic membrane transport disorders provide examples of this. In Glucose-Galactose Malabsorption patients, the Na^+/glucose cotransporter (SGLT1) mutations A304V and R449H cause impaired sugar transport because of the

transporters' failure to traffick normally to the plasma membrane (81). The majority of cystic fibrosis cases result from the deletion of a single amino acid residue (F508) from the cystic fibrosis transmembrane conductance regulator (CFTR)(121). This mutation causes decreased targeting of the protein to the plasma membrane (121).

To determine whether the effect of a site-directed mutagenesis substitution is on the intrinsic activity of a membrane transport protein or on its trafficking to the plasma membrane, it is necessary to estimate the amount of the protein expressed on the cell surface. This can be achieved by Western analysis of plasma membrane preparations from cells expressing the recombinant protein.

In my experiments, I adopted a method of oocyte plasma membrane isolation that has been used successfully in several different laboratories (34,37,113). This procedure produces a 10,000*g* plasma membrane-enriched pellet (and, if required intracellular membrane fractions), which show (i) the expected distribution of membrane enzyme markers (34,113) and (ii) the correct ultrastructure and composition by electron microscopy (34). Using this fractionation method, Thomas and coworkers (113) studied the subcellular distributions of three recombinant equilibrative glucose transporters (GLUT2, GLUT3 and GLUT4) expressed in *Xenopus* oocytes. Immunoblot analysis showed that GLUT2 and GLUT3 were expressed predominantly in the plasma membrane, while GLUT4 was localized mainly in intracellular membranes. This distribution correlated with the relative functional activities of the three proteins. In my experiments, plasma membranes prepared by this procedure from oocytes injected with wild-type and mutant rCNT1

RNA transcripts showed comparable levels of expression of each of the recombinant proteins.

4.3 FUTURE DIRECTIONS

4.3.1 Human CNT Transporters

hCNT1 has been shown to have transport activity with respect to both physiological pyrimidine nucleosides (and adenosine) and antiviral pyrimidine nucleoside analogs (102). It will be important to establish the tissue and cellular distribution of this transporter and to understand the factors which regulate expression of the hCNT1 gene. Initial confocal immunocytochemistry studies of rCNT1 using rCNT1 antipeptide antibodies have demonstrated expression of the transporter in the brush border membrane of enterocytes of rat jejunum (Dr. S.A. Baldwin, personal communication). It will be important to analyse other rat tissues, including kidney, and to extend the study to hCNT1. It would also be informative to undertake parallel *in situ* hybridization studies to quantify tissue and cellular levels of CNT1 message. Cloning and sequencing of the hCNT1 gene and its regulatory elements is also required. Chromosomal fluorescence *in situ* hybridization (FISH) analysis of human lymphocyte metaphase chromosomes has been used to map a 2 kb hCNT1 probe to chromosome 15q25-26 (102). The same chromosomal band location was determined by screening a human P1-derived artificial chromosome (PAC) library (102). To date, approximately 10 kb of hCNT1 genomic sequence has

been obtained from two PAC clones that mapped exclusively to 15q25-26 (M.W.L. Ritzel, personal communication). The full hCNT1 genomic sequence will provide information not only about regulation of gene expression, but also about transporter topology, the potential for alternate splicing of hCNT1 transcript (*eg* to generate an N4/*cit*-type phenotype), and whether or not the two anomolous regions of hCNT1 clones A and B correspond to introns.

It will also be important to establish whether the human genome contains genes for other Na^+-linked nucleoside transporters, including, for example, that corresponding to rCNT2.

4.3.2 Mutagenesis Studies

In the rCNT1 mutagenesis experiments described in this thesis, Western blotting was used to compare expression of mutant and wild-type recombinant rCNT1 proteins in the oocyte plasma membrane. Cell surface expression of the different recombinant rCNT1 constructs should be verified by other methods, including confocal immunocytochemistry (35), charge movement measurements (81) and freeze-fracture electron microscopy (81). These methods, in combination with quantification of rCNT1 functional activity using the two electrode voltage clamp (81) would allow, in theory, transport activity (nucleoside-dependent Na^+-currents) and plasma membrane transporter density to be determined in the same oocyte.

As discussed in Section 4.2.1 of this Chapter, it will also be important to characterise each mutant functionally with respect to both K_m and V_{max}. It may also

be informative to study their handling of permeants other than uridine and to assess whether any of the amino acid substitutions alter the protein's interaction with Na^+.

Figure 4.1. Comparison of the deduced amino acid sequences of hCNT1 and rCNT1. The alignment was performed using the GCG BESTFIT program. Lines denote identical residues. Two dots represent highly conserved residues and a single dot shows weakly conserved residues. The two sequences are 83% identical.

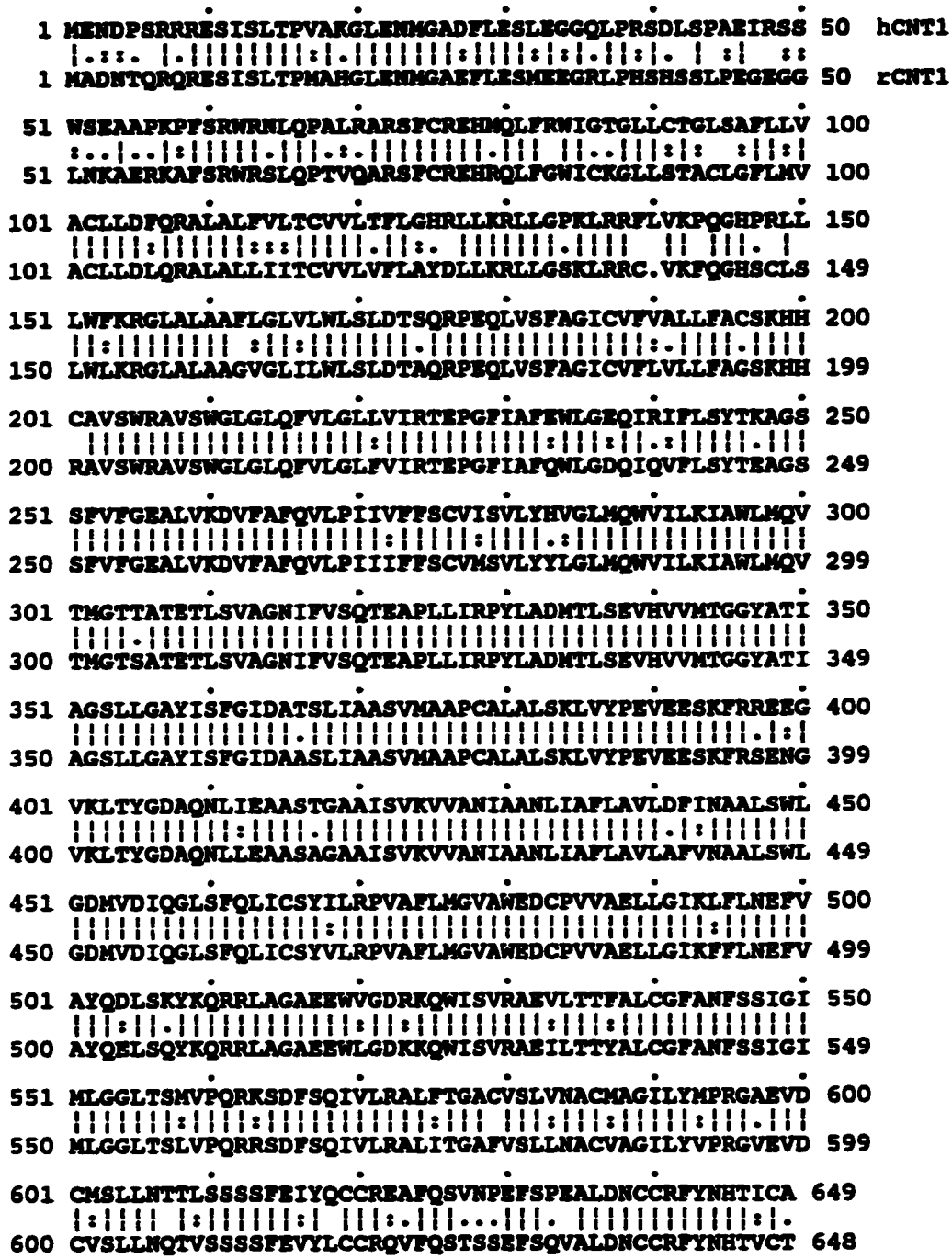
1 MENDPSRRRESISLTPVAKGLENMGADFLESLEGGQLPRSDLSPAEIRSS 50 hCNT1
1 MADNTQRQRESISLTPMAHGLENMGAEFLESMEEGRLPHSHSSLPEGEGG 50 rCNT1
51 WSEAAPKPFSRWRNLQPALRARSFCREHMQLFRWIGTGLLCTGLSAFLLV 100
51 LNKAERKAFSRWRSLQPTVQARSFCREHRQLFGWICKGLLSTACLGFLMV 100
101 ACLLDFQRALALFVLTCVVLTFLGHRLLKRLLGPKLRRFLVKPQGHPRLL 150
101 ACLLDLQRALALLIITCVVLVFLAYDLLKRLLGSKLRRC.VKFQGHSCLS 149
151 LWFKRGLALAAFLGLVLWLSLDTSQRPEQLVSFAGICVFVALLFACSKHH 200
150 LWLKRGLALAAGVGLILWLSLDTAQRPEQLVSFAGICVFLVLLFAGSKHH 199
201 CAVSWRAVSWGLGLQFVLGLLVIRTEPGFIAFEWLGEQIRIFLSYTKAGS 250
200 RAVSWRAVSWGLGLQFVLGLFVIRTEPGFIAFQWLGDQIQVFLSYTEAGS 249
251 SFVFGEALVKDVFAFQVLPIIVFFSCVISVLYHVGLMQWVILKIAWLMQV 300
250 SFVFGEALVKDVFAFQVLPIIIFFSCVMSVLYYLGLMQWVILKIAWLMQV 299
301 TMGTTATETLSVAGNIFVSQTEAPLLIRPYLADMTLSEVHVVMTGGYATI 350
300 TMGTSATETLSVAGNIFVSQTEAPLLIRPYLADMTLSEVHVVMTGGYATI 349
351 AGSLLGAYISFGIDATSLIAASVMAAPCALALSKLVYPEVEESKFRREEG 400
350 AGSLLGAYISFGIDAASLIAASVMAAPCALALSKLVYPEVEESKFRSENG 399
401 VKLTYGDAQNLIEAASTGAAISVKVVANIAANLIAFLAVLDFINAALSWL 450
400 VKLTYGDAQNLLEAASAGAAISVKVVANIAANLIAFLAVLAFVNAALSWL 449
451 GDMVDIQGLSFQLICSYILRPVAFLMGVAWEDCPVVAELLGIKLFLNEFV 500
450 GDMVDIQGLSFQLICSYVLRPVAFLMGVAWEDCPVVAELLGIKFFLNEFV 499
501 AYQDLSKYKQRRLAGAEEWVGDRKQWISVRAEVLTTFALCGFANFSSIGI 550
500 AYQELSQYKQRRLAGAEEWLGDKKQWISVRAEILTTYALCGFANFSSIGI 549
551 MLGGLTSMVPQRKSDFSQIVLRALFTGACVSLVNACMAGILYMPRGAEVD 600
550 MLGGLTSLVPQRRSDFSQIVLRALITGAFVSLLNACVAGILYVPRGVEVD 599
601 CMSLLNTTLSSSSFEIYQCCREAFQSVNPEFSPEALDNCCRFYNHTICA 649
600 CVSLLNQTVSSSSFEVYLCCRQVFQSTSSEFSQVALDNCCRFYNHTVCT 648

Figure 4.2. Comparison of the deduced amino acid sequences of hCNT1 and rCNT2. The alignment was performed using the GCG BESTFIT program. Lines denote identical residues. Two dots represent highly conserved residues and a single dot shows weakly conserved residues. The two sequences are 64% identical.

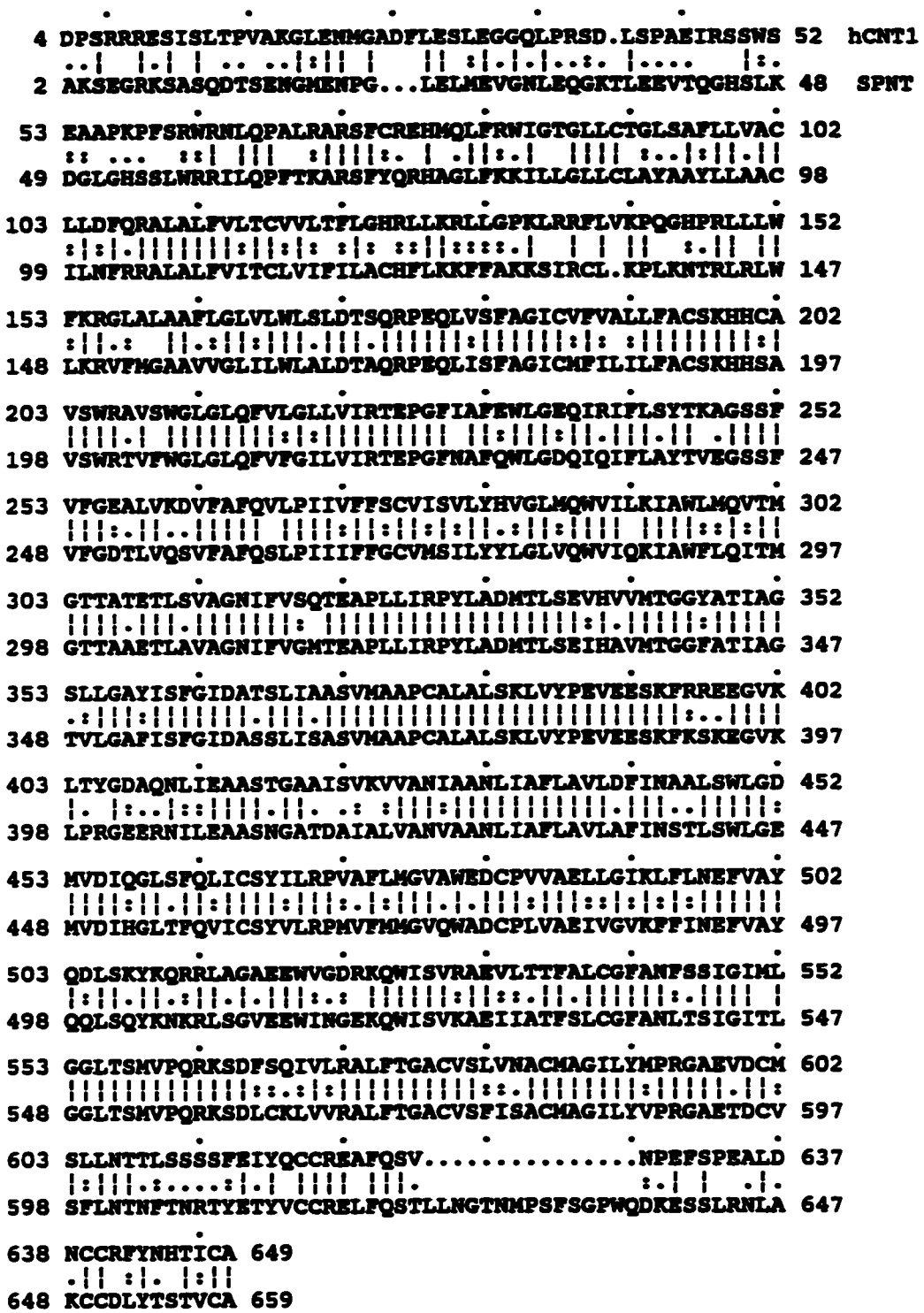
4 DPSRRRESISLTPVAKGLENMGADFLESLEGGQLPRSD.LSPAEIRSSWS 52 hCNT1
2 AKSEGRKSASQDTSENGMENPG...LELMEVGNLEQGKTLEEVTQGHSLK 48 SPNT
53 EAAPKPFSRWRNLQPALRARSFCREHMQLFRWIGTGLLCTGLSAFLLVAC 102
49 DGLGHSSLWRRILQPFTKARSFYQRHAGLFKKILLGLLCLAYAAYLLAAC 98
103 LLDFQRALALFVLTCVVLTFLGHRLLKRLLGPKLRRFLVKPQGHPRLLLW 152
99 ILNFRRALALFVITCLVIFILACHFLKKFFAKKSIRCL.KPLKNTRLRLW 147
153 FKRGLALAAFLGLVLWLSLDTSQRPEQLVSFAGICVFVALLFACSKHHCA 202
148 LKRVFMGAAVVGLILWLALDTAQRPEQLISFAGICMFILILFACSKHHSA 197
203 VSWRAVSWGLGLQFVLGLLVIRTEPGFIAFEWLGEQIRIFLSYTKAGSSF 252
198 VSWRTVFWGLGLQFVFGILVIRTEPGFNAFQWLGDQIQIFLAYTVEGSSF 247
253 VFGEALVKDVFAFQVLPIIVFFSCVISVLYHVGLMQWVILKIAWLMQVTM 302
248 VFGDTLVQSVFAFQSLPIIIFFGCVMSILYYLGLVQWVIQKIAWFLQITM 297
303 GTTATETLSVAGNIFVSQTEAPLLIRPYLADMTLSEVHVVMTGGYATIAG 352
298 GTTAAETLAVAGNIFVGMTEAPLLIRPYLADMTLSEIHAVMTGGFATIAG 347
353 SLLGAYISFGIDATSLIAASVMAAPCALALSKLVYPEVEESKFRREEGVK 402
348 TVLGAFISFGIDASSLISASVMAAPCALALSKLVYPEVEESKFKSKEGVK 397
403 LTYGDAQNLIEAASTGAAISVKVVANIAANLIAFLAVLDFINAALSWLGD 452
398 LPRGEERNILEAASNGATDAIALVANVAANLIAFLAVLAFINSTLSWLGE 447
453 MVDIQGLSFQLICSYILRPVAFLMGVAWEDCPVVAELLGIKLFLNEFVAY 502
448 MVDIHGLTFQVICSYVLRPMVFMMGVQWADCPLVAEIVGVKFFINEFVAY 497
503 QDLSKYKQRRLAGAEEWVGDRKQWISVRAEVLTTFALCGFANFSSIGIML 552
498 QQLSQYKNKRLSGVEEWINGEKQWISVKAEIIATFSLCGFANLTSIGITL 547
553 GGLTSMVPQRKSDFSQIVLRALFTGACVSLVNACMAGILYMPRGAEVDCM 602
548 GGLTSMVPQRKSDLCKLVVRALFTGACVSFISACMAGILYVPRGAETDCV 597
603 SLLNTTLSSSSFEIYQCCREAFQSV.....NPEFSPEALD 637
598 SFLNTNFTNRTYETYVCCRELFQSTLLNGTNMPSFSGPWQDKESSLRNLA 647
638 NCCRFYNHTICA 649
648 KCCDLYTSTVCA 659

REFERENCES

1. Baldwin, S.A., Beaumont, N., Barros, L.F., Young, J.D. and Cass, C.E. (1994). Antibodies as probes of nitrobenzylthioinosine-sensitive nucleoside transporters. *Drug Development Res.* **31**, 245.

2. Barros, L.F., Beaumont, N., Jarvis, S.M., Young, J.D., Henderson, P.J.F., Yudilevich, D.L., Thrasivoulou, C., and Baldwin, S.A. (1992). Immunological detection of nucleoside transporters in human placental trophoblast brush-border plasma membranes and placental capillary endothelial cells. *J. Physiol. London* **452**, 348P.

3. Barros, L.F., Beaumont, N., Jarvis, S.M., Young, J.D., Yudelivich, D.L., Thrasivoulou, C., and Baldwin, S.A. (1994). Immunological detection of nucleoside transporters in human placenta. *Eur. J. Physiol.* (in press).

4. Beaumont, N., Baldwin, S.A., Cass, C.E., and Young, J.D. (1994). In *Adenosine and adenine nucleotides: from molecular biology to integrative physiology*. (eds. Belardinelli, L., and Pelleg, A.), Kluwer Academic Publishers, Norwell, M.A. (in press).

5. Belardinelli, L., Linden, J., and Berne, R.M. (1989). The cardiac effects of adenosine. *Prog. Cardiovasc. Dis.* **32**, 73-97.

6. Belt, J.A. (1983). Nitrobenzylthioinosine-insensitive uridine transport in human lymphoblastoid and murine leukemia cells. *Biochem. Biophys. Res. Commun.* **110**, 417-423.

7. Belt, J.A. (1983). Heterogeneity of nucleoside transport in mammalian cells. Two types of transport activity in L1210 and other cultured neoplastic cells. *Mol. Pharmacol.* **24**, 479-484.

8. Belt, J.A., and Noel, L.D. (1985). Nucleoside transport in Walker 256 rat carcinosarcoma and S49 mouse lymphoma cells. *Biochem. J.* **232**, 681-687.

9. Belt, J.A., and Harper, E., Byl, J. (1992). Na^+-dependent nucleoside transport in human myeloid leukemia cell lines and freshly isolated myeloblasts. *Proc. Am. Assoc. Cancer Res.* **33**, 20.

10. Belt, J.A., Marina, N.M., Phelps, D.A., and Crawford, C.R. (1993). Nucleoside transport in normal and neoplastic cells. *Adv. Enzyme Regul.* **33**, 235-252.

11 Bendahan, A. and Kanner, B.I. (1993). Identification of domains of a cloned rat brain GABA transporter which are not required for its functional expression. *FEBS Lett.* **318**, 41-44.

12. Betcher, S.L., Forrest, J.N.Jr., Knickelbein, R.G., and Dobbins, J.W. (1990). Sodium-adenosine cotransport in brush-border membranes from rabbit ileum. *Am. J. Physiol.* **259**, G504-G510.

13. Boumah, C.E., Harvey, C.M., Paterson, A.R.P., Baldwin, S.A., Young, J.D., and Cass, C.E. (1993). Candidate cDNA clones encoding the nitrobenzylthioinosine-sensitive transporter of nucleosides in cultured human choriocarcinoma (BeWo) cells. *Biochem. Cell. Biol.* **71**, AXVI.

14. Brandl, C.J. and Deber, C.M. (1986). Hypothesis about the function of membrane-buried proline residues in transport proteins. *Proc. Natl. Acad. Sci. U.S.A.* **83**, 917-921.

15 Brooker, R. and Wilson, T.M. (1985). Isolation and nucleotide sequencing of lactose carrier mutants that transport maltose. *Proc. Natl. Acad. Sci. U.S.A.* **82**, 3959-3963.

16. Cabantchik, Z.I. (1989). Nucleoside transport across red cell membranes. *Methods Enzymol.* **230**, 13-40.

17. Casari, G., Andrade, M.A., Bork, P., Boyle, J., Daruvar, A., Ouzounis, C., Schnelder, R., Tamames, J., Valencia, A. and Sander, C. (1995). Challenging times for bioinformatics. *Nature* **376**, 647-648.

18. Cass, C.E., Gaudette, L.A., and Paterson, A.R.P. (1974). Mediated transport of nucleosides in human erythrocytes. Specific binding of the inhibitor nitrobenzylthioinosine to nucleoside transport sites in the erythrocyte membrane. *Biochim. Biophys. Acta* **345**, 1-10.

19. Cass, C.E., and Paterson, A.R.P. (1976). Nitrobenzylthioinosine binding sites in the erythrocyte membrane. *Biochim. Biophys. Acta* **419**, 285-294.

20. Cass, C.E., Belt, J.A., and Paterson, A.R.P. (1987). Adenosine transport in cultured cells. *Prog. Clin. Biol. Res.* **230**, 13-40.

21. Cass, C.E. Nucleoside transport. (1995). In: *Drug transport in antimicrobial and anticancer chemotherapy*, edited by N.H. Georgopapadakou. New York: Marcel Dekker p. 403-451.

22. Che, M., Nishida, T., Gatmaitan, Z., and Arias, I.M. (1992). A nucleoside transporter is functionally linked to ectonucleotidases in rat liver canalicular membrane. *J. Biol. Chem.* **267**, 9684-9688.

23 Che, M., Ortiz, D.F., and Arias, I.M. (1995). Primary structure and functional expression of a cDNA encoding the bile canalicular purine-specific Na^+-nucleoside cotransporter. *J.Biol.Chem.* **270**, 13596-13599.

24. Clumeck, N. (1993). Current use of anti-HIV drugs in AIDS. *J. Antimicrobiol. Chemother.* **32**, Suppl.A, 133-138.

25. Craig, J.E., Zhang, Y., and Gallagher, M.P. (1994). Cloning of the *nupC* gene of *Escherichia coli* encoding a nucleoside transport system, and identification of an adjacent insertion element, IS *186*. *Mol. Microbiol.* **11**, 1159-1168.

26. Crawford, C.R., Ng, C.Y.C., Ullman, B., and Belt, J.A. (1990). Identification and reconstitution of the nucleoside transporter of CEM human leukemia cells. *Biochim. Biophys. Acta* **1024**, 289-297.

27. Dacal, J.-L., Nehlig, A., and Nicolas, F. (1991). Physiological and pharmacological properties of adenosine: therapeutic implications. *Life Sci.* **49**, 1435-1453.

28. Dagnino, L., Bennett, L.L., and Paterson, A.R.P. (1991). Sodium-dependent nucleoside transport in mouse leukemia L1210 cells. *J. Biol. Chem.* **266**, 6308-6311.

29. Dagnino, L., Bennett, L.J., and Paterson, A.R.P. (1991). Substrate specificity, kinetics, and stoichiometry of sodium-dependent adenosine transport in L1210/AM mouse leukemia cells. *J. Biol. Chem.* **266**, 6312-6317.

30. Dahlig-Harvey, E., Eilam, Y., Paterson, A.R.P., and Cass, C.E. (1981). Binding of nitrobenzylthioinosine to high-affinity sites on the nucleoside transport mechanism of HeLa cells. *Biochem. J.* **200**, 295-305.

31. Due, A.D., Qu, Z.C., Thomas, J.M., Buchs, A., Powers, A.C. and May, J.M. (1995). Role of the C-terminal tail of the GLUT1 glucose transporter in its expression and function in *Xenopus laevis* oocytes. *Biochemistry* **34**, 5462-5471.

32. Engleman, D.M., Steitz, T.A., and Goldman, A. (1986). Identifying nonpolar transbilayer helices in amino acid sequences of membrane proteins. *Annu. Rev. Biophys. Chem.* **15**, 321-353.

33. Fang, X. Parkinson, D.A., Young, J.D. and Cass, C.E. (1996). Functional characterization of a recombinant sodium-dependent nucleoside transporter with selectivity for pyrimidine nucleosides ($cNT1_{rat}$) by transient expression in cultured mammalian cells. *Biochem. J.* **317**, 457-465.

34. Finidori-Lepicard, J., Schorderet-Slatkine, S., Hanoune, J. and Baulieu, E.E. (1981). Progesterone inhibits membrane-bound adenylate cyclase in *Xenopus laevis* oocytes. *Nature* **292**, 255-257.

35. Garcia, J.C., Strube, M., Leingang, K., Keller, K. and Mueckler, M.M. (1992). Amino acid substitutions at tryptophan 388 and tryptophan 412 of the HepG2 (Glut1) glucose transporter inhibit transport activity and targeting to the plasma membrane in *Xenopus* oocytes. *J. Biol. Chem.* **267**, 7770-7776.

36. Gati, W.P. and Paterson, A.R.P. (1989). Nucleoside transport. In *Red blood cell membranes.* (eds. Agre, P. and Parker, J.C.), Marcel Dekker, New York, pp635-661.

37. Geering, K., Theulaz, I., Verrey, F., Hauptle, M.T. and Rossier, B.C. (1989). A role for the ß-subunit in the expression of functional Na^+-K^+-ATPase in *Xenopus* oocytes. *Am. J. Physiol.* **257**, C851-858.

38. Good, S.S., Kobel, C.S., Crouch, R., Rideout, R.L. and De Miranda, P. (1990). Isolation and characterization of an ether glucuronide of zidovudine, a major metabolite in monkeys and humans. *Drug Metab. Disp.* **18**, 321-326.

39. Griffith, D.A. Hall, S.D. and Sokol, P.P. (1992). Effects of 3'-azido3'-deoxythymidine (AZT) on organic ion transport in rat renal brush membrane vesicles. *J. Pharmacol. Exptl. Therap.* **260**, 128-133.

40. Griffith, J.K., Baker, M.E., Rouch, D.A., Page, M.G.P., Skurray, R.A., Paulsen, I.T., Chater, K.F., Baldwin, S.A., and Henderson, P.J.F. (1992). Membrane transport proteins: implications of sequence comparisons. *Curr. Opin. Cell. Biol.* **4**, 684-695.

41. Griffiths, M., Beaumont, N, Yao, S.Y.M., Sundaram, M., Boumah, C.E., Davies, A., Kwong, F.Y.P., Coe, I., Cass, C.E., Young, J.D. and Baldwin, S.A. (1996). Cloning of a human nucleoside transporter implicated in the

cellular uptake of adenosine and chemotherapeutic drugs. *Nat. Med.* (submitted)

42. Gutierrez, M.M., and Giacomini, K.M. (1993). Substrate selectivity, potential sensitivity and stoichiometry of Na^+-nucleoside transport in brush-border membrane vesicles from human kidney. *Biochim. Biophys. Acta* **1149**, 202-208.

43. Gutierrez, M.M. and Giacomini, K.M. (1994). Expression of a human renal sodium nucleoside cotransporter in *Xenopus laevis* oocytes. *Biochem. Pharmacol.* **48**, 2251-2253.

44. Hammer-Jespersen, K. (1983). Nucleoside catabolism. In *Metabolism of nucleosides and nucleobases in microorganisms.* (ed. Munch-Petersen, A.), Academic Press, London, pp203-238.

45. Hediger, M.A., Coady, M.J., Ikeda, T.S., and Wright, E.M. (1987). Expression cloning and cDNA sequencing of the Na^+/glucose cotransporter. *Nature* **330**, 379-381.

46. Henderson, P.J.F. (1993). The 12-transmembrane helix transporters. *Curr. Opinion Cell. Biol.* **5**, 708-721.7.

47. Hogue, D.L., Hodgson, K.C. and Cass, C.E. (1990). Effects of inhibition of N-linked glycosylation by tunicamycin on nucleoside transport polypeptides of L1210 leukemia cells. *Biochem. Cell Biol.* **68**, 199-209.

48. Hogue, D.L., Ellison, M.J., Young, J.D., and Cass, C.E. (1994). Molecular cloning of a cDNA encoding a novel protein associated with golgi membranes of mammalian cells by complementation of the thymidine transport deficiency of *Saccharomyces cerevisiae*. *EMBO J.* (submitted).

49. Huang, Q.-Q., Harvey, C.M., Paterson, A.R.P., Cass, C.E. and Young, J.D. (1993). Functional expression of Na^+-dependent nucleoside transport systems of rat intestine in isolated oocytes of *Xenopus laevis*. Demonstration that rat jejunum expresses the purine-selective system N1 (*cif*) and a second novel system N3 having board specificity for purine and pyrimidine nucleosides. *J. Biol. Chem.* **268**, 20613-20619.

50. Huang, Q.Q., Yao, S.Y.M., Ritzel, M.W.L., Paterson, A.R.P., Cass, C.E., and Young, J.D. (1994). Cloning and functional expression of a complementary DNA encoding a mammalian nucleoside transport protein. *J. Biol. Chem.* **269**, 17757-17760.

51. Jackowski, S., and Alix, J.-H. (1990). Cloning, sequence and expression of the pantothenate permease (*pan F*) gene of *Escherichia coli* B. *J. Bacteriol.* **172**, 3842-3848.

52. Jacobson, K.A., Daly, J.W. and Mangeniello, V. (1990). Purines in Cellular Signalling: targets for new drugs. Springer Verlag, New York.

53. Jarvis, S.M., and Young, J.D. (1980). Nucleoside transport in human and sheep erythrocytes: evidence that nitrobenzylthioinosine binds specifically to functional nucleoside transport sites. *Biochem. J.* **190**, 377-383.

54. Jarvis, S.M., and Young, J.D. (1981). Extraction and partial purification of the nucleoside-transport system from human erythrocytes based on the assay of nitrobenzylthioinosine-binding activity. *Biochem. J.* **194**, 331-339.

55. Jarvis, S.M., and Young, J.D. (1986). Nucleoside transport in rat erythrocytes: two components with differences in sensitivity to inhibition by nitrobenzylthioinosine and p-chloromercuriphenyl sulphonate. *J. Membr. Biol.* **43**, 1-10.

56 Jarvis, S.M., Ellory, J.C. and Young, J.D. (1986). Radiation inactivation of the human erythrocyte nucleoside and glucose transporters. *Biochim. Biophys. Acta.* **855**, 312-315.

57. Jarvis, S.M., and Young, J.D. (1987) Photoaffinity labelling of nucleoside transporter polypeptides. *Pharmac. Therapeut.* **32**, 339-359.

58. Jarvis, S.M. (1989). Characterization of sodium-dependent nucleoside transport in rabbit intestinal brush-border membrane vesicles. *Biochim. Biophys. Acta* **979**, 132-138.

59. Jarvis, S.M., and Griffith, D.A. (1991). Expression of the rabbit intestinal N2 Na^+/nucleoside transporter in *Xenopus leavis* oocytes. *Biochem. J.* **278**, 605-607.

60. Jasper, J.R. and Insel, P.A. (1992). Evolving concepts of partial agonism. The ß-adrenergic receptor as a paradigm. *Biochem. Pharmacol.* **43**, 119-130.

61. Joost, H.G., Wandel, S. and Schürmann, A. (1994). Structure-function relationship of glucose transporters catalyzing facilitated diffusion. *Exp. Clin. Endocrinol.* **102**, 434-438.

62. Kitayama, S., Shimada, S., Xu, H. Markham, L., Donovan, D.M. and Uhl, G.R. (1992). Dopamine transporter site-directed mutations differentially alter substrate transport and cocaine binding. *Proc. Natl. Acad. Sci. U.S.A.* **89**, 7782-7785.

63. Komatsu, Y., and Tanaka, K. (1970). Mechanism of action of showdomycin. II. Effect of showdomycin on the synthesis of deoxyribonucleic acid in *Escherichia coli*. *Agric. Biol. Chem.* **34**, 891-899.

64. Komatsu, Y., and Tanaka, K. (1971). Mechanism of action of showdomycin. IV. Interactions between the mechanisms for transport of showdomycin and various nucleosides in *Escherichia coli*. *Agric. Biol. Chem.* **35**, 1328-1339.

65. Komatsu, Y., and Tanaka, K. (1972). A showdomycin resistant mutant of *Escherichia coli* K12 with altered nucleoside transport character. *Biochim. Biophys. Acta* **288**, 390-403.

66. Kuttesch, J.F. and Nelson, J.A. (1982). Renal handling of 2'-deoxyadenosine and adenosine in humans and mice. *Cancer Chemoth. Pharmacol.* **8**, 221-229.

67. Kwon, H.M., Yamauchi, A., Uchida, S., Preston, A.S., Garcia-Perez, A., Burg, M.B., and Handler, J.S. (1992). Cloning of the cDNA for a Na^+/myo-inositol cotransporter, a hypertonicity stress protein. *J. Biol. Chem.* **267**, 6297-6301.

68. Kwong, F.Y.P., Tse, C.M., Jarvis, S.M., Choy, M.Y., and Young, J.D. (1987). Purification and reconstitution studies of the nucleoside transporter from pig erythrocytes. *Biochim. Biophys. Acta* **904**, 105-116.

69. Kwong, F.Y.P., Davies, A., Tse, C.M., Young, J.D., Henderson, P.J.F., and Baldwin, S.A. (1988). Purification of the human erythrocyte nucleoside transporter by immunoaffinity chromatography. *Biochem. J.* **255**, 243-249.

70. Kwong, F.Y.P., Fincham, H.E., Davies, A., Beaumont, N., Henderson, P.J.F., Young, J.D., and Baldwin, S.A. (1992). Mammalian nitrobenzylthioinosine-sensitive nucleoside transport proteins. *J. Biol. Chem.* **267**, 21954-21960.

71. Kwong, F.Y.P., Wu, J.S.R., Shi, M.M., Fincham, H.E., Davies, A., Henderson, P.J.F., Baldwin, S.A., and Young, J.D. (1993). Enzymatic

cleavage as a probe of the molecular structures of mammalian equilibrative nucleoside transporters. *J. Biol. Chem.* **268**, 22127-22134.

72. Lee, C.W., Cheeseman, C.I., and Jarvis, S.M. (1990). Transport characteristics of renal brush-border Na^+- and K^+-dependent uridine carriers. *Am. J. Physiol.* **258**, F1203-F1210.

73. Le Hir, M., and Dubach, U.C. (1984). Sodium gradient-energized concentrative transport of adenosine in renal brush border vesicles. *Pflugs Arch.* **401**, 58-63.

74. Le Hir, M. (1990). Evidence for separate carriers for purine nucleosides and for pyrimidine nucleosides in the renal brush border membrane. *Renal Physiol. Biochem.* **13**, 154-161.

75. Li, S.C., Goto, N.K., Williams, K.A. and Deber, C.M. (1996). α-Helical, but not ß-sheet, propensity of proline is determined by peptide environment. *Proc. Natl. Acad. Sci. U.S.A.* **93**, 6676-6681.

76. Lobsanov, Y.D., Gitt, M.A., Leffler, H., Barondes, S.H. and Rini, J.M. (1993). Crystallization and preliminary X-ray diffraction analysis of the human dimeric S-Lac lectin (L-14-II). *J. Mol. Biol.* **233**, 553-555.

77. Lobsanov, Y.D., Gitt, M.A., Leffler, H., Barondes, S.H. and Rini, J.M. (1993). X-ray crystal structure of the human dimeric S-Lac lectin, L-14-II, in complex with lactose at 2.9-A resolution. *J. Biol. Chem.* **268**, 27034-27038.

78. Lostao, M.P., Hirayama, B.A., Panayotova-Heiermann, M., Sampogna, S.L., Bok, D. and Wright, E.M. (1995). Arginine-427 in the Na^+-/glucose transporter (SCLT1) is involved in trafficking to the plasma membrane. *FEBS Lett.* **377**, 181-184.

79. Margraf, M., Bocklage, H. and Mueller-Hill, B. (1985). A change of threonine 266 to isoleucine in the *lac* permease of *Escherichia coli* diminishes the transport of lactose and increases the transport of maltose. *Mol. Gen. Genet.* **198**, 473-475.

80. Marshall, B.A., Murata, H. Hresko, R.C. and Mueckler, M. (1993). Domains that confer intracellular sequestration of the Glut4 glucose transporter in *Xenopus* oocytes. *J. Biol. Chem.* **268**, 26193-26199.

81. Martin, M.G., Turk, E., Lostao, M.P., Kerner, C. and Wright, E.M. (1996). Defects in Na^+/glucose cotransporter (SGLT1) trafficking and function cause glucose-galactose malabsorption. *Nat. Genet.* **12**, 216-220.

82. McKenna, E., Hardy, D. and Kaback, H.R. (1992). Insertional mutagenesis of hydrophillic domains in the lactose permease of *Escherichia coli*. *Proc. Natl. Acad. Sci. U.S.A.* **89**, 11954-11958.

83. Melvin, G.C., Ellison, S.R., Monk, C.M. and Bates, T.R. (1990). Existence of a flip-flop kinetic model for zidovudine (AZT) after oral administration. *Res. Commun. Chem. Pathol. Pharmacol.* **70**, 193-204.

84. Munch-Petersen, A., and Mygind, B. (1976). Nucleoside transport systems in *Escherichia coli* K12: specificity and regulation. *J. Cell. Physiol.* **89**, 551-560.

85. Munch-Petersen, A., Mygind, B., Nicolaisen, A., and Pihl, N.J. (1979). Nucleoside transport in cells and membrane vesicles from *Escherichia coli* K12. *J. Biol. Chem.* **254**, 3730-3737.

86. Munch-Petersen, A., and Mygind, B. (1983). Transport of nucleic acid precursor. In *Metabolism of nucleotides, nucleosides and nucleobases in microorganisms* (ed. Munch-Petersen, A.), Academic Press, London, pp258-305.

87. Mygind, B., and Munch-Petersen, A. (1975). Transport of pyrimidine nucleosides in cells of *Escherichia coli* K12. *Eur. J. Biochem.* **59**, 365-372.

88. Nakao, T., Yamato, I., and Anraku, Y. (1987). Nucleotide sequence of Put P, the proline carrier gene of *Escherichia coli* K_{12}. *Mol. Gen. Genet.* **208**, 70-75.

89. Nelson, J.A., Kuttesch, J.F. and Herbert, B.H. (1983). Renal secretion of purine nucleosides and their analogs in mice. *Biochem. Pharmacol.* **32**, 2323-2327.

90. Pajor, A.M., and Wright, E.M. (1992). Cloning and functional expression of a mammalian Na^+/nucleoside cotransporter. A member of the SGLT family. *J. Biol. Chem.* **267**, 3557-3560.

91. Pajor, A.M. (1994). Molecular cloning and expression of SNST1, a renal sodium/nucleoside cotransporter. *Drug Development Res.* **31**, 305.

92. Park, G.B. and Mitra, A.K. (1992). Mechanism and site dependency of intestine mucosal transport and metabolism of thymidine analogs. Pharmaceut. Res. 9, 326-331.

93. Paterson, A.R.P., and Cass, C.E. (1986). Transport of nucleoside drugs in animal cells. In *Membrane transport of antineoplasmic agents.* (ed. Goldman, I.D.), Pergamon Press, Oxford, pp309-329.

94. Paterson, A.R.P., Clanachan, A.S., Craik, J.D., Gati, W.P., Jakobs, J.S., and Cass, C.E. Plasma membrane transport of nucleosides, nucleobases and nucleotides: an overview. In *Role of adenosine and adenine nucleotides in biological systems.* (eds. Imai, S., and Nakazawa, M.), Elsevier Science Publisher BV, pp133-148.

95. Paterson, A.R.P., Gati, W.P., Vijayalakshmi, D. (1993). Inhibitor-sensitive, Na^+-linked transport of nucleoside analogs in leukemia cells from patients. *Proc. Amer. Assoc. Cancer Res.* **34**, 14.

96. Plagemann, P.G.W. and Wohlhueter, R.M. (1985). Nitrobenzylthioinosine-sensitive and -resistant nucleoside transport in normal and transformed rat cells. *Biochim. Biophys. Acta* **816**, 387-395.

97. Plagemann, P.G.W., Wohlhueter, R.M., and Woffendin, C. (1988). Nucleoside and nucleobase transport in animal cells. *Biochim. Biophys. Acta* **947**, 405-443.

98. Plagemann, P.G.W., and Aran, J.M. (1990). Characterization of Na^+-dependent, active nucleoside transport in rat and mouse peritoneal macrophages, a mouse macrophage cell line and normal rat kidney cells. *Biochim. Biophys. Acta* **1028**, 289-298.

99. Plagemann, P.G.W., Aran, J.M., and Woffendin, C. (1990). Na^+-dependent, active and Na^+-independent, facilitated transport of formycine B in mouse spleen lymphocytes. *Biochim. Biophys. Acta.* **1022**, 93-102.

100. Plagemann, P.G.W. (1991). Na^+-dependent, concentrative nucleoside transport in rat macrophages. Specificity for natural nucleosides and nucleoside analogs, including dideoxynucleosides, and comparison of nucleoside transport in rat, mouse and human macrophages. *Biochem. Pharmacol.* **42**, 247-252.

101. Reizer, J., Reizer, A., and Saier, M.H.Jr. (1994). A functional superfamily of sodium/solute symporters. *Biochim. Biophys. Acta* **1197**, 133-166.

102 Ritzel, M.W.L., Yao, S.Y.M., Huang, M.Y., Elliott, J.F., Cass, C.E. and Young, J.D. (1996). Molecular cloning, functional expression and chromosomal localization of cDNAs encoding a human Na^+/nucleoside cotransporter (hCNT1). *Am. J. Physiol.* (in press)

103. Roy-Burman, S., and Visser, D.W. (1975). Transport of purines and deoxyadenosine in *Escherichia coli*. *J. Biol. Chem.* **250**, 9270-9275.

104. Roy-Burman, S., von Dippe, P., and Visser, D.W. (1978). Mechanism of energy coupling for transport of deoxycytidine, uridine, uracil, adenine and hypoxanthine in *Escherichia coli*. *Biochim. Biophys. Acta* **511**, 285-296.

105. Saier, M.H., Jr. and Reizer, J. (1991). Families and superfamilies of transport proteins common to prokaryotes and eukaryotes. *Curr. Opin. Struct. Biol.* **1**, 362-368

106. Sambrook, J., Fritsch, E.F. and Maniatis, T. (1989). In: *Molecular cloning - A laboratory manual*, edited by N. Ford. Cold Spring Harbor Laboratory Press.

107. Sankararamakrishnan, R. and Vishveshwara, S. (1992). Geometry of proline-containing alpha-helicex in proteins. *Int. J. Peptide Protein Res.* **39**, 356-363.

108. Sankararamakrishnan, R. and Vishveshwara, S. (1993). Characterization of proline-containing α-helix (helix F model of bacteriorhodopsin) by molecular dynamics studies. *Proteins* **15**, 26-41.

109. Sansom, M.S.P. (1992). Proline residues in transmembrane helices of channel and transport proteins: a molecular modelling study. *Protein Eng.* **5**, 53-60.

110. Saxild, H.H., Andersen, L.N. and Hammer, K. (1996). Dra-nupC-pdp operon of *Bacillus subtilis*: nucleoside sequence, induction by deoxy ribonucleosides, and transcriptional regulation by the deoR-encoded DeoR repressor protein. *J. Bacteriol.* **178**, 424-434.

111. Strader, C.D., Sigal, I.S. and Dixon, R.A.F. (1989). Structural basis of ß-adrenergic receptor function. *FASEB J.* **3**, 1825-1832.

112. Suchyna, T.M., Xu, L.X., Gao, F., Fourtner, C.R. and Nicholson, B. (1993). Identification of a proline residue as a transduction element involved in voltage gating of gap junctions. *Nature* **28**, 847-849.

113. Thomas, H.M., Takeda, J. and Gould, G.W. (1993). Differential targeting of glucose transporter isoforms heterologously expressed in *Xenopus* oocytes. *Biochem. J.* **290**, 707-715.

114. Trimble, M.E. and Coulson, R. (1984). Adenosine transport in perfused rat kidney and renal cortical membrane vesicles. *Am. J. Physiol.* **15**, F749-F803.

115. Uratani, Y. and Hoshino, T. (1989). Difference in sodium requirement of branched chain amino acid carrier between Pseudomonas aeruginosa PAO and PML strains is due to substitution of an amino acid at position 292. *J. Biol. Chem.* **264**, 18944-18950.

116. Vijayalakshimi, D. and Belt, J.A. (1988). Sodium-dependent nucleoside transport in mouse intestinal epithelial cells. Two transport systems with differing substrate specificities. *J.Biol. Chem.* **263**, 19419-19423.

117. Vilson, B. (1992). Functional consequences of alterations to Pro^{328} and Leu^{332} located in the 4th transmembrane segment of the α-subunit of the rat kidney Na^+, K^+-ATPase. *FEBS Lett.* **314**, 301-307.

118. von Heijne, G. (1989). Control of topology and mode of assembly of a polytopic membrane protein by positively charged residues. *Nature* **341**, 456-458.

119 Wandel, S., Schurmann, A., Becker, W., Summers, S.A., Shanahan, M.F. and Joost, H.G. (1994). Substitution of conserved tyrosine residues in helix 4 (Y143) and 7 (Y293) affects the activity, but not IAPS-forskoline binding, of the glucose transporter GLUT4. *FEBS Lett.* **348**, 114-118.

120. Wang, C.D., Buck, M.A. and Fraser, C.M. (1991). Site-directed mutagenesis of α_{2a}-adrenergic receptors: identification of amino acids involved in ligand binding and receptor activation by agonists. *Mol. Pharmacol.* **40**, 168-179.

121. Ward, C.L. and Kopito, R.R. (1994). Intracellular turnover of cystic fibrosis transmembrane conductance regulator. *J. Biol. Chem.* **269**, 25710-25718.

122. Wellner, M., Monden, I., Mueckler, M.M. and Keller, K. (1995). Functional consequences of proline mutations in the putative transmembrane segments 6 and 10 of the glucose transporter GLUT1. *Eur. J. Biochem.* **227**, 454-458.

123. Wells, R.G., Pajor, A.M., Kanai, Y., Turk, E., Wright, E.M., and Hediger, M.A. (1992). Cloning of a human cDNA with similarity to the sodium-glucose cotransporter. *Am. J. Physiol.* **263**, F459-F465.

124. Westh Hansen, S.E., Jensen, N., and Munch-Petersen, A. (1987). Studies on the sequence and structure of the *Escherichia coli* K-12 *nupG* gene, encoding a nucleoside-transport system. *Eur. J. Biochem.* **168**, 385-391.

125. Williams, T.C., Doherty, A.J., Griffith, D.A., and Jarvis, S.M. (1989). Characterization of sodium-dependent and sodium-independent nucleoside transport systems in rabbit renal brush-border and basolateral plasma-membrane vesicles from the renal outer cortex. *Biochem. J.* **264**, 223-231.

126. Williams, T.C., and Jarvis, S.M. (1991). Multiple sodium-dependent nucleoside transport systems in bovine renal brush-border membrane vesicles. *Biochem. J.* **274**, 27-33.

127. Wright, E.M., Hager, K.M., and Turk,E (1992). Sodium cotransport proteins. *Curr. Opin. Cell Biol.* **4**, 696-702

128. Wu, J.S.R., Jarvis, S.M., and Young, J.D. (1983). The human erythrocyte nucleoside and glucose transporters are both band 4.5 membrane polypeptides. *Biochem. J.* **214**, 995-997.

129. Wu, J.S.R., Kwong, F.Y.P., Jarvis, S.M., and Young, J.D. (1983). Identification of the erythrocyte nucleoside transporter as a band 4.5 polypeptide. Photoaffinity labelling studies using nitrobenzylthioinosine. *J. Biol. Chem.* **258**, 13745-13751.

130. Wu, X., Yuan, G., Brett, C.M., Hui, A.C., and Giacomini, K.M. (1992). Sodium-dependent nucleoside transport in choroid plexus from rabbit. Evidence for a single transporter for purine and pyrimidine nucleosides. *J. Biol. Chem.* **267**, 8813-8818.

131. Wu, X., Gutierrez, M.M., and Giacomini, K.M. (1994). Further characterization of the sodium-dependent nucleoside transporter (N3) in choroid plexus from rabbit. *Biochim. Biophys. Acta* **1191**, 190-196.

132. Wu, X. and Giacomini, K.M. (1994). Expression of the choroid plexus sodium-nucleoside cotransporter (N3) in *Xenopus* laevis oocytes. *Biochem. Pharmacol.* **48**, 432-434.

133. Yao, S.Y.M. (1995). Expression cloning and functional characterisation of cDNAs encoding nucleoside transporter and amino acid/nucleoside transport regulator proteins from rat jejunum. Thesis.

134 Yao, S.Y.M., Cass, C.E., and Young, J.D. (1996). Transport of the antiviral nucleoside analogs 3'-azido-3'-deoxythymidine (AZT) and 2',3'-dideoxycytidine (ddC) by a recombinant nucleoside transporter (rCNT1) expressed in *Xenopus* oocytes. *Mol. Pharmacol.* (in press)

135 Yao, S.Y.M., Ng, A.M.L., Ritzel, M.W.L., Cass, C.E., and Young, J.D. (1996). Transport of adenosine by recombinant N1/cif and N2/cit sodium/nucleoside cotransporters from rat jejunum expressed in *Xenopus* oocytes. *Mol. Pharmacol.* (submitted)

136. Yaron, A. and Naider, F. (1993). Proline-dependent structural and biological properties of peptides and proteins. *Crit. Rev. Biochem. Mol. Biol.* **28**, 31-81.

137. Young, J.D., Jarvis, S.M., Robins, M.J., and Paterson, A.R.P. (1983). Photoaffinity labelling of the human erythrocyte nucleoside transporter by N^6-(p-azidobenzyl)adenosine and nitrobenzylthioinosine. Evidence that the transporter is a band 4.5 polypeptide. *J. Biol. Chem.* **258**, 2202-2208.

138. Young, J.D., Paterson, A.R.P., and Henderson, J.F. (1985). Nucleoside transport and metabolism in erythrocytes from the Yucatan miniature pig. Evidence that inosine functions as *in vivo* energy substrate. *Biochim. Biophys. Acta* **842**, 214-224.

139. Young, J.D., Jarvis, S.M., Clanachan, A.S., Henderson, J.F. and Paterson, A.R.P. (1986). Nitrobenzylthioinosine-an *in vivo* inhibitor of pig erythrocyte energy metabolism. *Am. J. Physiol.* **251**, C90-C94.

140. Young, J.D., and Jarvis, S.M. (1983). Nucleoside transport in animal cells. *Biosci. reports* **3**, 309-322.

141. Young, J.D. (1989). Structures and functions of mammalian nucleoside transporters. *Biochem Soc Trans* **17**, 444-447

142. Zhang, Y., Craig, J.E., and Gallagher, M.P. (1992). Location of the *nupC* gene on the physical map of *Escherchia coli* K-12. *J. Bacteriol.* **174**, 5758-5759.